32831

NATIONAL LIBRARY
OTTAWA

CANADA

BIBLIOTHÈQUE NATIONALE
OTTAWA

NAME OF AUTHOR THOMAS LESLIE SAYER

TITLE OF THESIS NUCLEAR MAGNETIC RESONANCE STUDIES OF THE ACID-BASE CHEMISTRY OF AMINO ACIDS AND THE SOLUTION CHEMISTRY OF TRIMETHYLLEAD

UNIVERSITY UNIVERSITY OF ALBERTA

DEGREE FOR WHICH THESIS WAS PRESENTED Ph. D.

YEAR THIS DEGREE GRANTED 1976

Permission is hereby granted to THE NATIONAL LIBRARY OF CANADA to microfilm this thesis and to lend or sell copies of the film.

The author reserves other publication rights, and neither the thesis nor extensive extracts from it may be printed or otherwise reproduced without the author's written permission.

(Signed) Tom Sayer

PERMANENT ADDRESS:

3 HILL PLACE
STONEY CREEK, ONT

DATED July 19 1976

NL-91 (10-68)

National Library of Canada
Cataloguing Branch
Canadian Theses Division
Ottawa, Canada
K1A 0N4

Bibliothèque nationale du Canada
Direction du catalogage
Division des thèses canadiennes

NOTICE

The quality of this microfiche is heavily dependent upon the quality of the original thesis submitted for microfilming. Every effort has been made to ensure the highest quality of reproduction possible.

If pages are missing, contact the university which granted the degree.

Some pages may have indistinct print especially if the original pages were typed with a poor typewriter ribbon or if the university sent us a poor photocopy.

Previously copyrighted materials (journal articles, published tests, etc.) are not filmed.

Reproduction in full or in part of this film is governed by the Canadian Copyright Act, R.S.C. 1970, c. C-30. Please read the authorization forms which accompany this thesis.

THIS DISSERTATION
HAS BEEN MICROFILMED
EXACTLY AS RECEIVED

AVIS

La qualité de cette microfiche dépend grandement de la qualité de la thèse soumise au microfilmage. Nous avons tout fait pour assurer une qualité supérieure de reproduction.

S'il manque des pages, veuillez communiquer avec l'université qui a conféré le grade.

La qualité d'impression de certaines pages peut laisser à désirer, surtout si les pages originales ont été dactylographiées à l'aide d'un ruban usé ou si l'université nous a fait parvenir une photocopie de mauvaise qualité.

Les documents qui font déjà l'objet d'un droit d'auteur (articles de revue, examens publiés, etc.) ne sont pas microfilmés.

La reproduction, même partielle, de ce microfilm est soumise à la Loi canadienne sur le droit d'auteur, SRC 1970, c. C-30. Veuillez prendre connaissance des formules d'autorisation qui accompagnent cette thèse.

LA THÈSE A ÉTÉ
MICROFILMÉE TELLE QUE
NOUS L'AVONS REÇUE

NL-339 (3/77)

THE UNIVERSITY OF ALBERTA

NUCLEAR MAGNETIC RESONANCE STUDIES OF THE ACID-BASE CHEMISTRY OF AMINO ACIDS AND THE SOLUTION CHEMISTRY OF TRIMETHYLLEAD

by

© THOMAS LESLIE SAYER

A THESIS
SUBMITTED TO THE FACULTY OF GRADUATE STUDIES AND RESEARCH
IN PARTIAL FULFILMENT OF THE REQUIREMENTS FOR THE DEGREE
OF DOCTOR OF PHILOSOPHY

DEPARTMENT OF CHEMISTRY

EDMONTON, ALBERTA
FALL, 1976

THE UNIVERSITY OF ALBERTA

FACULTY OF GRADUATE STUDIES AND RESEARCH

The undersigned certify that they have read, and recommend to the Faculty of Graduate Studies and Research, for acceptance, a thesis entitled NUCLEAR MAGNETIC RESONANCE STUDIES OF THE ACID-BASE CHEMISTRY OF AMINO ACIDS AND THE SOLUTION CHEMISTRY OF TRIMETHYLLEAD

submitted by THOMAS LESLIE SAYER

in partial fulfilment of the requirements for the degree of DOCTOR OF PHILOSOPHY.

Dallas L Rabenstein
D.L. Rabenstein (Supervisor)

Gary Horlick
G. Horlick.

James A. Plambeck
J.A. Plambeck.

H B Dunford
H.B. Dunford

E. E. Knaus
E.E. Knaus

George H. Reed
G.H. Reed,
(External Examiner).

Date: July 15, 1976.

To my wife, Susan.

ABSTRACT

Part I

Methods have been developed for the determination of microscopic and macroscopic acid dissociation constants of polyprotic acids from nuclear magnetic resonance chemical shift measurements. Depending upon the position of a nmr-active nucleus relative to two simultaneously deprotonating functional groups, its chemical shift may reflect the state of protonation of one of the two groups (a unique resonance) or the state of both groups (a common resonance). The change in chemical shift of a unique resonance with changes in pH gives directly the fractional deprotonation of one of the two simultaneously deprotonating groups as a function of pH. In order to calculate fractional deprotonation values from common resonance data, it is necessary to determine the total change in the observed chemical shift due to the deprotonation of each of the two groups. Nonlinear least squares curvefitting techniques have been developed to calculate both macroscopic and microscopic acid dissociation constants from fractional deprotonation data. Also, a nonlinear technique has been developed to calculate macroscopic constants directly from common resonance chemical shift data.

Using these methods, microscopic and macroscopic acid dissociation constants were calculated from proton magnetic resonance chemical shift titration curves for the amino acids lysine and ornithine, the dipeptides lysylglycine and glycyllysine and the related compound ethylenediaminemonoacetic acid. Both macroscopic and microscopic constants were calculated from carbon-13 nmr titration curves for 2,3-diaminopropionic acid, ornithine and lysine. The carbon-13 data for 2,4-diaminobutyric acid proved to be anomalous and provided only macroscopic constants.

In connection with the carbon-13 nmr studies of the amino acids, linear parameterization schemes have been developed to predict the cmr chemical shifts of the alkyl and carboxyl carbons of amines, carboxylic acids, amino acids, and related compounds in aqueous solution. The parameters were determined by multiple, linear regression analysis of the observed chemical shifts of forty-five model compounds. The chemical shift parameters should be of value in the assignment of observed chemical shifts to the carbons of peptides and proteins as well as amines, carboxylic acids, and amino acids.

Part II

The aqueous solution chemistry of trimethyllead perchlorate and of the trimethyllead complexes of five carboxylic acids of pK_A values ranging from 3.40 to 4.95 has been studied by proton magnetic resonance spectroscopy and potentiometry. Pmr is shown to be a direct method for studying the solution chemistry of the trimethyllead cation; the chemical shift of methyl protons and, to a lesser extent, the coupling constant for spin-spin coupling between lead-207 ($I = \frac{1}{2}$, natural abundance 21.1%) and the protons of the methyl groups are sensitive to the nature of the ligands bonded to the trimethyllead and thus provide information at the molecular level. The equilibrium constant for the reaction of $(CH_3)_3Pb^+$ with hydroxide to form $(CH_3)_3PbOH$ has been determined from the pH dependence of the chemical shift of the methyl protons. Formation constants for the carboxylic acid complexes also were determined from the pH dependence of the chemical shift of the methyl protons in solutions containing both trimethyllead perchlorate and carboxylic acid. The formation constants of the trimethyllead complexes are found to increase linearly as the acid dissociation constants of the carboxylic acids decrease.

ACKNOWLEDGEMENTS

My most sincere thanks are given wholeheartedly to Dr. D.L. Rabenstein for his guidance and patience throughout the duration of this research. Special appreciation is given for the extra time and effort which he expended during the writing of this thesis.

Thanks must also go my colleagues in the research group for their assistance both in and out of the lab. In addition, I would like to thank Dr. T. Nakashima, Mr. Glen Bigam and Mr. Tom Brisbane for their technical assistance. Special thanks go to Miss Vi Melnychuk for an excellent typing job performed under most awkward conditions. To my friends, I would like to extend my appreciation for their friendship and encouragement during the course of my graduate work. It simply is not possible for me to express sufficient thanks to my wife, Susan, for her patience, encouragement and friendship. It would not have been possible for me to complete this work without her.

The financial support of the National Research Council, the I.W. Killiam Scholarship Foundation and the University of Alberta is gratefully acknowledged.

TABLE OF CONTENTS

CHAPTER PAGE

LIST OF TABLES xiii

LIST OF FIGURES xvii

Part I

NUCLEAR MAGNETIC RESONANCE STUDIES OF THE ACID-BASE CHEMISTRY OF AMINO ACIDS AND PEPTIDES

I. INTRODUCTION 2

A. Determination of Microscopic Acid Dissociation Constants 8

B. The Determination of Acid Dissociation Constants by Nuclear Magnetic Resonance Spectroscopy 14

C. Overview 18

II. EXPERIMENTAL 21

A. Chemicals 21

i. Proton Magnetic Resonance Studies 21

ii. Carbon-13 Magnetic Resonance Studies 21

iii. Potentiometric Studies 22

B. pH Measurements 22

C. NMR Measurements 22

i. ^{1}H NMR Measurements 22

ii. Carbon-13 Nmr Measurements . . . 23

D. Solution Preparation 24

i. PMR Studies 24

CHAPTER PAGE

ii. CMR Studies 25

iii. Potentiometric Titration Studies 26

E. Calculations 27

F. Clarification of the Definition of Acid Dissociation Constant 29

III. DEVELOPMENT OF METHODS FOR THE DETERMINATION OF MACROSCOPIC AND MICROSCOPIC ACID DISSOCIATION CONSTANTS BY NUCLEAR MAGNETIC RESONANCE SPECTROSCOPY 32

A. Introduction 32

B. The Nuclear Magnetic Resonance Technique for Studying Acid-Base Equilibria . . . 35

C. The Calculation of Acid Dissociation Constants from Common Resonance Data . 37

D. The Calculation of Acid Dissociation Constants from Fractional Deprotonation Data 41

i. Solitary Deprotonations 41

ii. Simultaneous Deprotonations . . . 44

E. Discussion 51

IV. APPLICATION OF METHODS FOR THE DETERMINATION OF ACID DISSOCIATION CONSTANTS BY NUCLEAR MAGNETIC RESONANCE SPECTROSCOPY 60

A. Introduction 60

B. Ethylenediaminemonoacetic Acid 61

i. NMR Spectra 61

ii. Determination of Acid Dissociation Constants 64

CHAPTER PAGE

C. Lysine 67

i. NMR Spectra 67

ii. Determination of Acid Dissociation Constants 72

D. Discussion 77

V. THE DETERMINATION OF MACROSCOPIC AND MICROSCOPIC ACID DISSOCIATION CONSTANTS OF α,ω-DIAMINOCARBOXYLIC ACIDS AND LYSINE PEPTIDES 98

A. Introduction 98

B. Results 98

i. α,ω-Diaminocarboxylic Acids . . . 98

ii. Lysine Dipeptides 108

C. Discussion 112

i. α,ω-Diaminocarboxylic Acids . . . 112

ii. Lysine Dipeptides 123

VI. CARBON-13 CHEMICAL SHIFT PARAMETERS FOR AMINES, CARBOXYLIC ACIDS AND AMINO ACIDS . 125

A. Introduction 125

B. Results and Discussion 129

i. Chemical Shift Data 129

ii. Alkyl Carbon Chemical Shift Parameters 137

iii. Carboxyl Carbon Chemical Shift Parameters 146

BIBLIOGRAPHY 150

CHAPTER Part II PAGE

THE AQUEOUS SOLUTION CHEMISTRY OF TRIMETHYLLEAD AND TRIMETHYLLEAD CARBOXYLIC ACID COMPLEXES

VII. INTRODUCTION 157

A. The Study of the Solution Chemistry of Metal Complexes by Nuclear Magnetic Resonance Spectroscopy 159

VIII. EXPERIMENTAL 160

A. Chemicals 160

B. pH Measurements 161

C. NMR Measurements 162

D. Solution Preparation 162

i. PMR Studies 162

ii. Potentiometric Studies 163

E. Calculations 164

F. Standardization of Trimethyllead Stock Solutions 164

IX. NUCLEAR MAGNETIC RESONANCE STUDIES OF THE AQUEOUS SOLUTION CHEMISTRY OF TRIMETHYLLEAD 166

A. The Acid-Base Chemistry of Trimethyllead 166

B. The Determination of Formation Constants of Trimethyllead Complexes of Selected Carboxylic Acids 179

BIBLIOGRAPHY 196

LIST OF TABLES

Table	Description	Page
1	Microscopic Acid Dissociation Constants of Cysteine	10
2	Spectral Data and Protonation Shift Constants for L-Cysteine and S-Methylcysteine	58
3	Proton Chemical Shift Titration Data for the Acetic Acid Protons of EDMA Below pH 4.0	63
4	Macroscopic and Microscopic Acid Dissociation Constants of EDMA	66
5	Macroscopic and Microscopic Acid Dissociation Constants of Lysine·HCl	74
6	Variation in the Macroscopic Acid Dissociation of Lysine with Concentration	76
7	Macroscopic Acid Dissociation Constants of Lysine Determined from Potentiometric Data	78
8	Macroscopic and Microscopic Acid Dissociation Constants of EDMA and Lysine Determined from pM Plots	83
9	Macroscopic and Microscopic Acid Dissociation Constants of EDMA and Lysine Calculated Using the Linear Modification of pM Plots	92
10	Macroscopic and Microscopic Acid Dissociation Constants of EDMA and Lysine Determined by Nonlinear Curvefitting	94
11	Macroscopic and Microscopic Acid Dissociation Constants of Ornithine·HCl and Lysine·HCl	102
12	Macroscopic Acid Dissociation Constants of α,ω-Diaminocarboxylic Acids Calculated from Carbon-13 Chemical Shift Data	107

Table	Description	Page
13	Microscopic Acid Dissociation Constants of 2,3-Diaminopropionic Acid, Ornithine, and Lysine from Carbon-13 Chemical Shifts Data	109
14	Macroscopic and Microscopic Acid Dissociation Constants of α-Glysyllysine·HCl and Lysylglycine·HCl	113
15	Effects of the Separation of the Alpha and Omega Ammonium Groups on the Acidities of the Ammonium Groups in α,ω-Diaminocarboxylic Acids	115
16	Acid Dissociation Constants for Symmetrical Diamines	119
17	Acid Dissociation Constants for Monoaminocarboxylic Acids	121
18	Predicted Macroscopic and Microscopic Acid Dissociation Constants for α,ω-Diaminocarboxylic Acids	122
19	Carbon-13 Chemical Shifts of Selected Monoamines in Aqueous Solution	130
20	Carbon-13 Chemical Shifts of Selected Diamines in Aqueous Solution	131
21	Carbon-13 Chemical Shifts of Selected Monocarboxylic Acids in Aqueous Solution	132
22	Carbon-13 Chemical Shifts of Selected Dicarboxylic Acids in Aqueous Solution	133
23	Carbon-13 Chemical Shifts of Selected Aminocarboxylic Acids in Aqueous Solution	134
24	Carbon-13 Chemical Shifts of Aminodicarboxylic Acids in Aqueous Solution	135
25	Carbon-13 Chemical Shifts of α,ω-Diaminocarboxylic Acids in Aqueous Solution	136
26	Chemical Shift Parameters for Alkyl Carbons of Amines, Carboxylic Acids and Amino Acids	139

Table	Description	Page
27	Chemical Shift Parameters for Primary, Secondary and Tertiary Carbons of Amines, Carboxylic Acids and Amino Acids	141
28	Chemical Shift Parameters for Primary, Secondary and Tertiary Carbons of Amino Acids	142
29	Chemical Shift Parameters for Carboxyl Carbons of Carboxylic Acids and Amino Acids	147
30	Proton Magnetic Resonance Data and Log K_1 Values for 0.069 M Trimethyllead Perchlorate	173
31	Proton Magnetic Resonance Data and Log K_1 Values for 0.034 M Trimethyllead Perchlorate	174
32	Proton Magnetic Resonance Data and Log K_1 Values for 0.014 M Trimethyllead Perchlorate	175
33	Proton Magnetic Resonance Data and Log K_1 Values for 0.005 M Trimethyllead Perchlorate	176
34	Proton Magnetic Resonance Data for the Trimethyllead-Pivalic Acid System	180
35	Proton Magnetic Resonance Data for the Trimethyllead-Pivalic Acid System	181
36	Proton Magnetic Resonance Data for the Trimethyllead-Propionic Acid System	182
37	Proton Magnetic Resonance Data for the Trimethyllead-Acetic Acid System	183
38	Proton Magnetic Resonance Data for the Trimethyllead-Formic Acid System	185
39	Proton Magnetic Resonance Data for the Trimethyllead-Acetylglycine System	186

Table	Description	Page
40	Acid Ionization Constants and Formation Constants of the Trimethyllead and the Methylmercury Complexes of Selected Carboxylic Acids, and the Trimethyllead Chemical Shifts of Their Trimethyllead Complexes	192

LIST OF FIGURES

Figure Page

1 Fractional deprotonation errors inherent in the model used for a diprotic acid in Equation 81 (36,44). The numbers by the curves are the ratio K_1/K_2. The fractional deprotonation error is defined as the fractional deprotonation predicted by the model in Equation 81 minus the true fractional deprotonation. The model gives negative fractional deprotonation errors for titration of the first proton (the lower set of curves) and positive errors for the titration of the second proton (the upper set of curves). 54

2 pH dependence of the chemical shifts of the carbon-bonded protons of ethylenediaminemonoacetic acid in a 0.02 M aqueous solution. 62

3 Microscopic acid dissociation scheme for the ammonium groups of ethylenediaminemonoacetic acid. 68

4 Microscopic acid dissociation scheme for the ammonium groups of lysine. 69

5 PMR spectrum of the carbon bonded protons of lysine in a 0.5 M aqueous solution at approximately neutral pH. 70

6 pH dependence of the chemical shifts of the protons on the alpha (lower curve) and epsilon (upper curve) carbons of lysine in a 0.19 M aqueous solution. 71

7 pM_2 vs $f_{2,d}$, the fractional deprotonation of the secondary ammonium group for EDMA. 84

8 pM_2 vs $f_{2,d}$, the fractional deprotonation of the alpha ammonium group, for lysine. 85

9 pM_3 vs $f_{3,d}$, the fractional deprotonation of the epsilon ammonium group, for lysine. 86

Figure Page

10 $a_{H^+}(k_{12}-M_2)$ vs M_2 for EDMA. The slope yields k_{13} and the intercept $- k_{13}k_{123}$. 89

11 $a_{H^+}(k_{12}-M_2)$ vs M_2 for lysine. The slope yields k_{13} and the intercept $- k_{13}k_{123}$. 90

12 $a_{H^+}(k_{13}-M_3)$ vs M_3 for lysine. The slope yields k_{12} and the intercept $- k_{12}k_{132}$. 91

13 Microscopic acid dissociation scheme for α,ω-diaminocarboxylic acids. 99

14 pH dependence of the chemical shifts of the protons on the alpha and delta carbons of ornithine. 100

15 pH dependence of the chemical shifts of the alkyl carbons of 2,3-diaminopropionic acid in a 0.185 M aqueous solution 103

16 pH dependence of the chemical shifts of the alkyl carbons of 2,4-diaminobutyric acid in a 0.185 M aqueous solution. 104

17 pH dependence of the chemical shifts of the alkyl carbons of ornithine in a 0.185 M aqueous solution 105

18 pH dependence of the chemical shifts of the alkyl carbons of lysine in a 0.185 M aqueous solution. 106

19 pH dependence of the chemical shifts of the protons on the glycyl alpha carbon and the lysine epsilon carbon of glycyl-lysine in a 0.099 M aqueous solution 110

20 pH dependence of the chemical shifts of the protons on the alpha and epsilon carbons of the lysyl residue of lysyl-glycine in a 0.11 M aqueous solution. 111

21 PMR spectrum of the methyl groups of trimethyllead in a 0.140 M solution at approximately neutral pH. 167

Figure Page

22 pH dependence of the methyl protons of trimethyllead in a 0.140 M aqueous solution, in an aqueous solution containing 0.153 M trimethyllead and 0.071 M pivalic acid and in an aqueous solution containing 0.102 M trimethyllead and 0.093 M pivalic acid. 168

23 pH dependence of the lead 207-proton coupling constant in a 0.140 M aqueous solution. 169

24 Plot of the pK_A's of selected carboxylic acids vs the formation constants of their trimethyllead complexes. 194

Part I

NUCLEAR MAGNETIC RESONANCE STUDIES OF THE ACID-BASE CHEMISTRY OF AMINO ACIDS AND PEPTIDES

CHAPTER I

INTRODUCTION

The acid-base chemistry of polyprotic molecules is generally described in terms of stepwise, macroscopic acid dissociation constants. For example, the titration of the fully protonated form of the amino acid glycine yields two

$$H_3^{+}NCH_2CO_2H$$

macroscopic acidity constants, $pK_1 = 2.3$ and $pK_2 = 9.8$ (1). The macroscopic deprotonation scheme can be described by:

$$H_2^{+}A \rightleftarrows H^{+} + HA \qquad (1)$$

$$K_1 = \frac{[H^{+}][HA]}{[H_2^{+}A]} \qquad (2)$$

$$HA \rightleftarrows H^{+} + A^{-} \qquad (3)$$

$$K_2 = \frac{[H][A^{-}]}{[HA]} \qquad (4)$$

On the molecular level, the monoprotonated form HA can be represented by two microscopic forms as illustrated in Scheme I.

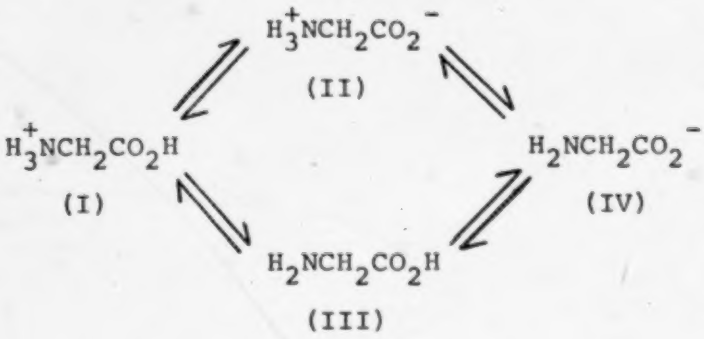

Scheme I

By analogy to acetic acid (pK_a = 4.76 (2)) and ethylamine (pK_a = 10.81 (3)), pK_1 of glycine can be assigned to the $-CO_2H$ group and pK_2 to the amino group. Due to the widely varying acidities of the two functional groups, the deprotonation will occur almost entirely via the upper pathway of Scheme I and very little of the glycine will be present as Form III at any pH.

When the strengths of the acid groups are similar, two or more functional groups may simultaneously deprotonate over the same pH range, and the macroscopic constants obtained by pH titration can no longer be assigned to a specific group. The amino acid cysteine,

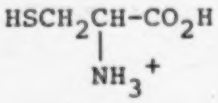

$$HSCH_2\underset{\displaystyle NH_3^+}{\underset{|}{C}}H\text{-}CO_2H$$

which has been studied quite intensively, is a molecule of this type. The macroscopic deprotonation scheme of cysteine can be represented as follows

$$H_3^+A \rightleftharpoons H_2A + H^+ \quad (5)$$

$$H_2A \rightleftharpoons HA^- + H^+ \quad (6)$$

$$HA^- \rightleftharpoons A^= + H^+ \quad (7)$$

where $pK_1 = 1.77$, $pK_2 = 8.33$ and $pK_3 = 10.78$ (4). pK_1 can be assigned to the carboxylic acid group but the assignment of pK_2 or pK_3 to either the sulfhydryl or amino group, by analogy to similar compounds, is ambiguous. Initially, Cohn and Edsall (5) assigned the higher pK to the sulfhydryl group, but this assignment was reversed by Calvin (6). Edsall, as cited by Ryklan and Schmidt (7), assumed the intrinsic proton affinities of the sulfhydryl and amino groups to be similar, and thus considered the macroscopic pK values to be due to the deprotonation of both groups. This latter interpretation has proven to be correct and the microscopic acid dissociation scheme for the second and third deprotonations of cysteine is illustrated in Scheme II (8).

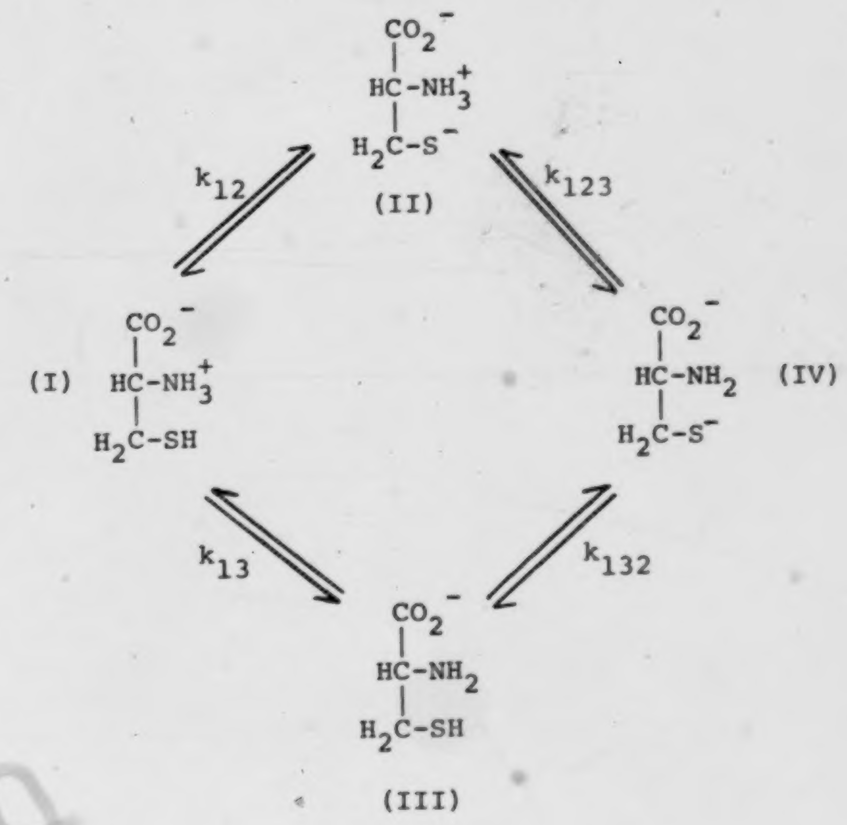
k12
k123
k13
k132
(I)
(II)
(III)
(IV)

Scheme II

The microscopic constants are denoted by lower case k's and are defined by Equations 8 through 11.

$$k_{12} = \frac{[H^+][II]}{[I]} \tag{8}$$

$$k_{13} = \frac{[H^+][III]}{[I]} \tag{9}$$

$$k_{123} = \frac{[H^+][IV]}{[II]} \tag{10}$$

$$k_{132} = \frac{[H^+][IV]}{[III]} \tag{11}$$

The acid dissociation step to which a given microconstant refers is indicated by the subscript, the last number denoting the group undergoing deprotonation and the preceding number(s) indicating groups which have previously undergone deprotonation. The carboxyl, sulfhydryl, and amino groups are denoted by the subscripts (1), (2) and (3) respectively. The macroscopic constants can be defined on the molecular level by:

$$K_2 = \frac{[H^+][HA^-]}{[H_2A]} = \frac{[H^+]([II] + [III])}{[I]} \tag{12}$$

$$K_3 = \frac{[H^+][A^=]}{[HA^-]} = \frac{[H^+][IV]}{[II] + [III]} \tag{13}$$

By substitution of Equations 8-11 into Equations 12 and 13, it can be shown that the macroscopic constants are composites of the microscopic constants.

$$K_2 = k_{12} + k_{13} \tag{14}$$

$$K_3 = \frac{k_{123}k_{132}}{(k_{123} + k_{132})} \qquad (15)$$

$$K_2K_3 = k_{12}k_{123} = k_{13}k_{132} \qquad (16)$$

From the preceding equations, it can be seen that in order to determine the microscopic dissociation constants, it is necessary to obtain quantitative information related to the concentrations of the monoprotonated tautomers. A pH titration, the most common method of determining acid dissociation constants, provides information regarding the mean number of protons lost and thus can be used to determine only the sum of the concentrations of the two monoprotonated forms.

A knowledge of the microscopic constants is important in several areas. The binding of metal ions by polydentate ligands, such as amino acids, often involves only one of the two monoprotonated tautomers. For example, the complexation of certain metal ions may involve only Form II (see Scheme II) or only Form III of cysteine. The binding by specific functional groups is particularly important in peptides since the large size of many peptides prohibits the chelation of a single metal ion by more than a few of the multiple binding sites available. The ionic character, and thus chemical behavior, of compounds containing more than one type of functional group is often affected by the degree of deprotonation of the individual groups. As an example, although the monoprotonated forms of cysteine both have a net one negative charge, Form II contains three point charges whereas Form III contains only one point charge. It's likely that the presence of these point charges will strongly affect the behavior of such a molecule, particularly at the ionic strengths typical of biological fluids. Similarly, knowledge of the microscopic ionization scheme is necessary to completely describe the chemical and biological nature of polyprotic compounds used in pharmaceutical applications (14).

A. Determination of Microscopic Acid Dissociation Constants

Through the use of model compounds, potentiometry with the glass electrode has been extended to the determination of microscopic dissociation constants. This is accomplished by replacing the labile proton(s) of one of the simultaneously deprotonating functional groups with a non-labile alkyl group, usually a methyl or ethyl group. The acid dissociation constant of the remaining functional group is then determined by a pH titration of the model compound and the resultant k_a is combined with the macroscopic constants of the parent compound to obtain the remaining microconstants from equations 14 through 16.

This approach assumes that the acidity of the group titrated is not affected by replacing the proton(s) of the other functional group with an alkyl group(s). This assumption is the principle of Wegscheider (9) and its validity is dependent upon the functional group to which the alkyl moiety is attached (10,11,12). Consequently, caution must be exercised in the choice of model compounds.

The microscopic constants of cysteine have been estimated from pH titration data by combining macroscopic constants with those of model compounds. Ryklan and Schmidt (7) assumed the pK_2 of S-ethylcysteine to be equivalent to pk_{13} of cysteine (see Scheme II) and thus obtained the values 8.60 and 8.67 for pk_{13} and pk_{12} respectively. The remaining constants obtained by these authors are reported in Table 1. Grafius and Nielands (13) used a similar approach to solve the same problem. These authors assumed the pK_2 of cysteine betaine

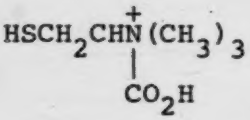

$$HSCH_2\underset{\displaystyle CO_2H}{CH}\overset{+}{N}(CH_3)_3$$

to be equivalent to pk_{12} of cysteine and the pK_2 of S-methylcysteine to represent pk_{13}. The constants obtained are listed in Table 1. The model compound approach has been used to approximate the microscopic dissociation schemes of other compounds of biological interest including

TABLE 1

Microscopic Acid Dissociation Constants of Cysteine[a]

pk_{12}	pk_{13}	pk_{123}	pk_{132}	μ(M)	Method	Reference
8.67	8.60	10.45	10.51	-	Potentiometry, Model Compounds	(7)
8.65	8.75	-	-	0.15	Potentiometry, Model Compounds	(8)
8.53	8.86	10.36	10.03	0.2	U.V. Spectroscopy	(15)
8.54	8.86	10.53	10.21	0.08	U.V. Spectroscopy	(13)
8.50	8.85	10.35	10.00	~1.0	Raman Spectroscopy	(19)
8.44	8.31	9.58	9.73	0.5	Calorimetry	(11)

a) See Scheme II for definition of the pk's.

glutathione (15) and citric acid (16,17).

The microscopic acid dissociation constants of cysteine have been estimated using calorimetric data obtained from model compounds. Wrathall et al (18) noted the four kilocalorie per mole difference in the heats of acid dissociation of the protonated sulfhydryl and amino groups of mercaptoacetic acid and S-methylcysteine, respectively, and assumed that the ΔH values represented the heats of acid dissociation for the analogous functional groups in cysteine. This approach also assumes that the heat of acid dissociation, for a given functional group, is the same for the diprotonated form as for the monoprotonated tautomer and has been criticized on this basis (19,20). The calorimetric results for the microconstants of cysteine are presented in Table 1. A similar approach has been used to calculate the microscopic constants for N-methyl and N,N-dimethylethylenediamine (21) from calorimetric data.

More favourable techniques are those which follow the deprotonation of at least one of the functional groups directly. Benesch and Benesch (22) used the ultraviolet absorption of the ionized sulfhydryl group to determine the microscopic scheme of cysteine. Although the position of the absorption maximum shifted from 236-238 nm to 230-232 nm as the pH was increased, it was assumed that the molar absorptivities of Forms II and IV (Scheme II) are equal. Consequently, the ratio of the absorbance at a given pH to the maximum absorbance at high pH represents α_{S^-}, the fraction of all sulfhydryl groups which are deprotonated.

$$\alpha_{S^-} = \frac{[R\text{-}S^-]}{[R\text{-}SH] + [R\text{-}S^-]} = \frac{A_{obs}}{A_{max}} \qquad (17)$$

Written in terms of the microscopic forms in Scheme II, Equation 17 becomes:

$$\alpha_{S^-} = \frac{[II] + [IV]}{[I] + [II] + [III] + [IV]} \qquad (18)$$

Equation 18, rewritten in terms of the microscopic acid dissociation constants, was solved by Benesch and Benesch using data at three different pH values to obtain k_{12}, k_{13}, and k_{132}. Their results are presented in Table 1. Several other research groups have repeated this work to elucidate the microscopic acid dissociation constants of cysteine (8,20,23). Coates, Marsden and Riggs (20) used the U.V. approach of Benesch and Benesch (22) to study the effects of temperature and ionic strength on the microscopic acid-base chemistry of cysteine. Their results, at 25°C and 0.1 M ionic strength, are presented in Table 1.

Although the U.V. approach is limited to molecules containing either a phenoxy or sulfhydryl group and a non-chromophore as the second simultaneously deprotonating functional group, the microscopic acid dissociation constants of a number of compounds have been determined using this technique. Edsall, Martin and Hollingworth (11) used the ultraviolet absorption of the deprotonated phenoxy group to determine the microscheme of tyrosine. The same paper introduced the pM plot method of calculating microconstants from U.V. absorption data. This graphical extrapolation technique has since been used by a number of authors to study a variety of compounds including L-3,4-dihydroxyphenylalanine (DOPA) (12), morphine.HCl (24) and phenolalkyl amines (25). Niebergall et al (14) also studied tyrosine using U.V. absorption-pH data but developed both linear and nonlinear regression techniques to calculate the microscopic and macroscopic acid dissociation constants. Comparisons between the constants obtained by the regression techniques and those obtained from pM plots, for tyrosine and morphine.HCl, indicated that the nonlinear regression gave better precision and lower residuals than did the other methods. Discussions of various calculation procedures appearing in the literature will be presented in Chapters III and IV.

In an approach similar to that used in the U.V. method, Elson and Edsall (26) used Raman spectroscopy to determine the microconstants of cysteine. By following the intensity of the S-H stretching band near 2580 cm^{-1}, the fraction of the sulfhydryl groups which were deprotonated at a given pH could be determined. Although the experiments were performed at relatively high ionic strengths (0.5-1.0 M), the results obtained compared favourably with those of Benesch and Benesch (see Table 1).

Of the preceding methods, those in which the deprotonation of a specific functional group is monitored depend upon a particular property of the given group and therefore can be applied only to those molecules which contain the specified groups. For example, the simultaneous deprotonation of the two carboxylic acid groups in glutathione or of the two amino groups in lysine cannot be resolved by ultraviolet spectroscopy. Consequently, a technique which is not dependent upon the characteristics of the functional groups undergoing deprotonation would have a wider range of applicability.

B. The Determination of Acid Dissociation Constants By Nuclear Magnetic Resonance Spectroscopy

Grunwald, Lowenstein and Meiboom (27) have shown that aqueous acid-base equilibria are generally rapid on the nuclear magnetic resonance (nmr) time scale and that the chemical shifts of the exchange averaged resonances are linearly related to the degree of protonation of the acidic functional groups. Since all polyprotic organic acids have nmr active nuclei whose chemical shifts are dependent upon the degree of protonation, the nuclear magnetic resonance technique has a wide potential range of application.

Lowenstein and Roberts (28) studied the deprotonation of citric acid using proton nmr. Since the observed resonances reflected the degree of protonation of more than one functional group,[1] a series of methyl esters was used to provide chemical shift data for the various partially deprotonated forms. However, their results have been criticized by Martin (15). Rigler et al (29) studied the acid-base chemistry of the antibiotic tetracycline by nmr and Kesserling and Benet (30) used pmr data to elucidate the protonation scheme of a related compound, isochlortetracycline. Both groups of workers employed quaternary methyl ammonium derivatives to separate the chemical shift effects of the deprotonating groups. More recently, Walters and Leyden (31) used pmr in an attempt to determine the ratio of protonated sulfhydryl groups to protonated amino groups in monoprotonated cysteine. However, their results showed poor agreement with those obtained by other spectroscopic methods and will be discussed in detail in Chapter III.

---

[1] Resonances which reflect the degree of protonation of a single functional group will be referred to as unique resonances and those which reflect the degree of protonation of more than one functional group will be referred to as common resonances.

In the NMR work cited thus far, the compounds studied have provided only common resonance data. However, if the spectrum contains at least one unique resonance, the microscopic acid dissociation constants can be calculated without the use of model compounds.

Creyf and co-workers (32) found that the chemical shifts of the methyl resonances of a series of N-methyldiamines reflected the deprotonation of only the substituted amino group. By combining the fractional protonation data obtained from the chemical shifts of the methyl resonances with macroscopic acid dissociation constants obtained by potentiometry, the microscopic constants for both amino groups were determined. Hine and co-workers (33,34) have also used pmr chemical shift data to study the microscopic deprotonation schemes of a series of N-methyl diamines.

The acid-base chemistry of the tripeptide

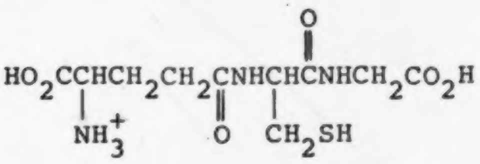

$$\mathrm{HO_2C\underset{NH_3^+}{\underset{|}{C}}HCH_2CH_2\underset{O}{\underset{\|}{C}}NH\underset{CH_2SH}{\underset{|}{C}}H\overset{O}{\overset{\|}{C}}NHCH_2CO_2H}$$

glutathione was studied by proton nmr (35). Microscopic acid dissociation constants for the simultaneous deprotonation of the two carboxylic acid groups and for the simultaneous deprotonation of the sulfhydryl and amino groups were all determined from chemical shift vs pH data. Due to the spatial separation of the deprotonating functional groups and the rapid attenuation of proton chemical shift effects, the spectrum of glutathione contains at least one unique resonance for each of the simultaneously deprotonating functional groups. As a result, the microscopic constants could be calculated using only the chemical shift-pH data. The macroscopic constants, calculated from the microscopic constants via Equations 14 and 15, agreed favourably with those in the literature.

Although the previously cited papers have utilized only proton nmr, the observed chemical shifts in carbon-13 nuclear magnetic resonance (cmr) are also dependent upon the degree of protonation of the acidic functional groups in the molecule. In proton decoupled cmr spectra, a singlet is observed for each non-equivalent carbon. Since each carbon can be monitored, the amount of information is usually greater than that contained in the pmr spectrum of the same molecule. In addition, the range of chemical shifts in cmr is generally at least an order of magnitude larger than those observed in ^{1}H-nmr. Thus, carbon-13 magnetic resonance should also be a useful tool for studying the acid-base chemistry of organic molecules.

A number of papers have appeared in the literature detailing the pH dependence of the carbon-13 chemical shift (36-43), but microscopic acid dissociation constants were not determined from the data. Freedman et al (44) studied a number of amino acids, peptides and proteins but reported only the macroscopic constants of histidine. Fairhurst (45) attempted to determine the microscopic acid dissociation constants of cysteine and several related compounds from carbon-13 chemical shift data using nonlinear regression techniques. Since each of the carbon resonances observed reflects the deprotonation of both functional groups in the microscheme, estimates of the intermediate chemical shifts are required. However, model compound data proved unsatisfactory as a source of intermediate shift values and only macroscopic constants could be determined.

C. Overview

Of the techniques for the determination of microscopic acid dissociation constants discussed in this introduction, the model compound approach lacks accuracy due to its inherent assumptions and the use of ultraviolet spectroscopy is limited to molecules in which one of the two simultaneously deprotonating functional groups is a chromophore. In addition, the calculation procedures presented in the literature tend to rely on uncertain estimates of vital parameters or are restricted to systems in which the ratios of the microscopic constants fall into a narrow range.

Since the nuclear magnetic resonance technique can be applied to molecules containing a variety of functional groups, a study was undertaken to determine the potential of nmr spectroscopy for the elucidation of acid-base equilibria on the molecular level. Chapter III contains the theoretical background and the development of methods for the determination of microscopic and macroscopic acid dissociation constants from nuclear magnetic resonance chemical shift data. The application of the methods developed in Chapter III is illustrated in Chapter IV by the determination of the acid dissociation constants of ethylenediaminemonoacetic acid and lysine; two compounds which are not suitable for study by the U.V. and Raman methods discussed previously. In addition, the data obtained for these compounds is analyzed by several calculation methods from the literature and the results are compared with those obtained using the methods developed in Chapter III.

Chapter V presents the results of a study of the determination of acid dissociation constants for a series of α,ω-diaminocarboxylic acids and two lysine dipeptides from both proton and carbon-13 nuclear magnetic resonance data. The acid-base chemistry of these compounds is discussed in the light of the previously unknown microscopic acid dissociation constants.

As part of the study of the application of CMR to the elucidation of the acid-base chemistry of polyprotic molecules, a linear parameterization scheme was developed to predict the carbon-13 chemical shifts of amines, carboxylic acids and amino acids in aqueous solution. The development of the scheme and the parameters obtained by the analysis of forty-five model compounds are presented and discussed in Chapter VI.

CHAPTER II

EXPERIMENTAL

A. Chemicals

i) Proton Magnetic Resonance Studies

L-lysine monohydrochloride (Eastman Organic Chemicals), L-ornithine monohydrochloride (Nutritional Biochemicals), α-glycyl-L-lysine monohydrochloride and L-lysylglycine monohydrochloride (Sigma Chemical Co.) were all used as received. The ethylenediaminemonoacetic acid (EDMA) was prepared by Dr. C.A. Evans using a literature method (46).

A stock solution of tetramethylammonium (TMA) nitrate was prepared by titrating a 25% aqueous solution of TMA-hydroxide (Eastman) with nitric acid to a neutral pH.

In the pmr titrations, the pH was adjusted with concentrated hydrochloric acid or potassium hydroxide pellets. Ionic strength adjustments were made using reagent grade potassium chloride.

ii) Carbon-13 Magnetic Resonance Studies

All chemicals were used as received from commercial sources. pH adjustments were made using concentrated HCl or KOH pellets.

iii) Potentiometric Studies

The lysine salt was used as received. The titrations were carried out using a carbonate-free potassium hydroxide stock solution prepared by the method described by Albert and Serjeant (47). The KOH solutions were standardized using dried potassium hydrogen phthalate (Matheson, Coleman, and Bell, alkimetric standard) as described by Vogel (48).

B. pH Measurements

The pH measurements were made using a digital pH meter (Orion Model 701 or 801, Fisher Model 502) equipped with either a standard glass electrode and a porous ceramic junction, saturated calomel electrode pair or a microcombination electrode. The pH meter was calibrated using Fisher standard solutions of pH 4.00, 7.00 and 10.00. All pH measurements were made at 25 ± 1°C.

C. NMR Measurements

i) ^{1}H NMR Measurements

Pmr spectra were obtained on Varian A60-D or HA-100-15 high resolution spectrometers at a probe temperature of 25 ± 1°C. Both spectrometers were equipped with Varian variable temperature control units and the temperature of the probe was monitored with a copper-constantan thermocouple.

Chemical shifts were measured relative to the central resonance of TMA and at a sweep rate of 0.1 Hz per second. The chemical shifts are reported relative to the methyl protons of DSS (sodium 2,2-dimethyl-2-silapentane-5-sulfonate), the conversion being made via Equation 25

$$\delta_{DSS} = \delta_{TMA} + 3.175 \qquad (25)$$

All chemical shifts are reported in units of parts per million (ppm), with positive shifts representing resonances which are downfield (less shielded) from the resonance of DSS. The chemical shifts are considered reproducible to within ± 0.1 Hz.

ii) Carbon-13 NMR Measurements

All CMR spectra were recorded on a Varian HA-100-15 NMR spectrometer operating at 25.1 MHz and equipped with a Digilab FTS/NMR-3 system. The Fourier transform mode was used with broadband proton decoupling. Each spectrum required 2K accumulations. The system was locked on the deuterium resonance of C_6D_6 in a concentric capillary in the 12 mm tube.

Chemical shifts were recorded relative to the carbon resonance of 1,4-dioxane, added as internal standard, and are reported relative to external TMS. The resonance of dioxane is 67.73 ppm downfield from TMS. Positive shifts correspond to less shielding than TMS.

The chemical shift measurements are considered accurate to ± 0.05 ppm.

D. Solution Preparation

i) PMR Studies

The appropriate amount of amino acid or peptide was dissolved in distilled water to give 100 ml of solution. Enough TMA-nitrate was added, prior to dilution, to make the final solution 0.01 M in TMA, which served as the internal chemical shift standard. Due to the lower concentration of EDMA studied (0.02 M), the concentration of TMA was reduced to 0.005 M.

The solutions of lysine and ornithine did not require any initial pH adjustment to obtain a solution of the fully diprotonated form. The lysylglycine solution was adjusted to pH 3.0 and the EDMA solution to pH 1.0 in order to obtain a sample of the diprotonated and fully protonated forms respectively. All four compounds were titrated with KOH pellets after the initial sample had been taken. The glycyllysine solution was adjusted to a pH of 12.9 in order to obtain a sample of the fully deprotonated form prior to titration with concentrated HCl. With the exception of EDMA, no inert salt was added to control the ionic strength. Potassium chloride was added to the EDMA solution to bring the initial ionic strength to 0.16 M.

All solutions were maintained at 25 ± 1°C with a water bath during the pH adjustments. Samples of about 0.5 ml were withdrawn at approximately 0.3 pH unit intervals during the course of the titration.

ii) CMR Studies

The titrations of lysine, ornithine, 2,4-diaminobutyric acid and 2,3-diaminopropionic acid were performed in essentially the same manner as described for the pmr solutions with the following modifications (a) 1,4-dioxane was used as the chemical shift standard and (b), the initial pH was reduced, prior to titration with base, to obtain a sample of the fully protonated form. All solutions were 0.185 M in α,ω-diaminocarboxylic acid.

For the model compound chemical shift studies, 25 to 50 ml of 0.3 M solution containing approximately 0.1 M dioxane were prepared. If the initial pH indicated the compound under study was basic, the pH was adjusted to above 13 with KOH pellets to obtain the fully deprotonated form. A sample was taken, and the pH was then reduced to a level, determined from literature pK_a values, where the molecule would be fully protonated. A second sample was then withdrawn from the solution. For acidic compounds, the fully protonated sample was obtained prior to increasing the pH to obtain the fully deprotonated sample. When the compound contained more than one type of functional group, the pH at which the intermediate form would predominate was calculated from literature pK_a values, when available, and a sample of the appropriate form obtained (an intermediate form has one type of functional group fully protonated and the other fully deprotonated).

All solutions were prepared at 25 ± 1°C. Approximately 2 ml of solution is required for each carbon-13 spectrum when 12 mm tubes are used.

iii) Potentiometric Titration Studies

The solutions used in the potentiometric titration studies of lysine were prepared with freshly boiled, double distilled water. All potentiometric determinations were carried out using 50 ml (pipette) of solution and were performed under a stream of nitrogen to reduce exposure to atmospheric carbon dioxide. For the series of titrations performed to determine the concentration dependence of the pK_a's of lysine, the pattern of change in the ionic strength of the pmr titration was duplicated by adding KCl both before and during the titration. This was necessary due to the wide variation in amino acid concentration. The titrations were carried out with carbonate-free potassium hydroxide at a concentration level at least ten times that of the lysine solution being titrated.

All titrations were performed at 25 ± 1°C.

E. Calculations

The overlapping macroscopic constants of lysine were calculated from potentiometric data using the correction term method of Irving and Rossotti (51). When $\bar{p}$ represents the average number of protonated groups per molecule, a plot of $\bar{p}$ vs pH for a diprotic acid will be symmetric about its midpoint. As a consequence, it can be shown that:

$$pK_1 = pH_{1+d} - y \tag{19}$$

$$pK_2 = pH_{1-d} + y \tag{20}$$

where d is greater than zero but less than 1 and y is defined by

$$y = \log\left(\frac{1-d}{d}\right) + \log\left\{1 - \frac{(1+d)[H^+]_{1-d}}{(1-d)[H^+]_{1+d}}\right\} \tag{21}$$

For the purpose of the calculation, the simultaneous deprotonations of the two ammonium groups of lysine may be treated as a diprotic acid.

The linear least squares programme for the determination of macroscopic and microscopic acid dissociation constants from fractional deprotonation data was written in WATFIV and run on the IBM 360/67 system at the University of Alberta computing centre.

The nonlinear curvefitting calculations were performed using an adapted form of 'KINET', a nonlinear regression programme developed by J.L. Dye and V.A. Nicely (52). The regression procedure used was the matrix technique described by Wentworth (53). The programme contains a weighting subroutine which utilizes estimates of the variances of the experimental data to calculate statistical weights for the variables. A plotting subroutine was used to compare the observed and calculated data.

In addition, KINET calculates a linear estimate of the standard deviation of each parameter and a multiple correlation coefficient. Due to the use of inexact values as constants in some of the calculations, the linear estimates of the standard deviations reflect the scatter in the data rather than the true uncertainty of the parameter estimate. The multiple correlation coefficient may vary from zero to one, values near unity indicating a high degree of correlation between the parameters.

The multiple linear regression performed to determine the carbon-13 chemical shift parameters utilized the programme *MULTREGR developed by the University of Alberta Computing Services (Public File Descriptions, Vol. II). The programme uses the abbreviated Doolittle method to compute the regression coefficients and utilizes a number of subroutines from *SSPLID (Scientific Subroutine Library).

F. Clarification of the Definition of Acid Dissociation Constant

Acid dissociation constants may be expressed as thermodynamic constants, mixed activity-concentration constants or concentration constants. To illustrate these three constants, consider the deprotonation of the acid, HA:

$$HA \rightleftarrows H^+ + A^- \tag{22}$$

The thermodynamic acid dissociation constant describing Equation 22 is defined as

$$K_a^T = \frac{(a_{H^+})(a_{A^-})}{(a_{HA})} = \frac{[H^+][A^-]}{[HA]} \cdot \frac{(\gamma_{H^+})(\gamma_{A^-})}{(\gamma_{HA})} \tag{23}$$

where K_a^T is the thermodynamic constant and is defined in terms of the activities, a_i, of the species in solution. The activity is related to concentration by the activity coefficient, γ_i.

When the two forms of the acid are expressed as concentrations, a mixed activity-concentration constant results.

$$K_a^M = \frac{(a_{H^+})[A^-]}{[HA]} \tag{24}$$

When the experimental determination is carried out under the conditions of dilute acid concentration and constant ionic strength, it is possible to obtain values of γ_{H^+} from the Davies (or some similar) equation (49,50). The hydrogen ion concentration can then be calculated, and the dissociation constant is reported as a concentration constant.

$$K_a{}^C = \frac{[H^+][A^-]}{[HA]} \qquad (25)$$

The concentrations of the acid and its conjugate base in Equations 24 and 25 are determined from the initial acid concentration.

Although the K_a values obtained using Equation 24 are dependent upon the experimental conditions, the calculation of mixed constants avoids the assumptions inherent in the activity-concentration interconversion and can be accurately performed under a wide range of experimental conditions. The acid dissociation constants reported in this thesis will be mixed activity-concentration constants. A factor which will facilitate the conversion to concentration constants will be given with the tabulated values of the acid dissociation constants.

In order to calculate the concentration constants, it is necessary to convert the pH meter readings to hydrogen ion concentrations. The meter readings are related to a_{H^+}, the hydrogen ion activity.

$$pH = -\log_{10}(a_{H^+}) \qquad (26)$$

The activity coefficient for the hydrogen ion was calculated from the Davies equation (49,50),

$$-\frac{\log \gamma^2}{Z_i} = \frac{0.511(\mu)^{½}}{1+1.5(\mu)^{½}} - 0.2\mu \qquad (27)$$

where γ represents the activity coefficient of an ion of charge Z_i and μ is the ionic strength. The ionic strength can be calculated from

$$\mu = ½\sum_i C_i Z_i^2 \qquad (28)$$

where C_i represents the concentration of ionic species i with charge Z_i. The concentrations of the various acid species present were calculated from the mixed activity-concentration constants, determined as described in Chapter III. The concentrations of the inert salts present were calculated from the amounts of acid, base, and salt added.

CHAPTER III

DEVELOPMENT OF METHODS FOR THE DETERMINATION OF MACROSCOPIC AND MICROSCOPIC ACID DISSOCIATION CONSTANTS BY NUCLEAR MAGNETIC RESONANCE SPECTROSCOPY

A. Introduction

The stepwise deprotonation of a diprotic acid can be described by the macroscopic sequence:

$$H_2A \overset{K_1}{\rightleftharpoons} HA \overset{K_2}{\rightleftharpoons} A \qquad (29)$$

Charges have been omitted for simplicity. At the molecular level, deprotonation proceeds by the two pathways shown in Scheme III.

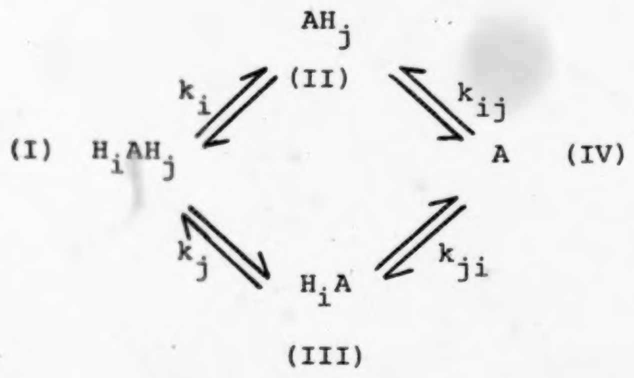

Scheme III

The macroscopic acid dissociation constants are represented by upper case K's and the subscripts 1 and 2 denote the macroscopic deprotonation step to which the constant refers. The lower case k's represent the microscopic acid dissociation constants. The acid dissociation step to which a given microconstant refers is given by the subscript, the last letter denoting the group undergoing deprotonation and any preceding letters indicating groups which have been previously titrated.

The macroscopic constants are defined in terms of the total concentration of monoprotonated acid present.

$$K_1 = \frac{a_{H^+}[HA]}{[H_2A]} \tag{30}$$

$$K_2 = \frac{a_{H^+}[A]}{[HA]} \tag{31}$$

The microscopic constants, however, are defined on the molecular level in terms of the two monoprotonated tautomers.

$$k_i = \frac{a_{H^+}[AH_j]}{H_iAH_j} \tag{32}$$

$$k_j = \frac{a_{H^+}[H_iA]}{[H_iAH_j]} \tag{33}$$

$$k_{ij} = \frac{a_{H^+}[A]}{[AH_j]} \tag{34}$$

$$k_{ji} = \frac{a_{H^+}[A]}{[H_iA]} \tag{35}$$

Since [HA] represents the total concentration of both monoprotonated tautomers, we may write:

$$[HA] = [AH_j] + [H_iA] \tag{36}$$

which, when substituted into Equations 30 and 31 leads to the following relationships between macroscopic and microscopic constants

$$K_1 = \frac{a_{H^+}([AH_j] + [H_iA])}{[H_iAH_j]} = k_i + k_j \tag{37}$$

$$K_2 = \frac{a_{H^+}[A]}{([H_iA] + [AH_j])} = \frac{k_{ij}k_{ji}}{(k_{ji} + k_{ij})} \tag{38}$$

$$K_1K_2 = k_ik_{ij} = k_jk_{ji} \tag{39}$$

For molecules in which the two functional groups are of widely differing acidities, only one of the two microscopic pathways will be of importance and the macroconstants are essentially equal to the microconstants which describe the major pathway. However, when simultaneous deprotonation of the two functional groups occurs, the macroscopic constants describe only the mean number of protons lost by the molecule.

From the preceding discussion, it can be seen that in order to determine microscopic acid dissociation constants, the acid-base equilibria must be followed on the molecular level. The remainder of this chapter will describe the development of methods for the determination of microscopic and macroscopic acid dissociation constants from nuclear magnetic resonance chemical shift data. The basis of the application of nmr to aqueous acid-base chemistry will be described, and the development of the calculation techniques will be presented. Several literature methods for the extraction of acid dissociation constants from chemical shift data will also be discussed.

B. The Nuclear Magnetic Resonance Technique for Studying Acid-Base Equilibria

In 1957, Grunwald, Lowenstein and Meiboom reported (27) that, in aqueous solutions of methylamine and methylamine hydrochloride, the chemical shift of the methyl protons is linearly related to the ratio of the concentration of methylamine hydrochloride to the total concentration of amine. As a result, they concluded that the exchange of acidic protons is rapid on the nmr time scale and that the observed chemical shift values are weighted averages of the limiting chemical shifts of the molecular forms present in solution. (A limiting shift will be defined as the observed value when only one molecular form is present in solution). The observed chemical shift is described by

$$\delta_{obs} = \sum_{i} \alpha_i \delta_i \qquad (40)$$

where δ_{obs} represents the observed chemical shift and α_i the fraction of all molecules in the form i with a limiting chemical shift δ_i. Depending upon the position of the nmr active nucleus relative to the functional groups in the molecule, a given resonance may reflect the deprotonation of one or both simultaneously deprotonating groups. If the resonance in question reflects the deprotonation of both groups, it will be termed a common resonance in this thesis, while those resonances which are affected by the degree of deprotonation of only one functional group will be referred to as unique resonances.

Fractional deprotonation data can be calculated directly from unique resonance data. Fractional deprotonation data can also be calculated from those common resonances for which the total change in chemical shift due to each deprotonating functional group can be determined. Microscopic and macroscopic acid dissociation constants can be calculated from fractional deprotonation data, but only macroscopic dissociation constants can be calculated from common resonance data for which the individual contributions of the two deprotonating groups to the total chemical shift change cannot be determined. As a consequence, different methods of calculation have been developed for the determination of acid dissociation constants from fractional deprotonation data and common resonance data.

C. The Calculation of Acid Dissociation Constants from Common Resonance Data

Equation 40 can be written in terms of the molecular forms in the microscopic scheme for the acid H_iAH_j

$$\delta_{obs} = \alpha_I\delta_I + \alpha_{II}\delta_{II} + \alpha_{III}\delta_{III} + \alpha_{IV}\delta_{IV} \qquad (41)$$

The subscripts refer to the molecular species as denoted in Scheme III. The fractions are defined in terms of the molecular species by the following expressions:

$$\alpha_I = [H_iAH_j]/C_T \qquad (42)$$

$$\alpha_{II} = [AH_j]/C_T \qquad (43)$$

$$\alpha_{III} = [H_iA]/C_T \qquad (44)$$

$$\alpha_{IV} = [A]/C_T \qquad (45)$$

where C_T represents the analytical concentration of acid.

$$C_T = [H_iAH_j] + [AH_j] + [H_iA] + [A] \qquad (46)$$

The fractions can also be written in terms of the microscopic acid dissociation constants by replacing the molecular forms with the expressions in Equations 32-35

$$\alpha_I = \frac{a_{H^+}^2}{a_{H^+}^2 + (k_i + k_j)a_{H^+} + k_i k_{ij}} \qquad (47)$$

$$\alpha_{II} = \frac{a_{H^+} k_i}{a_{H^+}^2 + (k_i + k_j)a_{H^+} + k_i k_{ij}} \qquad (48)$$

$$\alpha_{III} = \frac{a_{H^+} k_j}{a_{H^+}^2 + (k_i + k_j)a_{H^+} + k_i k_{ij}} \qquad (49)$$

$$\alpha_{IV} = \frac{k_i k_{ij}}{a_{H^+}^2 + (k_i + k_j)a_{H^+} + k_i k_{ij}} \qquad (50)$$

Substitution of Equations 47-50 into Equation 41 yields an expression for the chemical shift of a common resonance in terms of the microscopic acid dissociation constants and the limiting chemical shifts of the various molecular forms.

$$\delta_{obs} = \frac{a_{H^+}^2 \delta_I + a_{H^+} k_i \delta_{II} + a_{H^+} k_j \delta_{III} + k_i k_{ij} \delta_{IV}}{a_{H^+} + (k_i + k_j)a_{H^+} + k_i k_{ij}} \qquad (51)$$

If the limiting shifts of the four molecular forms can be determined, the microscopic acid dissociation constant can be evaluated from common resonance data by nonlinear least squares curvefitting to Equation 51. Since δ_I and δ_{IV} are the limiting chemical shifts of the fully protonated and fully deprotonated forms, respectively, δ_I and δ_{IV} values can generally be obtained from spectra at the low pH and high pH portions of the titration curve. However, δ_{II} and δ_{III} cannot be obtained directly from the experimental data. When the two acidic groups deprotonate simultaneously, there are no pH values at which a single monoprotonated species is the only molecular form present. When the chemical shift data is analyzed by nonlinear curvefitting to Equation 51, the values for $k_i\delta_{II}$, $k_j\delta_{III}$, k_ik_{ij} and $(k_i + k_j)$ will be strongly correlated. That is, errors in one parameter will be compensated for by errors in the other parameters. The net result will be a family of solutions, all of which will satisfy the regression criteria, but with no indication which, if any, of the solutions represents the actual values of the constants.

By replacing the microscopic constants with the appropriate macroscopic constants, we obtain

$$\delta_{obs} = \frac{a_{H^+}^2\delta_I + a_{H^+}K_1\delta_{HL} + K_1K_2\delta_{IV}}{a_{H^+}^2 + a_{H^+}K_1 + K_1K_2} \qquad (52)$$

where δ_{HL} is a chemical shift parameter related to the intermediate chemical shifts and the microscopic constants according to Equation 53

$$\delta_{HL} = \frac{k_i}{(k_i + k_j)}\delta_{II} + \frac{k_j}{(k_i + k_j)}\delta_{III} \qquad (53)$$

When related to the macroscopic acid dissociation scheme (Equation 29), δ_{HL} represents the chemical shift of the monoprotonated form, HA. Nonlinear regression analysis of the observed chemical shift data will yield estimates of K_1, K_2 and δ_{HL}. The nonlinear programme requires initial estimates of the parameters being determined. Approximate values can be obtained from a plot of $(\delta_{obs} - \delta_I)/(\delta_{IV} - \delta_I)$ vs pH. pK_1 and pK_2 can be approximated as equal to the pH at those pH values where this chemical shift ratio equals 0.25 and 0.75, respectively, and δ_{HL} as δ_{obs} when the ratio equals 0.5. If the chemical shift vs pH curve contains an inflection point, and is asymmetric about this point, better approximations can be obtained as follows:

(a) $\delta_{HL} \approx \delta_{obs}$ at the point of inflection

(b) $pK_1 \approx$ pH when $\dfrac{\delta_{obs} - \delta_I}{\delta_{HL} - \delta_I} = 0.5$

(c) $pK_2 \approx$ pH when $\dfrac{\delta_{obs} - \delta_{HL}}{\delta_{IV} - \delta_{HL}} = 0.5$

Although the estimates so obtained may be quite crude, they will generally be sufficient for rapid convergence of the nonlinear regression programme.

D. The Calculation of Acid Dissociation Constants from Fractional Deprotonation Data

i) Solitary Deprotonations

For monoprotic acids and for polyprotic acids with no overlapping dissociations, any resonance observed is, by definition, a unique resonance. Unique resonances which reflect a solitary deprotonation are also observed when one functional group of a polyprotic acid differs greatly, in acidity, from the other functional groups in the molecule. An example is the methylene resonance of the acetic acid group of EDMA when it reflects the deprotonation of the carboxylic acid group.

In these instances, the observed chemical shift is the weighted average of the chemical shifts of the protonated and deprotonated forms. That is,

$$\delta_{obs} = \alpha_p\delta_p + \alpha_d\delta_d \tag{54}$$

where the subscripts p and d refer to the protonated and deprotonated forms respectively. Since only two forms are present, $\alpha_p + \alpha_d = 1$, which when combined with Equation 54 gives the fraction deprotonated in terms of the observed shift.

$$\alpha_d = \frac{\delta_{obs} - \delta_p}{\delta_d - \delta_p} \tag{55}$$

The acid dissociation constant can be defined in terms of fractional deprotonation data by dividing the numerator and denominator of Equation 30 by the total concentration of acid present.

$$K_a = \frac{a_{H^+} \cdot \alpha_d}{\alpha_p} = \frac{a_{H^+} \cdot \alpha_d}{1 - \alpha_d} \tag{56}$$

Utilizing the relationship in Equations 55 and 56, the acid dissociation constant can be expressed in terms of chemical shift values.

$$K_a = a_{H^+} \cdot \frac{(\delta_{obs} - \delta_p)}{(\delta_d - \delta_{obs})} \tag{57}$$

When both limiting shifts can be obtained directly from the experimental data, a value of K_a can be calculated at each data point for which δ_{obs} falls between the values of δ_p and δ_d. However, for very strongly acidic (or basic) functional groups, one of the limiting shifts may be unobtainable since the functional group being monitored remains partially deprotonated (or protonated) beyond the experimental pH range for which a_{H^+} can be accurately determined. Alternatively, spectral overlap, due to other nmr active nuclei in the molecule, may hide one of the limiting shift values. In either case, Equation 57 can be used in the appropriate linear form to simultaneously obtain both K_a and the limiting chemical shift which cannot be directly measured.

$$\delta_{obs} = \delta_p + \left\{ \frac{(\delta_d - \delta_{obs})}{a_{H^+}} \right\} K_a \qquad (58)$$

$$\delta_{obs} = \delta_d + (\delta_p - \delta_{obs}) a_{H^+} \cdot \frac{1}{K_a} \qquad (59)$$

For example, a plot of δ_{obs} vs $\left(\frac{\delta_d - \delta_{obs}}{a_{H^+}} \right)$ will yield δ_p as the intercept and the acid dissociation constant as the slope. In practice, both of the preceding expressions, 58 and 59, deviate from linearity as the observed shift approaches the known limiting shift. Consequently, if the unknown parameters are to be obtained by a computer-performed least squares analysis of the chemical shift data, it is advisable to plot the expression to determine the point at which the deviation from linearity becomes significant. The data beyond this point can then be excluded from the computer calculations. Bradbury and Brown (54) have used Equation 59 for the determination of the macroscopic constants of lysine. Their results will be discussed in Chapter IV.

When a large, high speed, digital computer is available, nonlinear regression techniques can be used to extract acid dissociation constants from unique resonance data. The chemical shift-pH data can be analyzed by non-linear regression using Equation 60

$$\delta_{obs} = \frac{K_a\delta_d + a_H\delta_p}{a_H + K_a} \qquad (60)$$

This method can be used to determine the acid dissociation constant alone or in combination with either or both of the limiting chemical shifts. However, when the limiting shifts are not available, corroborating calculations are advisable since the fraction of the total chemical shift range which is observable will affect the values obtained. The application of Equation 60 is illustrated in Chapter IV.

ii) Simultaneous Deprotonations

When the system under study is a polyprotic acid containing two functional groups which undergo simultaneous deprotonation, it is necessary to express the fractional deprotonation data in terms of the molecular forms of an individual group. From Scheme III, the fraction of group i which is protonated, $f_{i,p}$, and the fraction which is deprotonated, $f_{i,d}$, can be defined by:

$$f_{i,d} = \frac{[H_iAH_j] + [H_iA]}{[H_iAH_j] + [H_iA] + [AH_j] + [A]} = \alpha_I + \alpha_{III} \qquad (61)$$

$$f_{2,d} = \frac{[AH_j] + [A]}{[H_iAH_j] + [H_iA] + [AH_j] + [A]} = \alpha_{II} + \alpha_{IV} \qquad (62)$$

The equivalent expressions for group j are:

$$f_{j,p} = \frac{[H_iAH_j] + [AH_j]}{[H_iAH_j] + [H_iA] + [AH_j] + [A]} = \alpha_{I} + \alpha_{II} \qquad (63)$$

$$f_{i,d} = \frac{[H_iA] + [A]}{[H_iAH_j] + [H_iA] + [AH_j] + [A]} = \alpha_{III} + \alpha_{IV} \qquad (64)$$

If $\delta_{i,obs}$ is a unique resonance which reflects only the degree of protonation of group i, the observed chemical shift can be expressed in terms of $f_{i,p}$ and $f_{i,d}$.

$$\delta_{i,obs} = f_{i,p}\delta_{i,p} + f_{i,d}\delta_{i,d} \qquad (65)$$

where $\delta_{i,p}$ is the chemical shift when group i is protonated and $\delta_{i,d}$ the chemical shift when group i is deprotonated. Referring to Scheme III, we can write:

$$\delta_{i,p} = \delta_{i,I} = \delta_{i,III} \qquad (66)$$

$$\delta_{i,d} = \delta_{i,IV} = \delta_{i,II} \qquad (67)$$

Thus, the fraction of all molecules with acidic group i protonated and deprotonated can be calculated from

$\delta_{i,obs}$ using

$$f_{i,p} = \frac{\delta_{i,obs} - \delta_{i,IV}}{\delta_{i,I} - \delta_{i,IV}} \qquad (68)$$

$$f_{i,d} = \frac{\delta_{i,obs} - \delta_{i,I}}{\delta_{i,IV} - \delta_{i,I}} \qquad (69)$$

$\delta_{i,I}$ and $\delta_{i,IV}$ can generally be obtained from the experimental data as described in Section C.

If the observed chemical shift changes in $\delta_{i,obs}$ reflect the deprotonation of both functional groups, the observed chemical shift is described by

$$\delta_{i,obs} = f_{i,p}\delta_{i,p} + f_{i,d}\delta_{i,d} + f_{j,d}\Delta_{i,j} \qquad (70)$$

where $\Delta_{i,j}$ represents the total change in chemical shift of $\delta_{i,obs}$ due to the complete deprotonation of group j. The expression for the degree of deprotonation becomes:

$$f_{i,d} = \frac{\delta_{obs} - (\delta_{i,p} + f_{j,d}\Delta_{i,j})}{\delta_{i,d} - (\delta_{i,p} + \Delta_{i,j})} \qquad (71)$$

It should be noted that $\delta_{i,d}$ is the observed shift of the totally deprotonated form.

The concentrations of the microscopic forms in Equations 62 and 64 can be replaced by the appropriate microscopic acid dissociation constant expressions (see Equations 32-35) to yield $f_{i,d}$ and $f_{j,d}$ in terms of the microconstants.

$$f_{i,d} = \frac{a_{H^+}k_i + k_ik_{ij}}{a_{H^+}^2 + a_{H^+}(k_i + k_j) + k_ik_{ij}} \qquad (72)$$

$$f_{j,d} = \frac{a_{H^+}k_j + k_jk_{ji}}{a_{H^+}^2 + a_{H^+}(k_i + k_j) + k_jk_{ji}} \qquad (73)$$

The microscopic acid dissociation constants can be determined using Equation 72 or 73 by nonlinear regression analysis of fractional deprotonation data. The application of these equations to fractional deprotonation data will be discussed in Chapter IV.

The correlation of the errors associated with the estimates of the constants determined by using Equation 72 or 73 increases as the ratio k_i/k_j increases above 5 or decreases below 0.2. However, by recalling the expressions relating to the microscopic and macroscopic constants (Equations 37-39), the microconstants in the denominator of Equations 72 and 73 can be replaced by macroconstants. For Equation 72 we obtain

$$f_{i,d} = \frac{a_{H^+}k_i + k_ik_{ij}}{a_{H^+}^2 + a_{H^+}K_1 + K_1K_2} \qquad (74)$$

If the values for K_1 and K_2 are known, nonlinear regression analysis of the $f_{i,d}$ data according to Equation 74 will yield estimates of k_i and k_{ij}. k_j can then be calculated from $k_j = K_1 - k_i$ and k_{ji} from $k_{ji} = k_i k_{ij}/k_j$ as well as from the analysis of $f_{j,d}$ data. The use of predetermined values for the macroscopic constants is not a limitation since the macroscopic constants can be calculated from either a common resonance as described previously, or a combined $f_{i,d} - f_{j,d}$ data set as described below. The nmr spectra of most compounds will contain the necessary resonances. The initial estimates of the microscopic constants can be obtained from plots of pM_i vs $f_{i,d}$ where

$$pM_i = \frac{a_H + f_{i,d}}{1 - f_{i,d}} \qquad (75)$$

The application of nonlinear regression analysis using Equation 74 is illustrated for a number of compounds in Chapters IV and V.

When both $f_{i,d}$ and $f_{j,d}$ can be determined from the chemical shift data of the molecule under study, it is possible to calculate the macroscopic as well as the microscopic constants from the fractional deprotonation data. The average number of protons lost by a molecule of a dibasic acid, at a given pH, may be represented by $\bar{h}$, where

$$\begin{aligned} \bar{h} &= ([H_iA] + [AH_j] + 2[A])/C_T \\ &= \alpha_{II} + \alpha_{III} + 2\alpha_{IV} \qquad (76) \end{aligned}$$

The α values have been previously defined (Equations 42-45). By recalling the definitions of $f_{i,d}$ and $f_{j,d}$ given as Equations 62 and 63 we can see that, at any given pH

$$\bar{h} = \alpha_{II} + \alpha_{III} + 2\alpha_{IV} = f_{i,d} + f_{j,d} \qquad (77)$$

As a result, $\bar{h}$ can be determined directly from the fractional deprotonation data of two resonances. The expression for $\bar{h}$ can be rewritten in terms of the macroscopic acid dissociation constants to give

$$\bar{h} = \frac{K_1 a_{H^+} + 2K_1K_2}{a_{H^+}^2 + K_1 a_{H^+} + K_1K_2} \qquad (78)$$

Equation 78 can be used to analyze the $\bar{h}$ data by non-linear regression techniques to determine overlapping macroscopic acid dissociation constants. The initial estimates of the macroscopic constants required by the curvefitting programme, can be obtained from a plot of $\bar{h}$ vs pH. That is $pK_1 \approx$ pH when $\bar{h} = 0.5$ and $pK_2 \approx$ pH when $\bar{h} = 1.5$. The results obtained with chemical shift vs pH data from a variety of molecules are presented in Chapters IV and V. The values of K_1 and K_2 obtained from the analysis of $\bar{h}$ data can be used in Equation 74 to obtain estimates of microscopic acid dissociation constants. Equation 78 has also been applied to the analysis of potentiometric data (55).

7

Since most nonlinear regression programmes require a large digital computer for their execution, a method for the determination of macroscopic and microscopic constants by the linear least squares analysis of fractional deprotonation data has been developed.

The macroscopic constants can be defined in terms of the molecular fractions, as was illustrated by Equations 37 and 38. By combining these two equations, the definition of $\bar{h}$, and the mass balance of all forms of the acid, it can be shown that

$$\frac{a_{H^+} \cdot \bar{h}}{(1-\bar{h})} = \left\{ \frac{(2-\bar{h})}{a_{H^+}(1-\bar{h})} \right\} K_1 K_2 + K_1 \qquad (79)$$

This expression is of the form $y = mx + b$ and can be treated by standard least squares and/or graphical techniques to obtain values of K_1 and K_2 from $\bar{h}$ vs a_{H^+} data. Data points in the proximity of $\bar{h} = 1$ must be avoided in the least squares approach (51).

The value of K_2 obtained using Equation 79 can be used to determine the individual molecular fractions from the fractional deprotonation data. Combining the expressions relating the macroscopic constants and the molecular fractions with the definition of $\bar{h}$ (Equation 77) leads to:

$$\alpha_{IV} = (f_{i,d} + f_{j,d}) \left\{ \frac{K_2}{a_{H^+} + 2K_2} \right\} \qquad (80)$$

Values of α_{IV} so obtained can be substituted into expressions for $f_{i,d}$ and $f_{j,d}$ (Equations 62 and 64) to obtain α_{II} and α_{III}. Since the sum of all four molecular forms is unity at all pH's, the value of α_I is readily obtained. The calculation of the microscopic constants from the appropriate molecular forms (see Equations 32-35) is straightforward. The precision of the values so obtained is best in the range $(0.25 < f_{i,d}; f_{j,d} < 0.75)$. This method has been used to evaluate the microscopic constants of several molecules and the results are presented and discussed in Chapters IV and V.

E. Discussion

Of the methods just described for the determination of macroscopic acid dissociation constants, it has been found that nonlinear regression analysis using either Equations 52 or 78 will yield precise values which are in good agreement with potentiometric results. Having obtained estimates of the macroscopic constants, fractional deprotonation data may be treated, using Equation 74, in a similar manner to obtain microscopic acid dissociation constants. This approach will be illustrated with a number of compounds in Chapters IV and V. The remainder of this chapter will be devoted to a discussion of some of the methods for the determination of acid dissociation constants, from chemical shift data, which have appeared in the literature.

Cohen and coworkers (36,44) have described a curve-fitting method for determining macroscopic constants from chemical shift titration curves which is based on a composite Henderson-Hasselbach equation. These authors have applied this method to the determination of the macroscopic constants of histidine and related compounds from pmr and cmr data. Their model equation is of the form:

$$\delta_{obs} = \delta_{min} + \Sigma(\Delta_i 10^{pH-pK_i})/(1 + 10^{pH-pK_i}) \quad (81)$$

where δ_{min} is the chemical shift of the fully protonated form and pK_i and Δ_i are the acid dissociation constant and the total change in the chemical shift for the ith proton transition. The chemical shift titration curves are computer fitted to obtain both pK_i and Δ_i for each deprotonation. For a diprotic acid, when i = 1 the expression $(10^{pH-pK_i})/(1 + 10^{pH-pK_i})$ assumes the fraction of the acid in the monoprotonated form to be $[HA]/(H_2A] + [HA])$. If overlapping dissociations occur, the fraction of the acid in the monoprotonated form is $[HA]/([H_2A] + [HA] + [A])$, and macroscopic constants determined by Equation 81 will be in error. For consecutive macroscopic constants which vary by more than 3 pK units, $(10^{pH-pK_i})/(1 + 10^{pH-pK_i})$ will represent the fraction from which the ith proton has been removed to within 1 ppt. However, as the separation between pK_i and pK_{i+1} decreases, the errors in the fractional concentrations of the various protonated forms will increase. Figure 1 illustrates the errors in fractional concentrations, as defined by Cohen et al for the first and second proton transitions of a diprotic acid, as a function of pH for different values of the ratio K_1/K_2.

Recalling Equation 51, one can see that intermediate chemical shift values are required in order to calculate microscopic constants from common resonance chemical shift data. The technique of approximating intermediate chemical shifts with the limiting chemical shifts of model compounds has been utilized by a number of authors (28-31,33). For example, Rigler et al (29) and Kesselring and Benet (30) used a chemical shift of tetracycline methiodide to correct for common resonance effects in tetracycline and isochlorotetracycline respectively. The correction applied was small enough that its effect on the results may be considered marginal, particularly when compared to the errors introduced by the assumptions and interpolations involved in the method of calculation (30).

Martin (16) has pointed out, when discussing the ionization of citric acid as determined by nmr (28), that small errors in the values chosen as the intermediate chemical shifts may lead to large errors in the calculated microscopic dissociation constants. This point can be

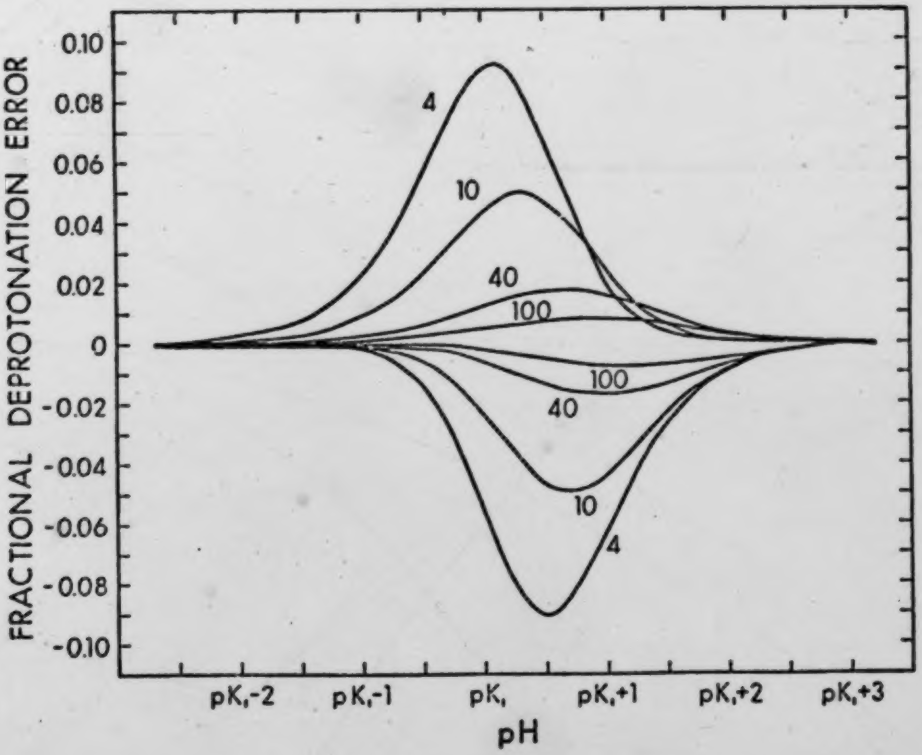

Figure 1. Fractional deprotonation errors inherent in the model used for a diprotic acid in Equation 81 (36,44).

applied to most attempts to combine model compound data with common resonance chemical shift data in order to determine microscopic acid dissociation constants. In general, the success of this technique is limited to systems in which the applied correction is quite small.

Due to the interest in determining the macroscopic acid dissociation constants of cysteine (5-8,13,18,20,22, 23,26) the recent attempt by Walters and Leyden (31) to determine the relative acidities of the sulfhydryl and ammonium groups in cysteine deserves comment. These authors obtained the chemical shift titration curves for the carbon bonded protons of L-cysteine, S-methylcysteine and L-cysteine methyl ester. The change in the chemical shift of cysteine, due to the addition of acid to the completely deprotonated form, was expressed by

$$\Delta\delta = \Sigma f_i \Delta_i \qquad (82)$$

where f_i represents the average fraction of the ith site which is protonated and Δ_i the appropriate protonation shift constant. A protonation shift constant was defined as the net effect of the protonation of a particualr functional group on the observed chemical shifts of the -CH- and -CH_2- proton resonances.

The protonation shift constant of the sulfhydryl group, Δ_{SH}, for the methine proton of cysteine was calculated by subtracting the total change in the observed chemical shift of the CH resonance of S-methylcysteine from the net change observed for the equivalent resonance of cysteine. Similarly, the constant for the carboxyl group was calculated from the data for cysteine and the methyl ester. Δ_{SH} and Δ_{CO_2H} were then subtracted from the total observed change in the chemical shifts of cysteine to obtain the protonation constant of the amino group. Similar values were obtained for the methylene resonance to give a second equation of the form of Equation 82. A third relationship defined the normalization of the fractional values according to

$$n = \Sigma f_i \tag{83}$$

where n is the number of equivalents of acid added per equivalent of amino acid. The estimates of f_i at various values of n were obtained by minimizing $(\Delta\delta - \Sigma(f_i\Delta_i))^2$ for both resonances (31).

Careful examination of this approach raises several questions regarding its application to cysteine. The methylene protons of cysteine are magnetically nonequivalent at higher pH's; the observed resonance patterns undergoing a rapid transition from A_2X to ABC at pH 8.0. Since the CH_2 group of S-methylcysteine does not exhibit similar effects in its pmr spectra, the assumption that the chemical shift parameters of the methylene resonance of S-methylcysteine can be used as approximations for the parameters of cysteine is tenuous. Since, for deprotonated L-cysteine, the trans rotamer is preferred relative to the two gauche configurations (31), the observed chemical shift of the methylene resonance will be an unequally weighted average of the chemical shifts of the three rotameric configurations. Consequently, the protonation shift constants for the $-CH_2-$ resonance of cysteine can only be calculated when the populations and chemical shifts of the three configurations can be taken into account.

Due to the definite separation of the carboxyl deprotonation from the pH range over which the sulfhydryl and ammonium deprotonations occur, the use of the cysteine methyl ester data is unnecessary and can be seen to introduce error into the calculation of the protonation shift constants. Using the spectral parameters for 0.5 M cysteine and S-methylcysteine given in Table II of reference (31), the protonation shift constants were calculated and are presented in Table 2. The constant for the carboxyl deprotonation is calculated solely from the cysteine data below pH 5.0. Difficulty in obtaining the limiting chemical shift of the fully protonated form of cysteine will not affect the calculation of the fractions of the monoprotonated forms.

The change in the observed chemical shift of the methine proton, $\Delta\delta^{CH}$, upon protonation of the S^- and NH_2

TABLE 2

Spectral Data and Protonation Shift Constants for L-Cysteine and S-Methylcysteine[a]

Spectral Data

n[b]	$\Delta\delta_A$[c,d]	$\Delta\delta_B$[c,e]	$\Delta\delta_{CH}$[c]	Compound
1	.307	.018	.473	Cysteine
2	.292	.190	.408	
3	.100	.100	.417	
	$\Delta\delta_{CH_2}$			
1	.262		.520	S-Methylcysteine
2	.172		.462	

Protonation Shift Constants[c] for CH Protons of Cys

Δ_{SH}	.36	(.32)[f]
$\Delta_{NH_3^+}$	.52	(.53)[f]
Δ_{CO_2H}	.42	(.45)[f]

a) Data from Reference 31, Table II.
b) Number of equivalents of acid added to completely deprotonated form.
c) Units of ppm.
d) Upfield resonance of CH_2.
e) Downfield resonance of CH_2.
f) From Table IV, Reference 31.

groups can be described by

$$\Delta\delta^{CH} = f_{SH}\Delta_{SH} + f_{NH_3^+}\Delta_{NH_3^+} \qquad (84)$$

where f_{SH} and $f_{NH_3^+}$ are the fractions of the sulfhydryl and amino groups which are protonated. When the average number of functional groups protonated, per molecule, is unity $f_{SH} + f_{NH_3^+} = 1$. Combining this expression with Equation 84 yields

$$f_{NH_3^+} = \frac{\Delta\delta^{CH} - \Delta_{SH}}{\Delta_{NH_3^+} - \Delta_{SH}} \qquad (85)$$

By utilizing the data in Table II of reference 31 and Table 2 of this thesis, $f_{NH_3^+}$ can be estimated to be 0.704 and f_{SH} to 0.296, when one equivalent of acid has been added. The ratio, R, of protonated amino groups to protonated sulfhydryl groups is thus 2.4. This value varies considerably from the estimate of R = 0.60 calculated by Walters and Leyden but is in good agreement with the results of a number of other studies (20,22,26). The difference in the two estimates of R arises primarily from the inclusion of the methylene resonance data in the calculation by Walters and Leyden.

CHAPTER IV

APPLICATION OF METHODS FOR THE DETERMINATION OF ACID DISSOCIATION CONSTANTS BY NUCLEAR MAGNETIC RESONANCE SPECTROSCOPY

A. Introduction

In this chapter, the methods developed in Chapter III are applied to the determination of the microscopic and macroscopic acid dissociation constants of ethylenediaminomonoacetic acid (EDMA) and lysine (2,6-diaminehexanoic acid) from nmr chemical shift vs pH data. Both molecules contain simultaneously deprotonating ammonium groups and cannot be studied by the other spectroscopic techniques described in Chapter I.

Literature methods for the determination of acid dissociation constants also will be used to analyze the fractional deprotonation data of EDMA and lysine. Since the acidity ratio, for the two ammonium groups, is about 2 in EDMA and 8 in lysine, analysis of the fractional deprotonation data of these compounds will provide an indication of the reliable range of application of the method used. The constants obtained by the literature methods will be compared to the values derived using the methods developed in Chapter III.

B. Ethylenediaminemonoacetic Acid

i) NMR Spectra

The chemical shifts of the carbon bonded protons of EDMA are shown as a function of pH in Figure 2. The resonance due to the methylene protons of the acetic acid

$$H_3{}^+NCH_2CH_2N^+H_2CH_2CO_2H$$

group is a singlet over the entire pH range shown whereas the resonance pattern due to the ethylene protons varies from a singlet at low pH to an AA'BB' multiplet in basic solution. The chemical shift of the centre of the multiplet is plotted in Figure 2. The change in the chemical shift of the methylene resonance between pH's 1 and 4 is due to the deprotonation of the carboxylic acid group and between pH's 4 and 12 to the deprotonation of the secondary ammonium group. The chemical shift data for the methylene resonance between pH's 1 and 4 is presented in Table 3. It has been assumed that deprotonation of the primary amino group does not alter, to a significant degree, the chemical shift of the methylene resonance due to the rapid attenuation of the effects of deprotonation as the number of bonds between the site of deprotonation and the observed carbon-bonded protons increases (32,35). The changes in the chemical shift of the ethylene resonance reflect the deprotonation of both amino groups. Consequently, the methylene and ethylene resonances provide three

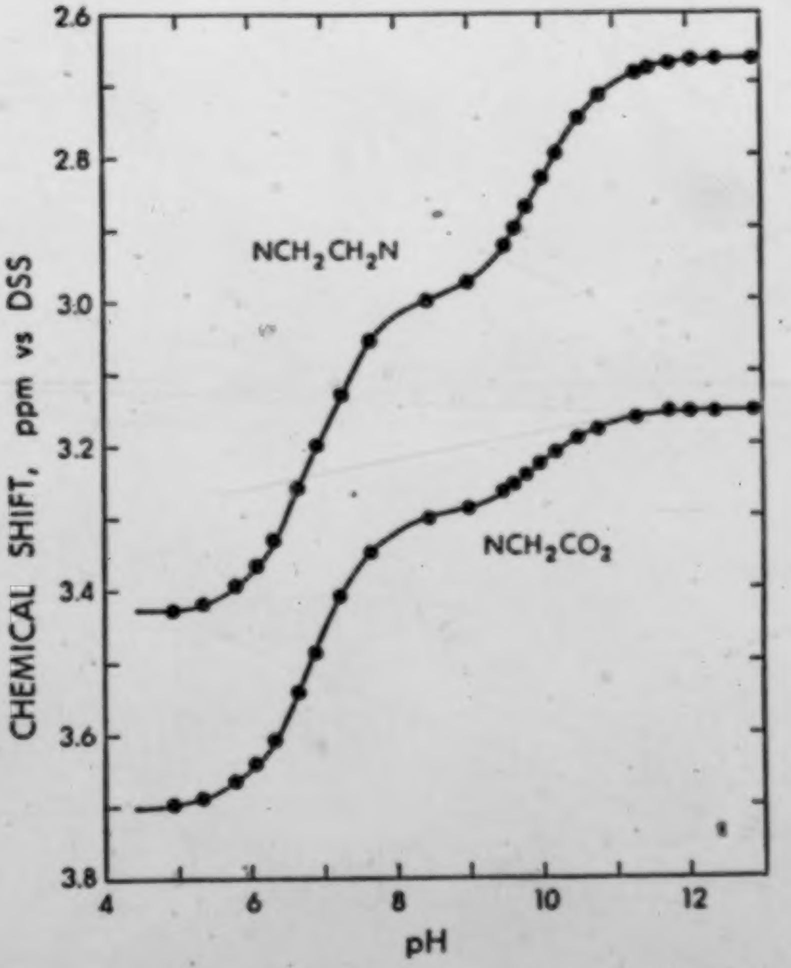

Figure 2. pH dependence of the chemical shifts of the carbon-bonded protons of ethylenediaminemonoacetic acid in a 0.02 M aqueous solution.

TABLE 3

Proton Chemical Shift Titration Data for the Acetic Acid Protons of EDMA Below pH 4.0

pH	Chemical Shift[a]
0.98	4.029
1.25	3.998
1.55	3.948
1.80	3.897
2.02	3.885
2.34	3.798
2.61	3.759
2.98	3.731
3.52	3.711

a) in ppm vs DSS.

types of nmr chemical shift data: the methylene resonance, up to pH 4, reflects the deprotonation of a solitary functional group; above pH 4 the methylene resonance is a unique resonance reflecting the deprotonation of one of two simultaneously deprotonating groups; and the ethylene resonance, above pH 4, is a common resonance affected by the two simultaneous deprotonations of the ammonium groups. As has been seen in Chapter III, the fractional deprotonation data obtained from the methylene resonance and the common resonance data obtained from the ethylene resonance are analyzed by different methods.

ii) Determination of Acid Dissociation Constants

a) Macroscopic Acid Dissociation Constants

K_1 of EDMA was determined by performing a nonlinear curvefitting of the data in Table 3 using Equation 86, which is the appropriate form of Equation 44

$$\delta_{obs,CH_2} = \frac{K_1\delta_d + a_{H^+}\delta_p}{a_{H^+} + K_1} \qquad (86)$$

As the chemical shift of the fully protonated form of EDMA was not obtained, and since the limiting chemical shift value at about pH 4.0 is not precisely defined, both limiting shifts were treated as unknowns. Using the curvefitting programme KINET (52), pK_1 was determined to be 1.77 ± .01 and the limiting chemical shifts were estimated to be 4.075 ppm for the fully protonated form and 3.709 ppm for the diprotonated form.

The macroscopic constants, K_2 and K_3, of the simultaneously deprotonating amino groups of EDMA were determined from the chemical shift titration data of the ethylene protons. Nonlinear curvefitting using Equation 87 yielded the macroconstants given in Table 4. The values for

$$\delta_{obs} = \frac{a_{H^+}^2\delta_I + a_{H^+}K_2\delta_{HL} + K_2K_3\delta_{IV}}{a_{H^+}^2 + a_{H^+}K_2 + K_2K_3} \qquad (87)$$

δ_I and δ_{IV} were obtained from Figure 2. The predicted value for δ_{HL} is 3.002 ppm (vs DSS). Initial estimates for K_2, K_3 and δ_{HL} were obtained from the chemical shift-pH data as described in Chapter III.

b) Microscopic Acid Dissociation Constants

The microscopic acid dissociation constants of EDMA were determined by nonlinear curvefitting of fractional deprotonation data using Equation 88:

$$f_{2,d} = \frac{a_{H^+}k_{12} + k_{12}k_{123}}{a_{H^+}^2 + K_2a_{H^+} + K_2K_3} \qquad (88)$$

The results are presented in Table 4. The $f_{2,d}$ values were calculated from the methylene resonance titration data using Equation 71. $\Delta_{i,j}$ was assumed to be zero. The values of K_2 and K_3 obtained from the ethylene resonance

TABLE 4

Macroscopic and Microscopic Acid Dissociation Constants of EDMA[a,b]

Constant	Value	Method of Calculation
pK_1[c]	1.77 ± .01[d]	Equation 60[e]
pK_2	6.88 ± .01	Equation 52[e]
pK_3	10.81 ± .01	Equation 52[e]
pk_{12}[i]	6.94 ± .01	Equation 74[f]
pk_{13}	7.39 ± .01	g
pk_{123}	9.85 ± .01	Equation 74[f]
pk_{132}	9.40 ± .02	h

a) Mixed-activity concentration constants. To convert to concentration constants subtract .09.
b) 0.02 M EDMA, μ = 0.12-0.16 M.
c) $pK_a = -\log K_a$.
d) Deviations are linear estimates of the standard deviation as calculated by KINET.
e) Nonlinear curvefitting of chemical shift data.
f) Nonlinear curvefitting of fractional deprotonation data.
g) $k_{13} = K_2 - k_{12}$.
h) $k_{132}^{-1} = K_3^{-1} - k_{123}^{-1}$.
i) The subscripts denote the functional groups undergoing deprotonation, as previously described. The carboxylic acid group, the secondary amino group and the primary amino group are denoted as 1, 2, and 3 respectively.

data were supplied as constants. The microscopic acid dissociation scheme for EDMA is illustrated in Figure 3.

C. Lysine

i) NMR Spectra

Lysine is an α,ω-diaminocarboxylic acid with three titratable protons. As can be seen from the acid dissociation scheme in Figure 4, the deprotonation of the carboxylic acid group occurs separately, at low pH, whereas the two amino groups undergo simultaneous deprotonation in the pH range 7.5 to 12.5. The pmr spectrum obtained for 0.5 M lysine HCl at approximately neutral pH is shown in Figure 5. The triplet centered at about 4.25 ppm is due to the methine proton and the triplet at approximately 3.75 ppm is assigned to the ε-methylene protons. The resonance pattern at 3.60 ppm is due to the methyl protons of TMA.NO_3 which was added as an internal chemical shift standard. The multiplet pattern over 2.00 to 2.75 ppm is the methylene envelope for the other methylene protons.

The chemical shift titration data of the methine and ε-methylene resonances is presented in Figure 6. The chemical shift changes of the methine resonance, above pH 6.0, are almost entirely due to the deprotonation of the α-ammonium group whereas the changes observed in the chemical shift of the ε-methylene are almost entirely due

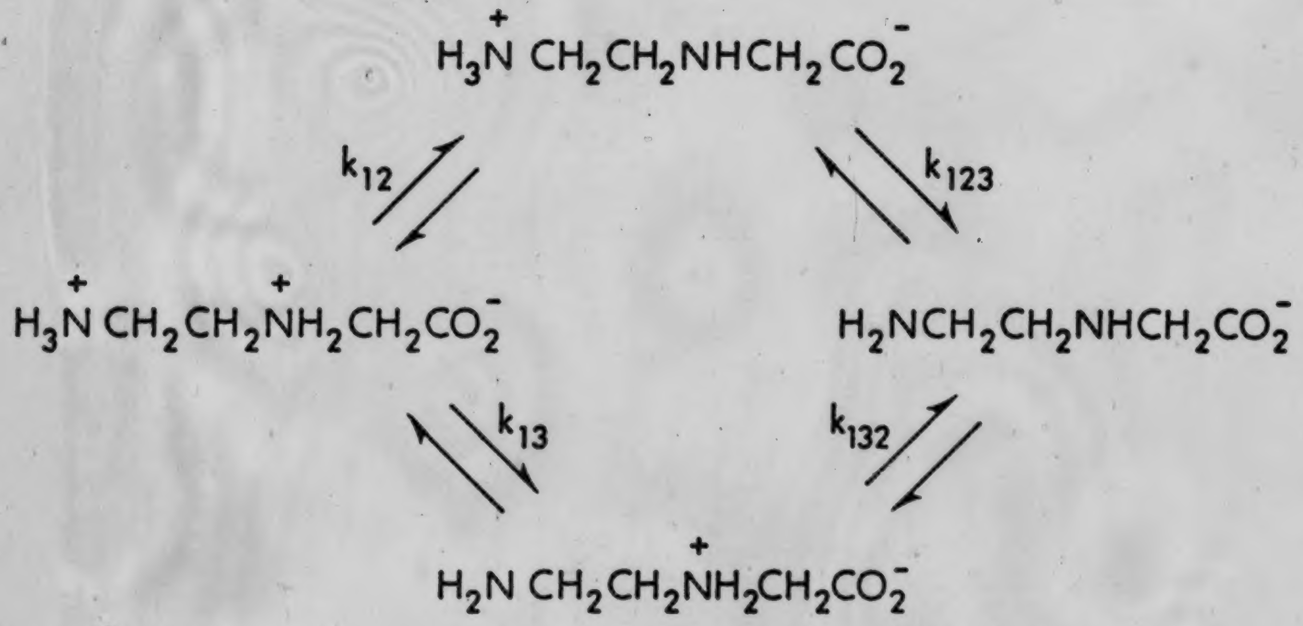
$H_3\overset{+}{N}CH_2CH_2NHCH_2CO_2^-$
k_{12}
k_{123}
$H_3\overset{+}{N}CH_2CH_2\overset{+}{N}H_2CH_2CO_2^-$
$H_2NCH_2CH_2NHCH_2CO_2^-$
k_{13}
k_{132}
$H_2NCH_2CH_2\overset{+}{N}H_2CH_2CO_2^-$

Figure 3. Microscopic acid dissociation scheme for the ammonium groups of ethylenediaminemonoacetic acid.

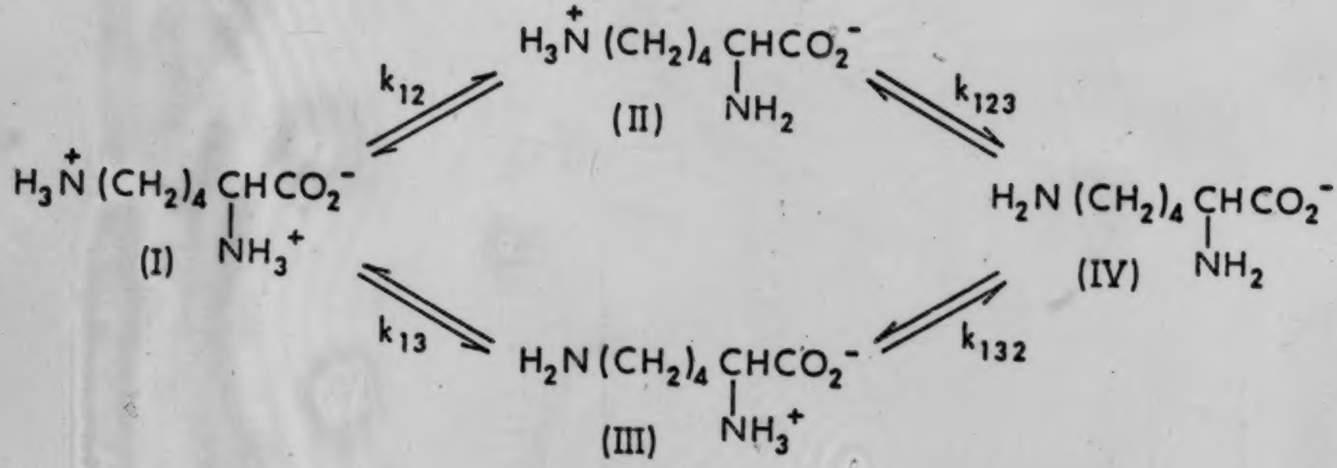
$H_3\overset{+}{N}(CH_2)_4CHCO_2^-$
(I)
NH_3^+
k_{12}
$H_3\overset{+}{N}(CH_2)_4CHCO_2^-$
(II)
NH_2
k_{123}
k_{13}
$H_2N(CH_2)_4CHCO_2^-$
(III)
NH_3^+
k_{132}
$H_2N(CH_2)_4CHCO_2^-$
(IV)
NH_2

Figure 4. Microscopic acid dissociation scheme for the ammonium groups of lysine.

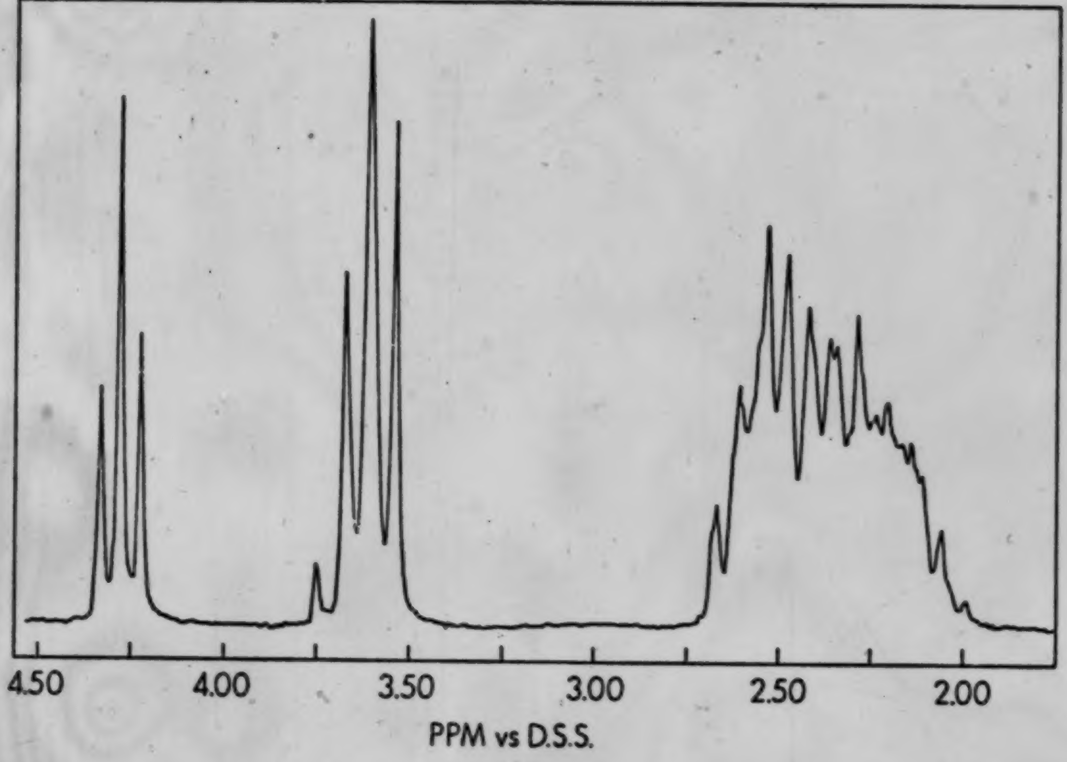

Figure 5. PMR spectrum of the carbon bonded protons of lysine in a 0.5 M aqueous solution at approximately neutral pH.

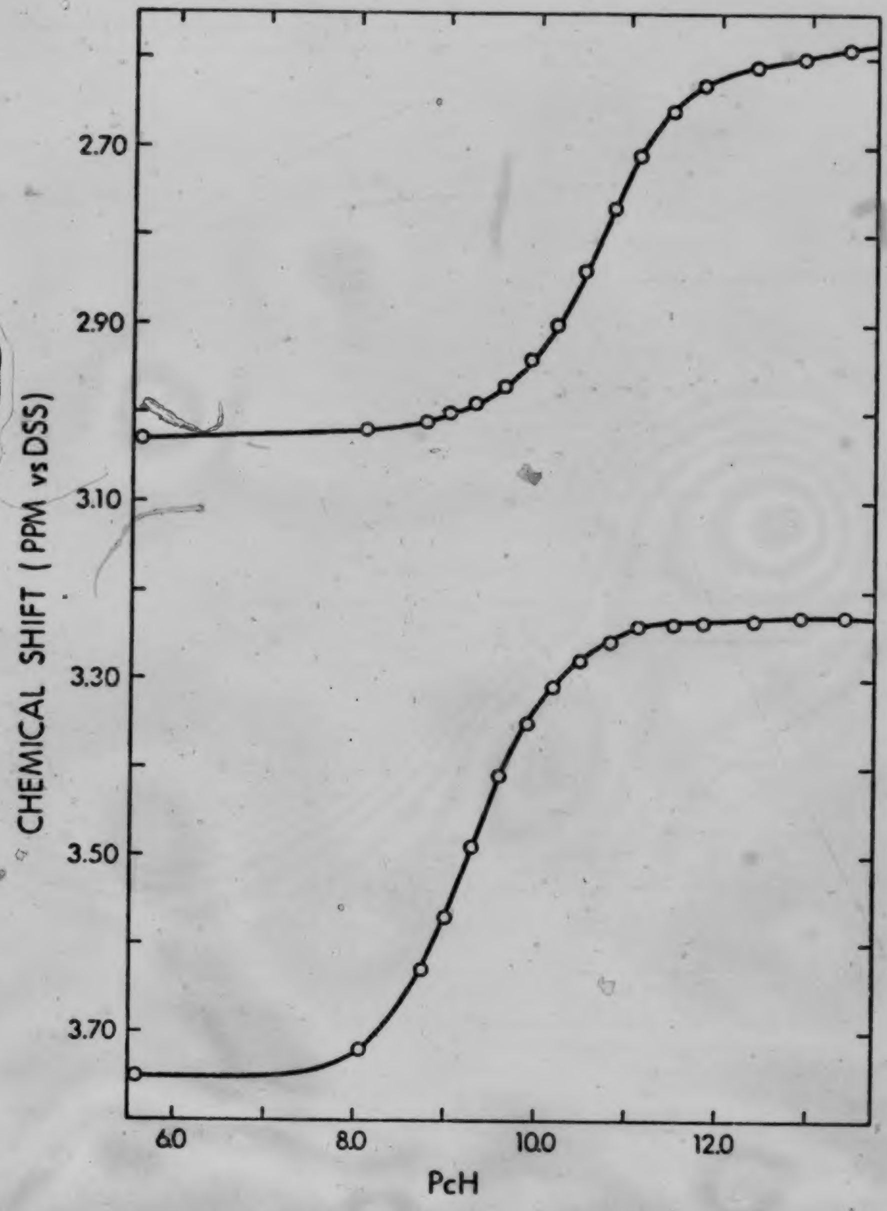

Figure 6. pH dependence of the chemical shifts of the protons on the alpha (lower curve) and epsilon (upper curve) carbons of lysine in a 0.19 M aqueous solution.

to the deprotonation of the omega ammonium group. For both resonances, it is the chemical shift of the central peak of the observed triplet pattern which is plotted in Figure 6.

ii) Determination of Acid Dissociation Constants

a) Macroscopic Acid Dissociation Constants

The macroscopic acid dissociation constants for the stepwise deprotonation of the two amino groups of lysine were determined using both linear and nonlinear methods. Fractional deprotonation data was calculated from the methine and ε-methylene chemical shift data using Equation 71. $\Delta_{2,3}$ and $\Delta_{3,2}$ were both assigned values of -1.7 Hz, as determined from chemical shift vs pH data for n-pentylamine, 2-aminohexanoic acid and 6-aminohexanoic acid. In all three compounds, complete deprotonation of the amino group results in a total change of -1.7 Hz in the resonance of proton(s) five bonds removed from the site of deprotonation. (The negative sign indicates an upfield shift.) The fractional deprotonation data, obtained from the methine and methylene chemical shifts, was combined according to Equation 77 to yield an $\bar{h}$ vs pH data set. Computer performed, linear least squares analysis of the $\bar{h}$ data according to Equation 88 and nonlinear curvefitting of the $\bar{h}$ data to

$$\frac{a_{H^+}\bar{h}}{(1-\bar{h})} = \left\{ \frac{(2-\bar{h})}{a_{H^+}(1-\bar{h})} \right\} K_2K_3 + K_2 \qquad (88)$$

Equation 89 resulted in the values of pK_2 and pK_3 given in Table 5.

$$\bar{h} = \frac{K_2 a_{H^+} + K_2 K_3}{a_{H^+}^2 + a_{H^+} K_2 + K_2 K_3} \tag{89}$$

Initial estimates of K_2 and K_3, required by KINET, were obtained from a plot of $\bar{h}$ vs pH at the points $\bar{h} = 1.5$ and $\bar{h} = 2.5$ respectively.

ii) Microscopic Acid Dissociation Constants

Three sets of estimates for the microscopic acid dissociation constants of the amino groups of lysine were calculated from the fractional deprotonation data obtained from the chemical shift data of methine and ε-methylene resonances. Nonlinear curvefitting of the methine fractional deprotonation data, $f_{\alpha,d}$, was performed by KINET using Equation 87. The $f_{\omega,d}$ data obtained from the ε-CH_2 resonance was similarly analyzed using Equation 90.

$$f_{\omega,d} = \frac{k_{13} a_{H^+} + k_{13} k_{132}}{a_{H^+}^2 + a_{H^+} K_2 + K_2 K_3} \tag{90}$$

The required values of K_2 and K_3 were obtained from fractional deprotonation data as previously described. The microscopic constants are presented in Table 5. The pk_{13} and pk_{132} values given for the methine data and the pk_{12} and pk_{123} values given for the ε-methylene data were calculated from K_2 and K_3 as described in Chapter III.

TABLE 5

Macroscopic and Microscopic Acid Dissociation Constants of Lysine.HCl[a,b]

pK_2[c]	pK_3	pk_{12}[d]	pk_{13}	pk_{123}	pk_{132}	Method of Calculation
9.27	10.82	-	-	-	-	Equation 78[e]
9.27	10.82	-	-	-	-	Equation 79[f]
-	-	9.31	10.33	10.78	9.74	Equation 74[g]
-	-	9.31	10.30	10.77	9.79	Equation 90[h]
-	-	9.33	10.22	10.76	9.87	Equation 80[f]

a) Mixed activity-concentration constants. To convert to approximate concentration constants, subtract .09.
b) 0.186 M lysine.HCl, $\mu = 0.186 - 0.372$ M.
c) Linear estimate of the standard deviation was ≤ 0.02 of a pK or pk unit for all constants listed.
d) Subscript 1 denotes the carboxylic acid group, 2 the α-amino group and 3 the ω-amino group.
e) Nonlinear curvefitting of fractional deprotonation data.
f) Linear least squares analysis of $\bar{h}$ data.
g) Nonlinear curvefitting of $f_{2,d}$ data.
h) Nonlinear curvefitting of $f_{3,d}$ data.

Table 5 also contains the microscopic acid dissociation constants of lysine calculated by the linear least-squares analysis of fractional deprotonation data. The value of K_3 obtained from the $f_{\alpha,d}$ and $f_{\omega,d}$ data using Equation 79 was substituted into Equation 91 to obtain α_{IV} data.

$$\alpha_{IV} = (f_{\alpha,d} + f_{\omega,d}) \left\{ \frac{K_3}{a_{H^+} + K_3} \right\} \qquad (91)$$

The microconstants were then calculated as described in Chapter III. The constants reported in Table 5 are the median values calculated from the data points in the range $(0.25 < f_{\alpha,d}; f_{\omega,d} > 0.75)$.

The variation of the macroscopic acid dissociation constants of lysine with concentration has been studied using potentiometry. The concentration of lysine was varied from approximately 0.2 to .005 M. The ionic strength was controlled using KCl so that the changes in ionic strength during the course of the titration were similar to those observed in the chemical shift titration. The macroscopic constants were calculated from the pH data using the correction term method described by Irving and Rossotti (51). The results are presented in Table 6.

TABLE 6

Variation in the Macroscopic Acid Dissociation Constants of Lysine With Concentration

Concentration (Molar)	Ionic Strength (M)[a]	$pK_2^{b,c}$	$pK_3^{b,c}$
.194	.2 - .35	9.25	10.80
.097	.2 - .35	9.21	10.79
.049	.2 - .29	9.21	10.81
.010	.2 - .27	9.21	10.68
.005	.2 - .28	9.21	10.65
.003	.1	9.17	10.60

a) Calculated using Equation 28.
b) Mixed activity-concentration constants.
c) Calculated using the correction term method described by Irving and Rossotti (51).

D. Discussion

No literature values are available for the macroscopic or microscopic acid dissociation constants of EDMA or for the microscopic constants of lysine. A number of workers have used pH titration data to determine pK_2 and pK_3 of lysine and the published results are presented in Table 7. Comparison of the results for the macroconstants presented in Table 5 with those in Table 7 shows a considerable discrepancy between the two sets of macroscopic constants. However, the results presented in Table 6 indicate that the differences are primarily due to the higher concentrations used in the nmr titration.

Although the application of the nmr technique is intended as a supplement to potentiometry with a glass electrode, it is inevitable that comparisons will be made between the two techniques. Examination of the equations developed in Chapter III and applied in this chapter will show that the nmr method, for the calculation of acidity constants, does not require that the concentration of the acid in solution be known. Thus, the purity of the solute need not be known. This is of particular advantage when dealing with biological compounds such as amino acids and peptides since the crystalline forms of these compounds are often difficult to purify and may contain non-stoichiometric waters of hydration and unknown concentrations of salt. Similarly, the presence of extraneous

TABLE 7

Macroscopic Acid Dissociation Constants of Lysine Determined From Potentiometric Data

pK_2	pK_3	Reference
9.19^b	10.62^b	45^d
9.24^b	10.58^b	46^d
9.23^c	10.79^c	47^e
9.17^b	10.60^b	This thesis

a) Mixed activity-concentration constants.
b) 0.003 M lysine.HCl, $\mu = 0.1$ M.
c) Lysine concentration not given, $\mu = 0.1$ M.
d) Calculated from the concentration constant using $\gamma = .771$.
e) Calculated from the thermodynamic constant using the value of $\gamma = .775$ given by the author.

sources of acid or base, such as the absorption of carbon dioxide, have no effect on the nmr calculations.

Aside from the complex and expensive equipment involved, and the time required to perform the data collection and calculations, the nmr method suffers from several disadvantages. Chemical shift measurements cannot be made with the same precision as is obtained for a carefully performed potentiometric titration. Secondly unless Fourier transform techniques are available, the concentration of compound, and thus the total ionic strength, are higher than those required for potentiometry and may be a limiting factor for compounds of low solubility.

As previously indicated, the microscopic acid dissociation constants of EDMA and lysine have not been previously determined and thus the results in Tables 4 and 5 cannot be compared to literature values. However, the α-methine and ε-methylene resonances of lysine are essentially two different data sets and as a consequence provide an internal check regarding the reliability of the values obtained for the microscopic acid dissociation constants. The excellent agreement between the nonlinear calculations using the two $f_{i,d}$ data sets and between the linear and nonlinear calculations (Table 5) serves as an indication of the reliability of the two methods.

Bradbury and Brown (54) used pmr chemical shift data to determine the macroscopic acid dissociation constants of lysine and several methylated derivatives of lysine in D_2O. They assumed that the methine and ε-methylene resonances of lysine were unique, which is essentially correct, but also assumed that the dissociation of one protonated ammonium group would not affect the acidity of the second protonated ammonium group. Examination of the results in Table 5 indicates that the second assumption is not valid. Consequently, Bradbury and Brown's use of Equation 59 to calculate the macroscopic acid dissociation constants is highly questionable.

The pM method has been the most frequently employed technique for the determination of microscopic acid dissociation constants from fractional deprotonation data, particularly that obtained by ultraviolet spectroscopy. This method was first presented by Edsall, Martin and Hollingworth (11) and is based on the function M_i.

$$M_i = \frac{a_{H^+} f_{i,d}}{1-f_{i,d}} = \frac{k_i a_{H^+} + k_i k_{ji}}{a_{H^+} + k_j} \qquad (92)$$

Examination of Equation 92 indicates that, when a plot of pM_i vs $f_{i,d}$ is extrapolated to zero, $pM_i = pk_i$ and when extrapolated to one, $pM_i = pk_{ji}$. The values obtained for k_i and k_{ji} can be treated as known quantities in order to determine the remaining constants.

In a plot of pM_i vs $f_{i,d}$, at the point where $f_{i,d} = 0.5$, $pM_i = pH$. As a result, when $f_{i,d} = 0.5$ Equation 92 can be rearranged to yield:

$$k_j = \frac{a_{H^+}(k_i - a_{H^+})}{a_{H^+} - k_{ji}} \tag{93}$$

In the instance where pk_i or pk_{ji} is approximately equal to the pH at $f_{i,d} = 0.5$, Equation 93 becomes dependent upon the determination of a relatively small difference between two large numbers and consequently suffers a loss in precision. As an alternative, the value of $f_{i,d}$ for which $pM_2 = (pk_i + pk_{ji})/2$ may be substituted into Equation 92 to yield:

$$pk_i = \log\left\{\frac{f_{i,d}}{1-f_{i,d}}\right\} + pk_{ij} \tag{94}$$

Both of the preceding equations are essentially one point calculations and are thus subject to the same errors and criticisms (51) as the $\bar{n} = 0.5$ technique used for determining formation constants. As has been previously noted (11,57) the extrapolation to determine k_i and k_{ji} is accurate for only a limited range of values for the ratio k_i/k_j. When $k_j >> k_i$, the extrapolation of the pM_i vs $f_{i,d}$ plot to obtain pk_{ji} is straightforward but the steepness of the function as $f_{i,d}$ approaches zero makes the determination of pk_i uncertain. Similarly, when

$k_j << k_i$, pk_i can be determined with confidence but the rapid change in the slope of the curve as $f_{i,d}$ approaches unity makes an accurate evaluation of pk_{ji} difficult. Edsall et al (11) determined that for both constants to be evaluated with a reasonable degree of accuracy, the ratio k_i/k_j must lie between the values of 5 and 0.2.

The values for the microscopic acid dissociation constants of EDMA and lysine have been determined from pM_i plots and are presented in Table 8. For lysine the extrapolation and calculation was performed for the fractional deprotonation data obtained from both the α-methine resonance and the ε-methylene resonance. The pM_i vs $f_{i,d}$ plots for EDMA and lysine are presented in Figures 7-9.

The k_{12}/k_{13} ratio for EDMA is 2.8 and comparison of the microscopic constants in Tables 4 and 8 shows that the constants obtained from the pM plot are in good agreement with those obtained by the methods used in Section B of this chapter. A comparison of the results for lysine, which has a k_{12}/k_{13} ratio of 7.8, indicates poor internal agreement for the constants determined from the pM_i vs $f_{i,d}$ plots (Tables 5 and 8). A possible explanation for the discrepancies observed lies in recalling exactly what information is present in the nmr chemical shift data. The expression for the observed chemical shift of a unique resonance can be written in terms of the fraction of the acid which is present in the various molecular

TABLE 8

The Macroscopic and Microscopic Acid Dissociation Constants[a] of EDMA and Lysine.HCl Determined From pM Plots

	EDMA	LYSINE	
pk_{12}	6.91	9.34[b]	9.56[c]
pk_{13}	7.32	10.38	10.15
pk_{123}	9.96	10.99	10.81
pk_{132}	9.55	9.95	10.22
pK_2	6.77	9.30	9.46
pK_3	10.10	10.99	10.91

a) Mixed activity concentration constants.
b) Calculated using $f_{2,d}$ data of lysine.
c) Calculated using $f_{3,d}$ data of lysine.

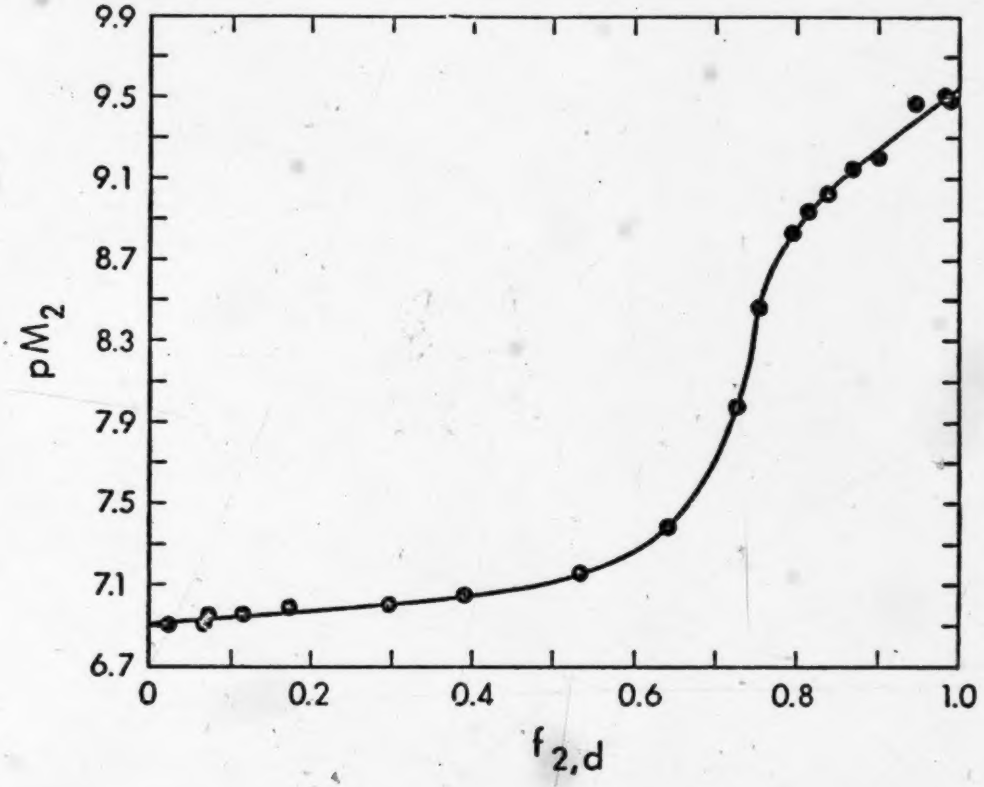

Figure 7. pM_2 vs $f_{2,d}$, the fractional deprotonation of the secondary ammonium group, for EDMA.

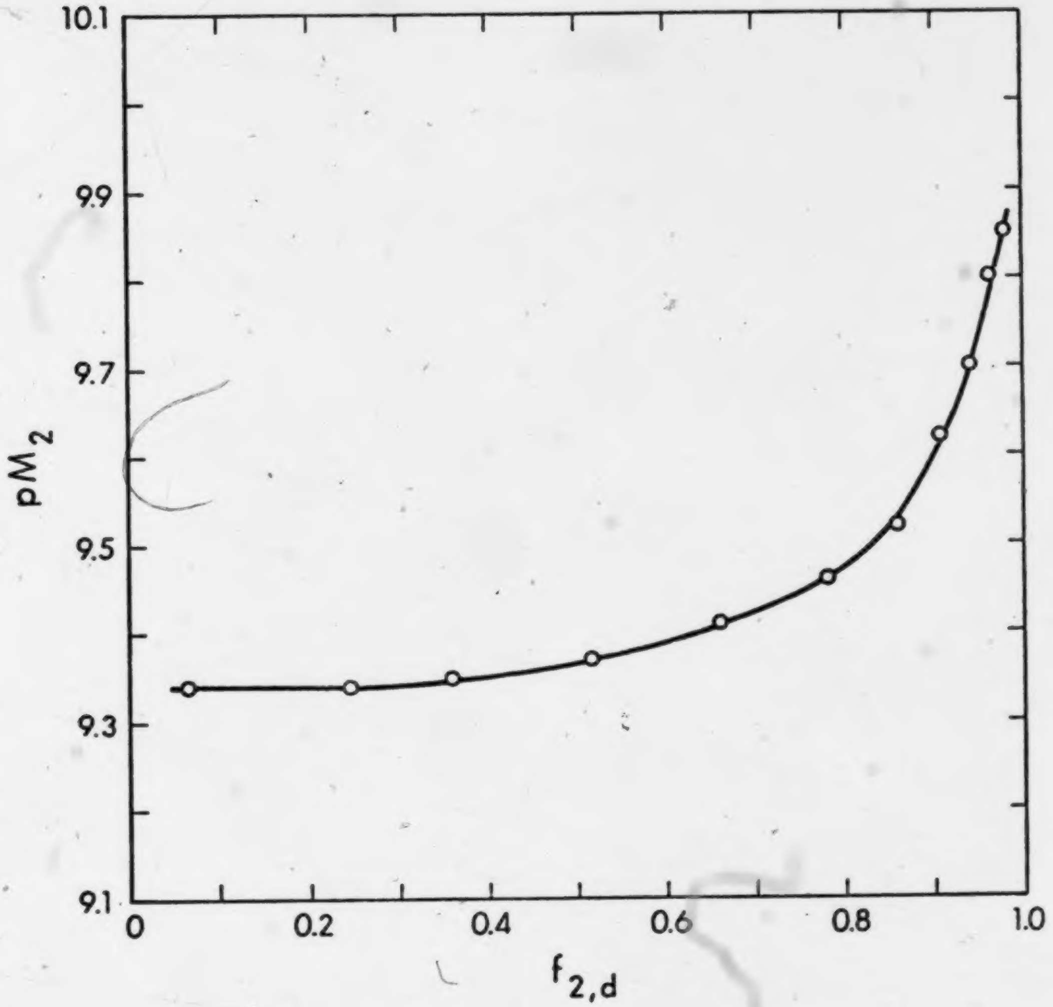

Figure 8. pM_2 vs $f_{2,d}$, the fractional deprotonation of the alpha ammonium group, for lysine.

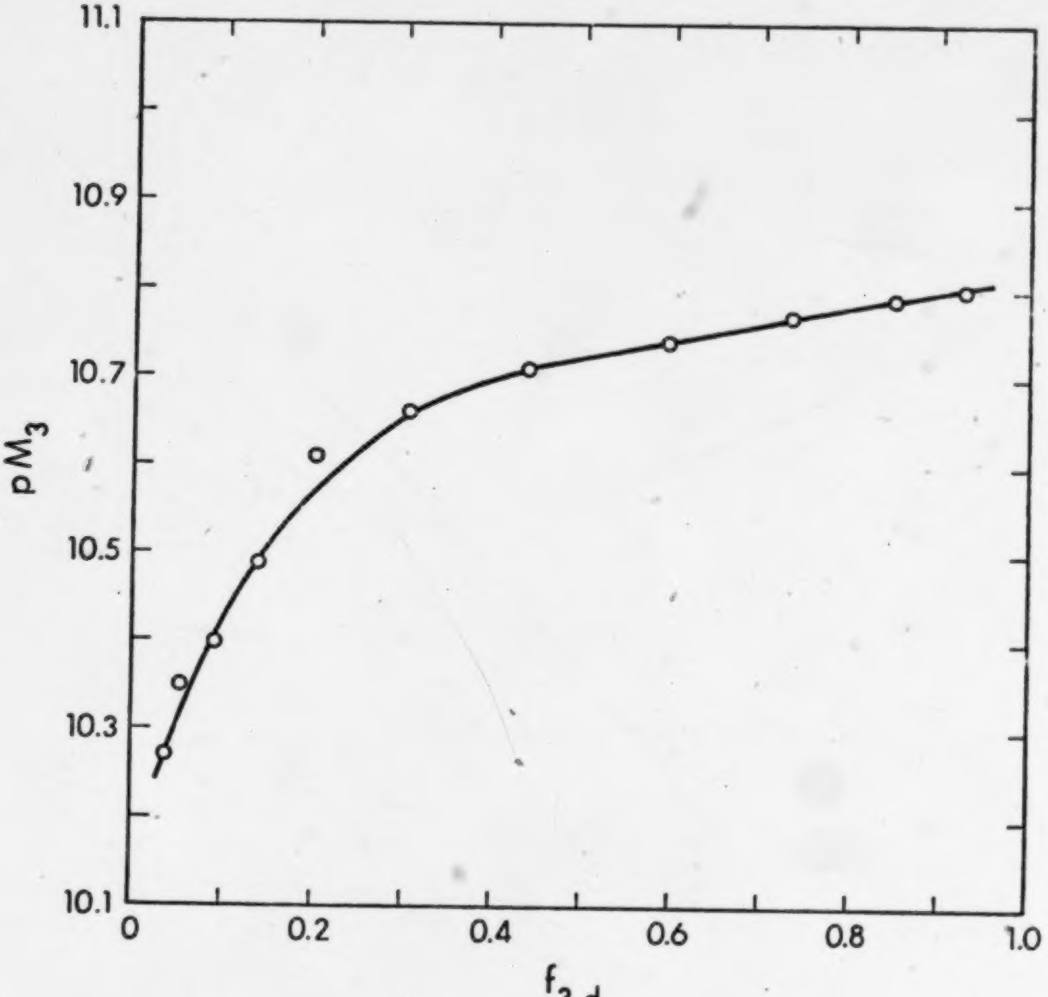

Figure 9. pM_3 vs $f_{3,d}$, the fractional deprotonation of the epsilon ammonium group, for lysine.

forms.

$$\delta_{i,obs} = (\alpha_I + \alpha_{III})\delta_{i,I} + (\alpha_{II} + \alpha_{IV})\delta_{i,IV} \qquad (95)$$

The magnitude of the ratio k_i/k_j is indicative of the fraction of all molecules which will dissociate by a given pathway and thus represents the ratio α_{II}/α_{III}. For a k_i/k_j ratio close to unity, approximately equal concentrations of the two monoprotonated tautomers will be present at a given pH. As the ratio moves away from unity, one or another of the two monoprotonated tautomers will begin to dominate in solution. For instance, at a k_i/k_j ratio of 5:1, eighty-three percent of the acid dissociation will occur via the upper pathway in Scheme III. If the value of α_{III} is always much less than that of α_{II}, the sensitivity of the observed chemical shift to changes in the amount of Form III present in solution will be low. As a result, the accuracy with which k_j and k_{ij} can be determined will also be low.

In addition, the extrapolation of the pM plot tends to weight the data taken at the two ends of the titration curve more heavily than that obtained in the middle of the titration. In those areas of the experiment where the values of $f_{i,d}$ are close to either zero or one, the ratio $f_{i,d}/(1-f_{i,d})$ is sensitive to small changes in $f_{i,d}$, and thus in δ_{obs}, and the relative experimental error increases. Consequently, the extrapolation depends on the least precise data. This is also true for $f_{i,d}$ values obtained from other spectroscopic techniques such as ultraviolet absorption. In contrast, the nonlinear curve-fitting technique utilizes all of the experimental data and weights the data points obtained from the different parts of the titration curve appropriately.

Fung and Chen (57) rearranged the equations used in calculating pM to obtain a linear form which would reduce the extrapolation errors for unfavourable values of the k_i/k_j ratio. When k_i is larger than k_j, the extrapolation to obtain k_i is straightforward but the value obtained for k_{ji} is imprecise. Equation 92 can be rearranged to obtain the linear form:

$$a_{H^+}(k_i - M_i) = k_j M_i - k_j k_{ji} \qquad (96)$$

Using the extrapolated value of k_i as a known quantity, a plot of $a_{H^+}(k_i - M_i)$ vs M_i should give a straight line of slope k_j and intercept $- k_j k_{ji}$. In practice, however, the range of experimental values for which a plot of Equation 96 is linear is somewhat limited and the plots are very sensitive to the value of k_i used (57). Plots of $a_{H^+}(k_{12} - M_2)$ vs M_2 for EDMA and of $a_{H^+}(k_{12} - M_2)$ vs M_2 and $a_{H^+}(k_{13} - M_3)$ vs M_3 for lysine are presented in Figures 10-12. The values obtained for the microscopic constants are in Table 9. As can be seen by examining

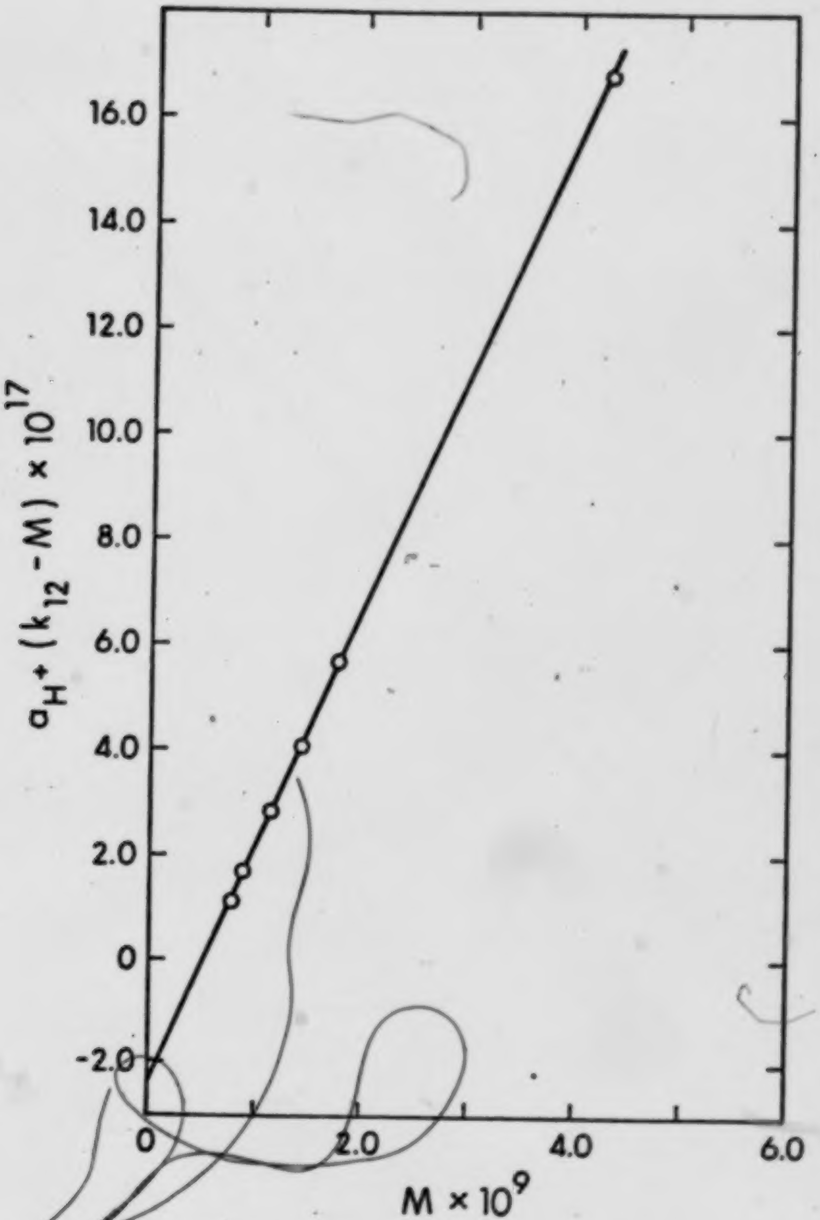

Figure 10. $a_{H^+}(k_{12}-M_2)$ vs M_2 for EDMA. The slope yields k_{13} and the intercept $-k_{13}k_{123}$.

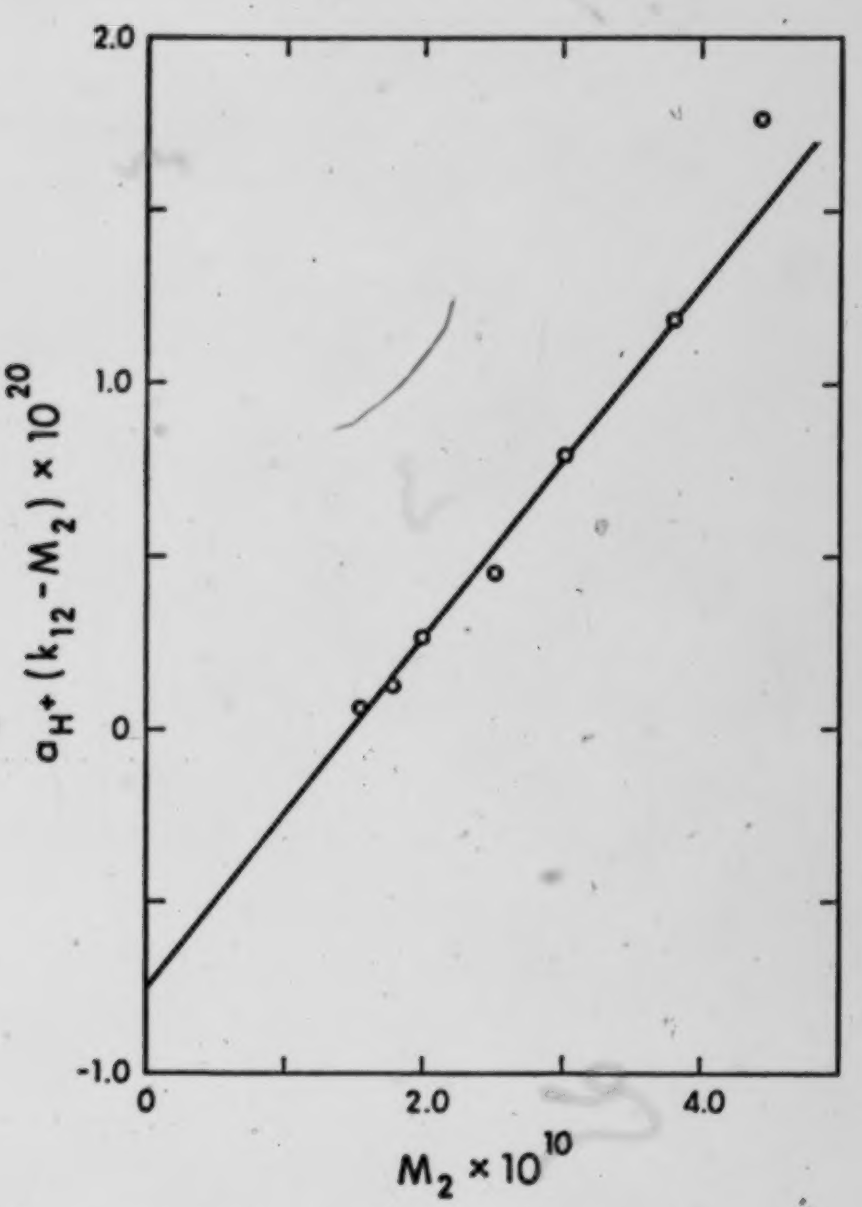

Figure 11. $a_{H^+}(k_{12}-M_2)$ vs M_2 for lysine. The slope yields k_{13} and the intercept $-k_{13}k_{123}$.

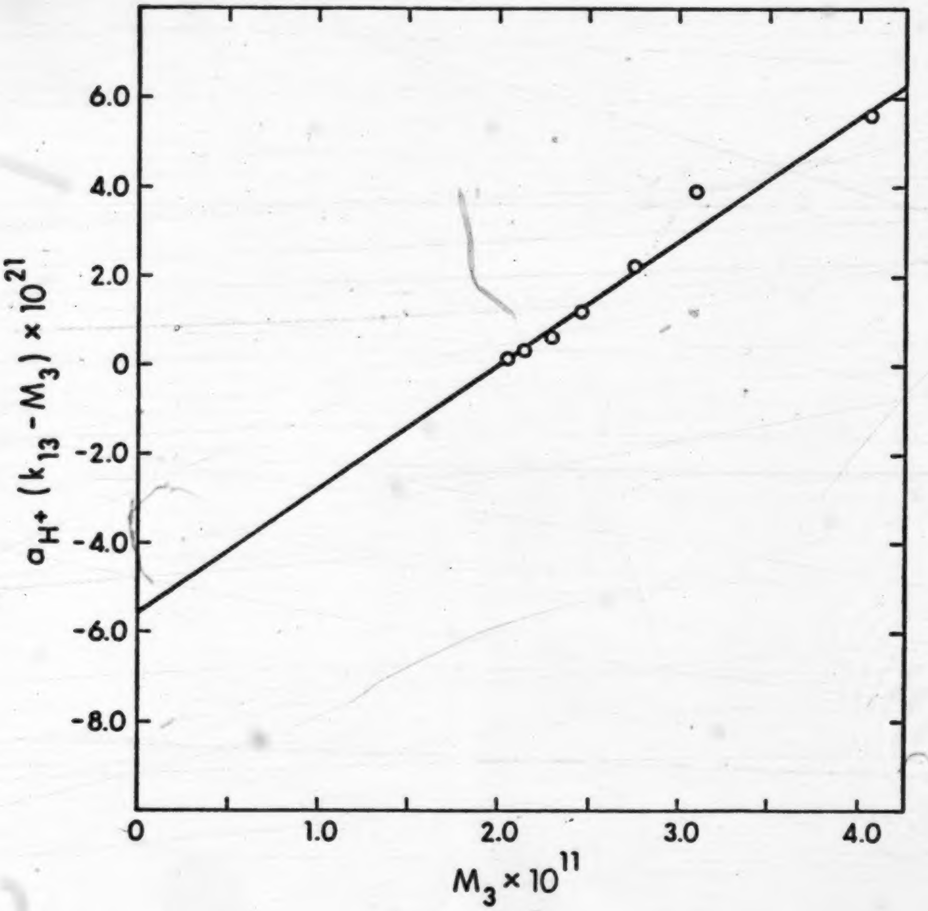

Figure 12. $a_{H^+}(k_{13}-M_3)$ vs M_3 for lysine. The slope yields k_{12} and the intercept $- k_{12}k_{132}$.

TABLE 9

Microscopic and Macroscopic Acid Dissociation Constants[a] of EDMA and Lysine Calculated Using the Linear Modification of pM[b] Plots

	EDMA	LYSINE	
pk_{12}	6.91	9.34[c]	9.40[d]
pk_{13}	7.39	10.38	10.19
pk_{123}	9.40	10.98	10.88
pk_{132}	9.88	9.94	10.02
pK_2	6.78	9.30	9.33
pK_3	10.00	10.92	10.88

a) Mixed activity-concentration constants.
b) Reference 57.
c) Calculated from $f_{2,d}$ data of lysine.
d) Calculated from $f_{3,d}$ data of lysine.

the results in Table 9, the linear modification does not provide a significant improvement over the values obtained from the pM plots for EDMA and lysine.

Niebergall, Schnaare, and Sugita have pointed out (14) that both the pM plot and the linear modification are susceptible to investigator bias. These authors have presented both linear least squares and nonlinear regression techniques for the determination of microscopic acid dissociation constants from the fractional deprotonation data obtained by ultraviolet absorption spectroscopy (14). The microscopic constants of D,L-tyrosine and morphine HCl were determined by performing a nonlinear regression analysis of $f_{i,d}$ data using Equation 97.

$$f_{i,d} = \frac{k_1 a_{H^+} + K_1K_2}{a_{H^+}^2 + a_{H^+}K_1 + K_1K_2} \qquad (97)$$

Equation 97 can be obtained by substituting the relationship in Equation 39 into the numerator of Equation 74.

Niebergall et al (14) obtained values for k_1, K_1 and K_1K_2 using Equation 97 and the remaining microconstants were determined using Equations 37-39. The $f_{2,d}$ data for EDMA and $f_{2,d}$ and $f_{3,d}$ data for lysine were analyzed by nonlinear curvefitting using Equation 97 and the results are in Table 10. The results for EDMA are essentially identical to those calculated using Equation 74 (see Table 4). Analysis of the lysine epsilon-

TABLE 10

Microscopic and Macroscopic Acid Dissociation Constants[a] of EDMA and Lysine Determined from Nonlinear Curvefitting[b]

	EDMA	LYSINE
pk_{12}	6.94	9.40[c]
pk_{13}	7.38	10.26
pk_{123}	9.85	10.70
pk_{132}	9.40	9.84
pK_2	6.80	9.34
pK_3	9.98	10.76

a) Mixed activity-concentration constants.
b) Using Equation 97.
c) From $f_{3,d}$ data.

methylene data yielded results in good agreement with those in Table 5 but the alpha-methine data gave a negative value for K_3. In addition, the statistical information provided by KINET indicated higher linear estimates of the standard deviations of the parameters and a high degree of correlation between the estimates of the three parameters. Analysis of $f_{i,d}$ data obtained from computer simulated chemical shift titration curves indicated that nonlinear curvefitting using Equation 97 is most reliable for systems with a low value for the ratio k_i/k_j. Although quantitative limits are somewhat difficult to define, the degree of correlation approached unity as the k_i/k_j ratio became progressively greater than 5. As a result, Equation 97 should only be used when other techniques indicate a low ratio for the microscopic constants.

Shrager *et al* (56) have described a computer curvefitting method which utilizes nmr chemical shift titration data to obtain both macroscopic and microscopic acid dissociation constants and have used their programme to determine the acid dissociation constants for L-histidine and several related compounds. The programme is designed to curvefit data from both solitary and overlapping dissociations; calculating macroscopic constants in the former cases and microscopic constants, from which the macroscopic constants are calculated, in the latter cases.

Their method is based upon a rearranged form of

Equation 51 and is written in terms of proton association or formation constants rather than dissociation constants. For systems in which common resonances are observed, the intermediate chemical shift values are defined in terms of a fraction, ρ, of the total observed change in chemical shift. As a result, the microscopic acid dissociation constants determined by this method will be dependent upon the values chosen for ρ. This is confirmed by examination of the constants presented for L-histidine methyl ester in Table 4 of reference 56.

There are several differences between the curve-fitting procedure presented by Schrager _et al_ (56) for the determination of microscopic constants and the procedure used in this chapter. The most notable differences are that Schrager _et al_ curvefit the observed chemical shift data, rather than $f_{i,d}$ data, and more important, attempt to determine both the macroscopic and microscopic acid dissociation constants from the chemical shift titration data of a single resonance. Analysis of computer simulated titration data, using equation 51, indicates that if the observed resonance is strongly affected by the degree of protonation of both groups, the microconstants obtained will be very sensitive to the values chosen for the intermediate chemical shifts. When the observed resonance is unique or is affected almost entirely by the deprotonation of only one of the two deprotonating functional groups, the reliability of the estimates obtained for the microscopic constants will decrease as the ratio k_i/k_j increases. Consequently, nonlinear curvefitting of chemical shift data to Equation 51 can be expected to yield reliable estimates for the macroscopic and microscopic constants of only a limited number of molecular systems.

CHAPTER V

THE DETERMINATION OF MACROSCOPIC AND MICROSCOPIC ACID DISSOCIATION CONSTANTS OF α,ω-DIAMINOCARBOXYLIC ACIDS AND LYSINE DIPEPTIDES

A. Introduction

The acid-base chemistry of the majority of amino acids and peptides has not been characterized on the molecular level. In this chapter, the results of the determination by nmr of the macroscopic and microscopic acid dissociation constants of a series of α,ω-diaminocarboxylic acids and of two lysine dipeptides are presented and discussed. As can be seen from the microscopic acid dissociation scheme in Figure 13, the compounds studied all contain two simultaneously deprotonating amino groups.

B. Results

i) α,ω-Diaminocarboxylic Acids

The chemical shift titration curves for the α-methine proton resonance and the γ-methylene protons resonance of ornithine are presented in Figure 14. The data for lysine has been presented previously (Figure 6). The chemical shift of the central peak of the observed triplet is plotted in units of ppm vs DSS. The chemical

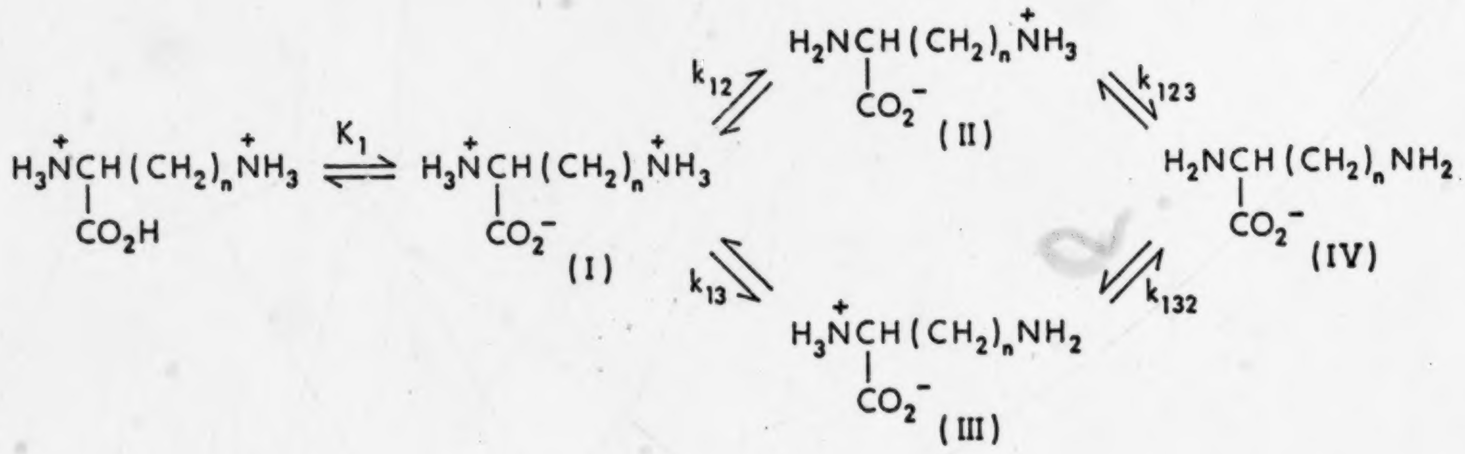

Figure 13. Microscopic acid dissociation scheme for α,ω-diaminocarboxylic acids.

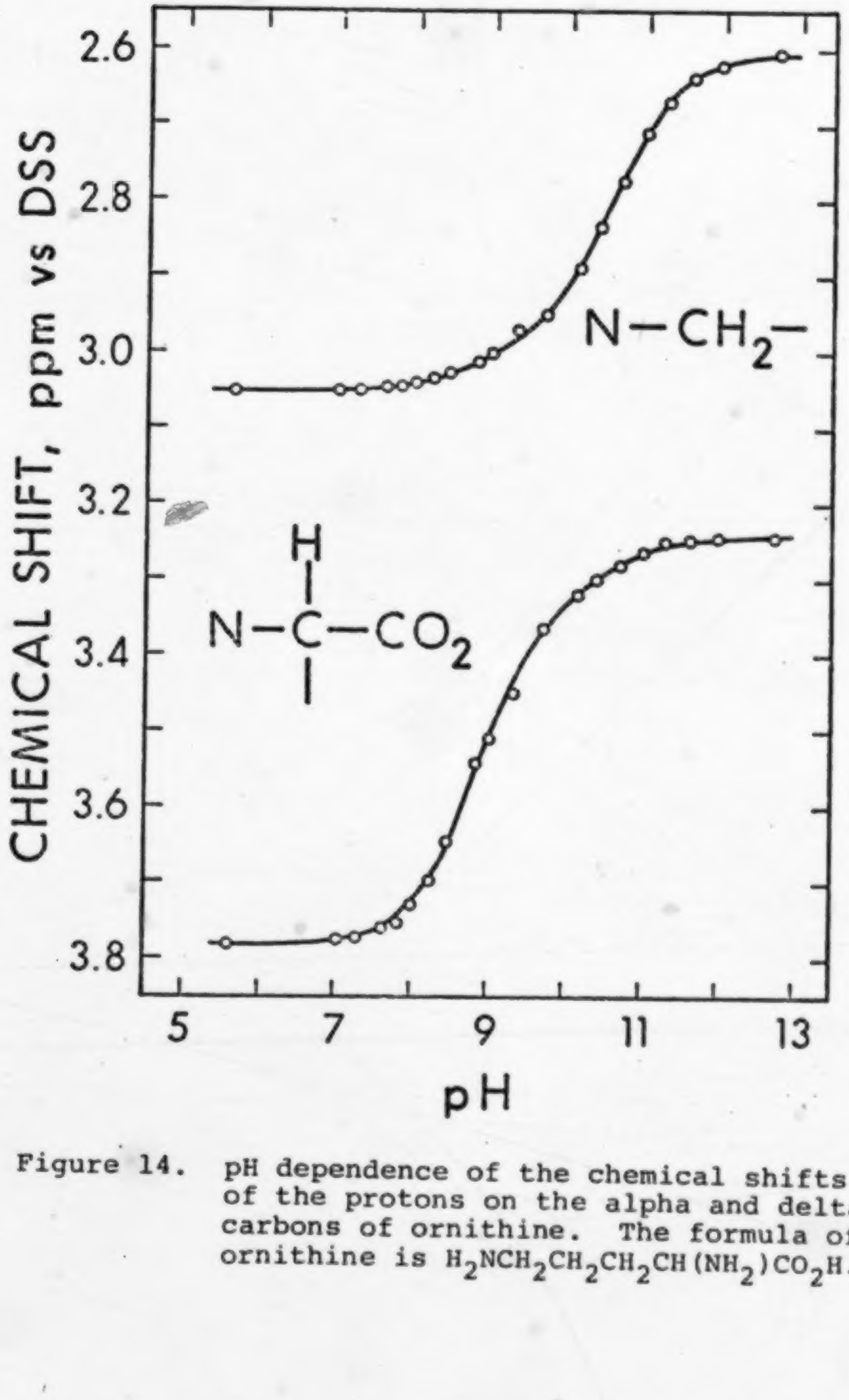

Figure 14. pH dependence of the chemical shifts of the protons on the alpha and delta carbons of ornithine. The formula of ornithine is $H_2NCH_2CH_2CH_2CH(NH_2)CO_2H$.

shift changes observed for each of these resonances are assumed to be almost entirely due to the deprotonation of one functional group and the microscopic and macroscopic acid dissociation constants have been calculated from fractional deprotonation data using the methods described for lysine in Chapter IV. The results for lysine and ornithine are presented in Table 11.

The CMR chemical shift data, as ppm vs internal dioxane for 2,3-diaminopropionic acid, 2,4-diaminobutyric acid, ornithine and lysine is shown in Figures 15-18. As is indicated by the data in Chapter VI, the effect of the deprotonation of an ammonium group will be reflected in chemical shift changes in the resonance of a carbon five bonds removed. As a consequence, the CMR chemical shift data of the alkyl carbons was treated by the common resonance techniques, described in Chapters III and IV, for the determination of macroscopic constants. The results are presented in Table 12.

Attempts to calculate the microscopic acid dissociation constants from carbon-13 chemical shift data using Equation 51 and intermediate chemical shifts predicted from the linear parameterization scheme in Chapter VI were unsuccessful due to the sensitivity of the calculation to the uncertainties in the predicted chemical shifts. However, the microscopic constants of 2,3-diaminopropionic acid, ornithine and lysine have been estimated from

TABLE 11

Macroscopic and Microscopic Acid Dissociation Constants of Ornithine.HCl and Lysine.HCl[a]

	ORNITHINE[b]		LYSINE[c]	
pK_2[d]	8.85[e]		9.27	
pK_3[d]	10.61		10.82	
pk_{12}[f]	8.91[e,g]	8.91[h]	9.31[g]	9.31[h]
pk_{13}	9.77	9.79	10.33	10.30
pk_{123}	10.55	10.56	10.78	10.77
pk_{132}	9.72	9.68	9.74	9.79

a) Mixed activity-concentration constants. To convert to approximate concentration constants, subtract .09.

b) 0.100 M ornithine.HCl; $\mu = 0.10 - .242$ M.

c) 0.186 M lysine.HCl; $\mu = 0.186 - .372$ M.

d) Nonlinear curvefitting of fractional deprotonation data to Equation 78.

e) The linear estimate of the standard deviation was ≤ 0.02 of a pK or pk-unit for all constants listed.

f) Subscript 1 denotes the carboxylic acid group, 2 the α-amino group and 3 the ω-amino group.

g) Nonlinear curvefitting of $f_{2,d}$ data to Equation 74. For ornithine $\Delta_{2,3} = -3.0$ Hz, for lysine $\Delta_{2,3} = -1.7$ Hz.

h) Nonlinear curvefitting of $f_{3,d}$ data to Equation 90. For ornithine $\Delta_{3,2} = -3.0$ Hz, for lysine $\Delta_{3,2} = -1.7$ Hz.

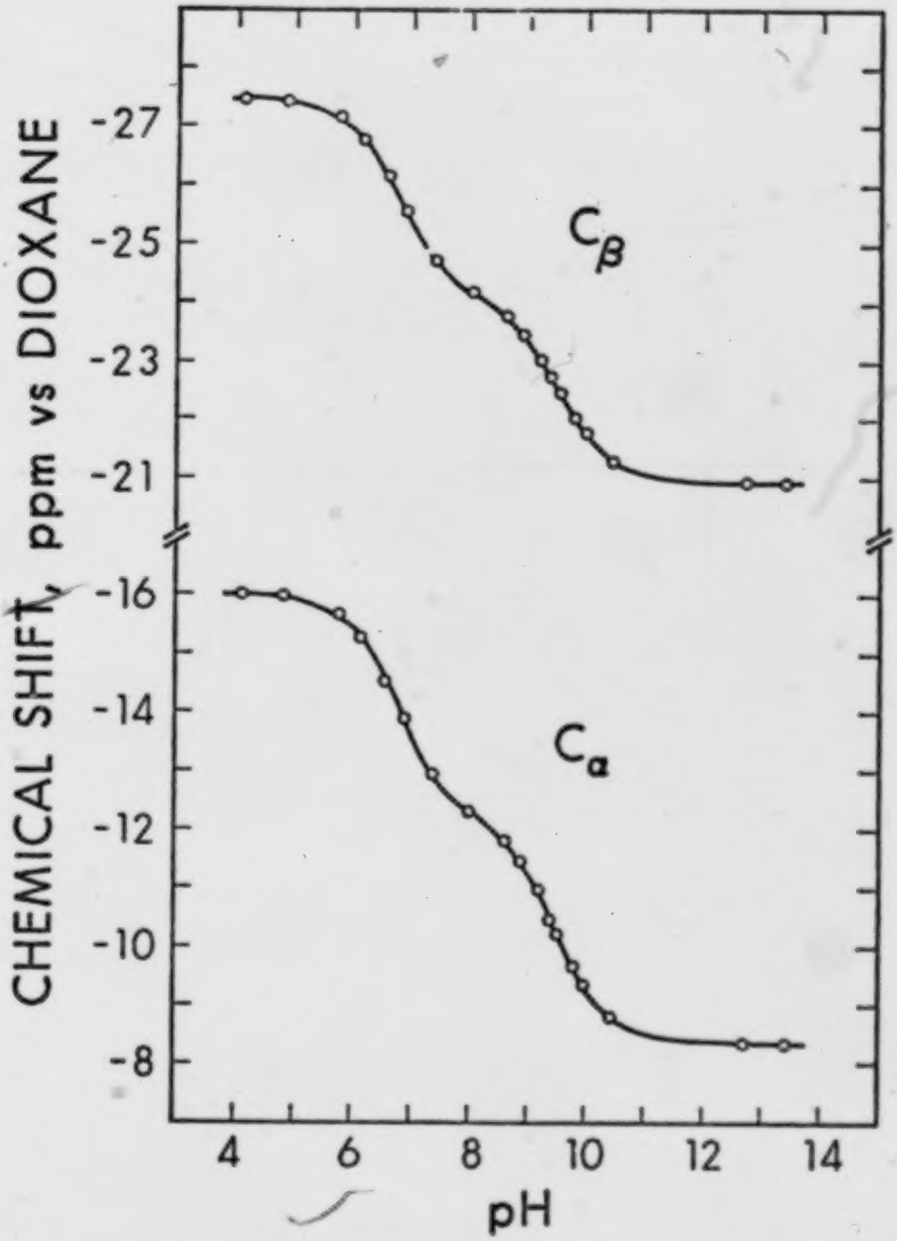

Figure 15. pH dependence of the chemical shifts of the alkyl carbons of 2,3-diaminopropionic acid in a 0.185 M aqueous solution.

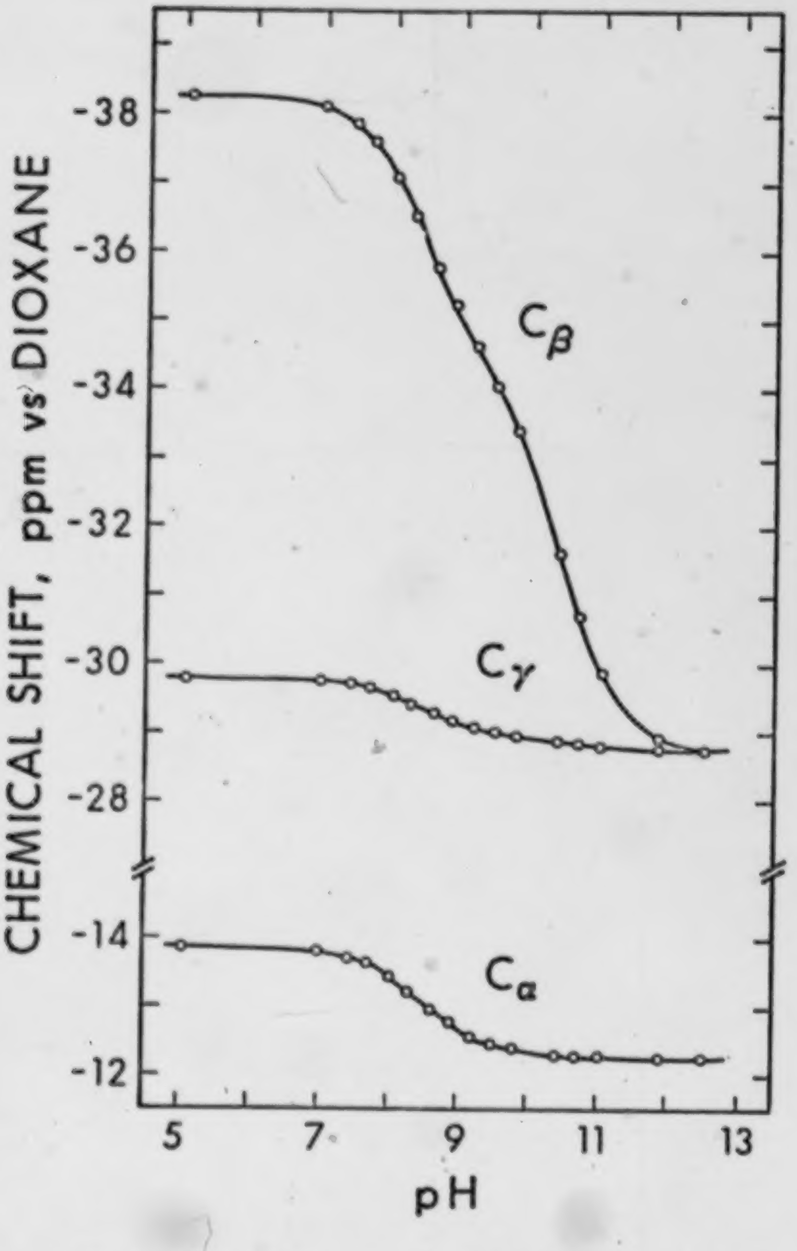

Figure 16. pH dependence of the chemical shifts of the alkyl carbons of 2,4-diaminobutyric acid in a 0.185 M aqueous solution.

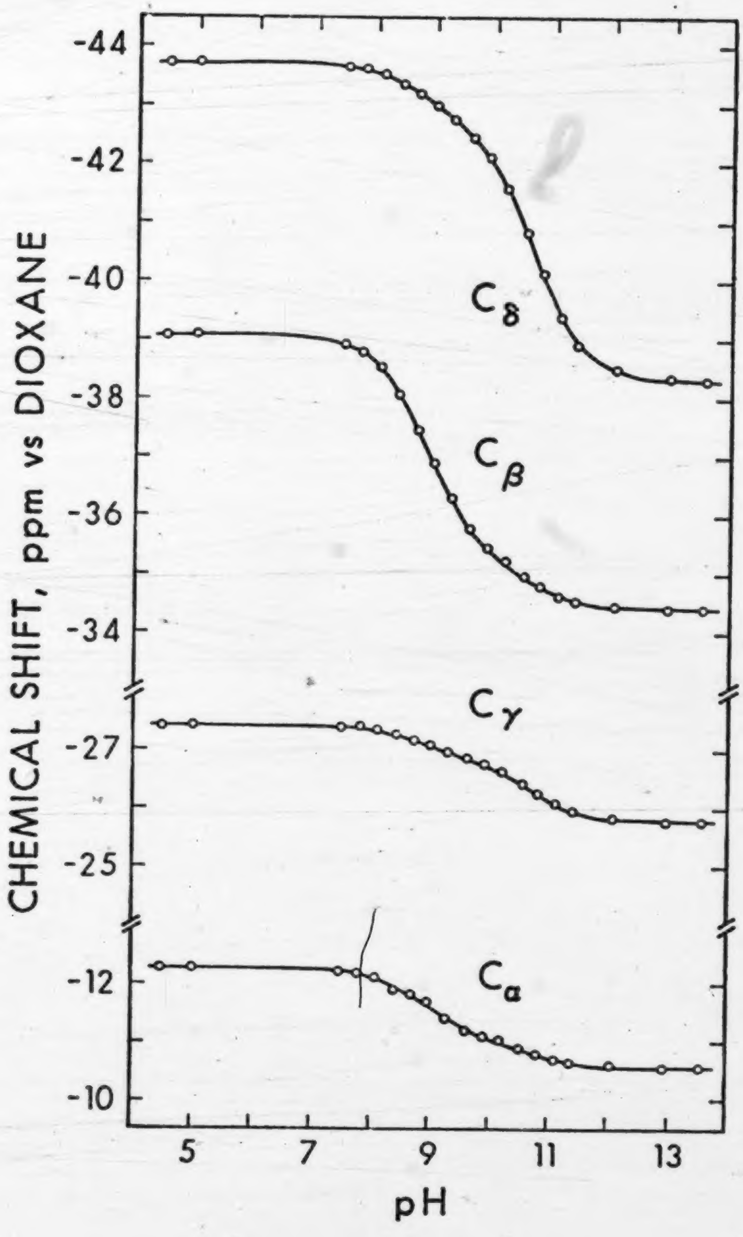

Figure 17. pH dependence of the chemical shifts of the alkyl carbons of ornithine in a 0.185 M aqueous solution.

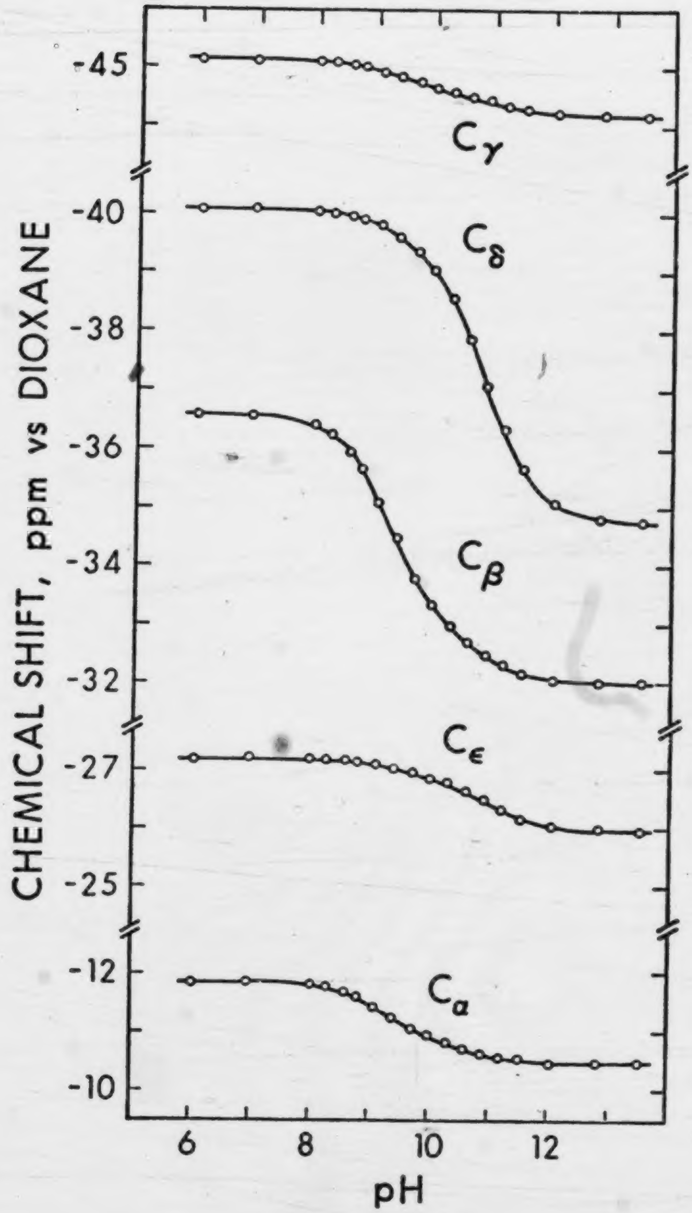

Figure 18. pH dependence of the chemical shifts of the alkyl carbons of lysine in a 0.185 M aqueous solution.

TABLE 12

Macroscopic Acid Dissociation Constants[a] of α,ω-Diaminocarboxylic Acids Calculated from Carbon-13 Chemical Shifts Data

	2,3-Diaminopropionic Acid			2,4-Diaminobutyric Acid			Ornithine			Lysine		
	pK_2[b]	pK_3	δ_{HA}[c]	pK_2	pK_3	δ_{HA}	pK_2	pK_3	δ_{HA}	pK_2	pK_3	δ_{HA}
C_α	6.79±.02	9.53±.02	-12.20±.03	d	d	-	8.92±.07	10.65±.18	-11.09±.07	9.26±.05	10.79±.15	-10.80±.05
C_β	6.77±.02	9.53±.01	-24.07±.02	8.40±.02	10.42±.01	-34.36±.04	8.86±.01	10.58±.04	-35.36±.03	9.29±.01	10.89±.04	-32.98±.03
C_γ	-	-	-	8.42±.04	10.51±.18	-28.98±.02	8.74±.07	10.65±.07	-42.70±.08	9.34±.08	10.99±.10	-44.63±.04
C_δ	-	-	-	-	-	-	8.88±.07	10.69±.03	-26.86±.03	9.41±.07	10.91±.01	-39.31±.06
C_ϵ	-	-	-	-	-	-	-	-	-	9.50±.20	11.03±.06	-26.88±.05
Avg.	6.78	9.53	-	8.41	10.46	-	8.86	10.65	-	9.31	10.91	-
Lit.	6.77	9.53	-	8.24	10.35	-	8.83	10.68	-	9.21	10.81	-
PMR	-	-	-	-	-	-	8.85	10.60	-	9.27	10.81	-

a) Mixed activity-concentration constants. To convert to approx. conc. constants, subtract .09 from each pK_a.
b) The uncertainty reported is the linear estimate of the standard deviation (52).
c) ppm vs internal dioxane.
d) Standard error of the fitted constant was greater than the constant.
e) Mixed constants calc. from the thermodynamic constants of Ref. 64, for $\mu = .3$ M for 2,3-DAP, orn, and lys and $\mu = .45$ M for 2,4-DAB. Activity coefficients calculated with the Davies equation (49,50).

fractional deprotonation data using $\Delta_{i,j}$ values predicted from the model compound data in Chapter VI. The predicted $\Delta_{i,j}$ values and the results are presented in Table 13.

ii) Lysine Dipeptides

The pmr spectra of α-glycyllysine and lysylglycine contain an essentially unique resonance for each of the two simultaneously deprotonating amino groups. For α-glycyllysine the chemical shifts of the glycyl methylene

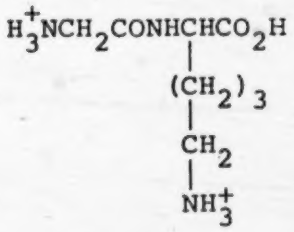

$$\mathrm{H_3\overset{+}{N}CH_2CONH\underset{\begin{array}{c}|\\(CH_2)_3\\|\\CH_2\\|\\NH_3^+\end{array}}{C}HCO_2H}$$

α-glycyllysine

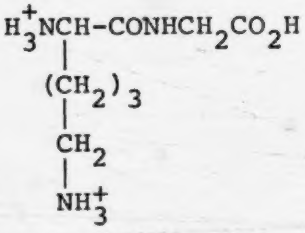

$$\mathrm{H_3\overset{+}{N}\underset{\begin{array}{c}|\\(CH_2)_3\\|\\CH_2\\|\\NH_3^+\end{array}}{C}H\text{-}CONHCH_2CO_2H}$$

lysylglycine

and of the ε-methylene of the lysine residue are presented in Figure 19. The glycyl protons give rise to a singlet over the entire pH range in which the ammonium groups are deprotonating whereas the ε-methylene of the lysine fragment yields a triplet which exhibits some broadening at the higher pH values. Both the α-methine and the ε-methylene of the lysine fragment of lysylglycine give rise to a triplet pattern over the pH range of interest and the chemical shift of the central peak of each triplet is presented as a function of pH in Figure 20. These chemical shift titration curves have been analyzed by the

TABLE 13

Microscopic Acid Dissociation Constants of 2,3-Diaminopropionic Acid, Ornithine and Lysine from Carbon 13 Chemical Shift Data.[a]

	2,3-DAP[b]		ORN[c]		LYS[d]	
	C_α	C_β	C_β	C_δ	C_β	C_γ
pk_{12}	7.06[e]	7.07	8.93	8.92	9.35	9.30
pk_{13}	7.10	7.09	9.63	9.67	10.02	10.43
pk_{123}	9.25	9.24	10.52	10.53	10.73	10.74
pk_{132}	9.21	9.21	9.82	9.79	10.06	9.66

a) Mixed acidity-concentration constants. To convert to approximate concentration constants subtract .09.

b) 0.185 M 2,3-DAP.HCl μ = 0.185 - 0.400 M. $\Delta_{2,3}$ = -5.23 ppm $\Delta_{3,2}$ = -6.53 ppm.

c) 0.185 M Ornithine.HCl μ = 0.4 - 0.55 M, $\Delta_{2,3}$ = -0.27 ppm $\Delta_{3,2}$ = -0.22 ppm.

d) 0.185 M Lysine.HCl μ = 0.4 - 0.55 M, $\Delta_{2,3}$ = -0.20 ppm $\Delta_{3,2}$ = -0.20 ppm.

e) The linear estimate of the standard deviation of each pk or pK is $\leq$ .03.

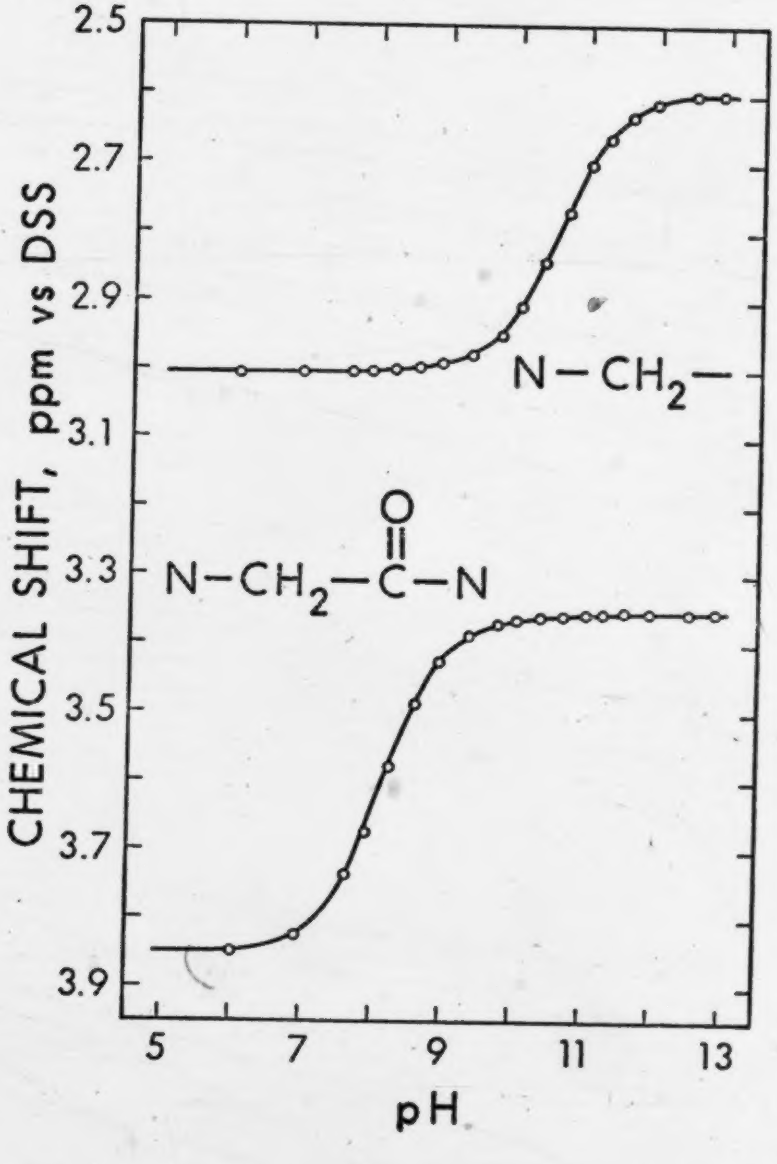

Figure 19. pH dependence of the chemical shifts of the protons on the glycyl alpha carbon and the lysine epsilon carbon of glycyllysine in a 0.099 M aqueous solution.

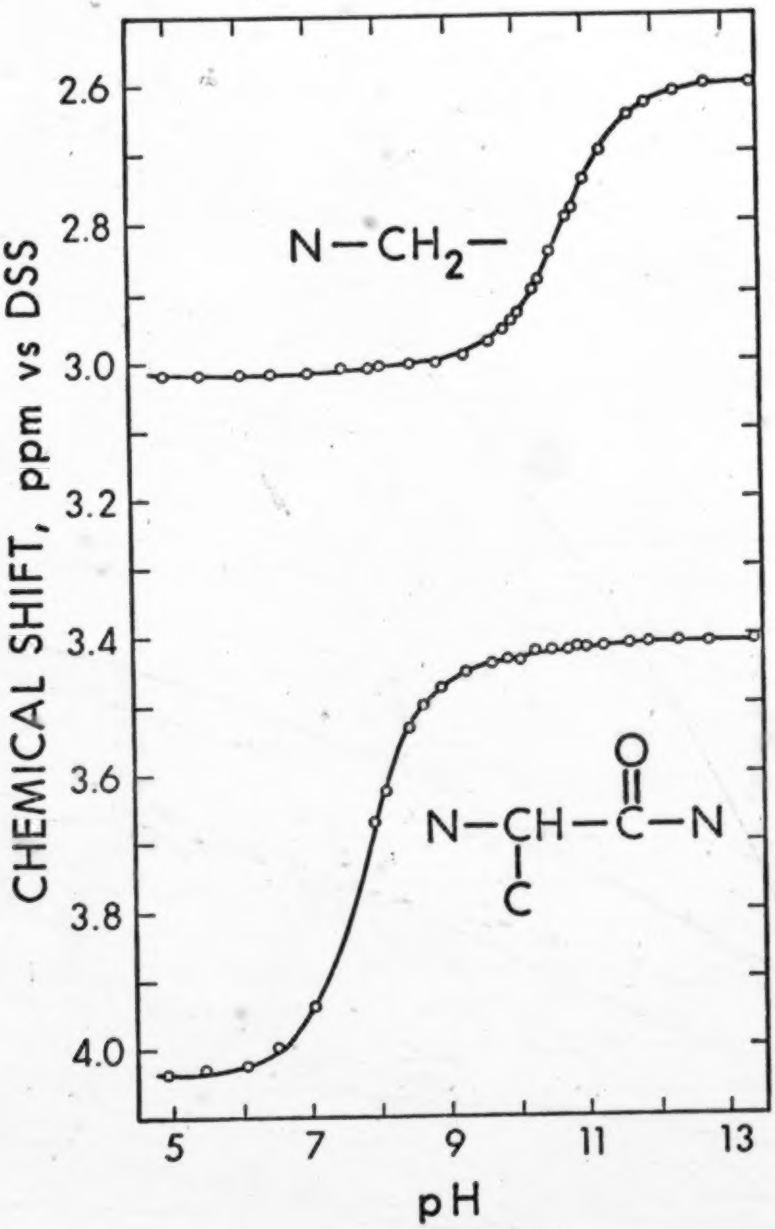

Figure 20. pH dependence of the chemical shifts of the protons on the alpha and epsilon carbons of the lysyl residue of lysylglycine in a 0.11 M aqueous solution.

methods developed in Chapter III for unique resonance data and the constants obtained are presented in Table 14.

C. Discussion

i) α,ω-Diaminocarboxylic Acids

The macroscopic acid dissociation constants of the α,ω-diaminocarboxylic acids presented in Table 12 indicate that the two amino groups of all four compounds undergo simultaneous deprotonation. Consequently, the acid base chemistry of these acids is described by the microscheme shown in Figure 13.

Upon examination of the macroscopic constants in Table 12 and the microscopic constants in Tables 11 and 13, several trends become apparent. As the number of intervening methylene groups increases, the acidity of the ammonium groups decreases, as does the separation between the two macroscopic constants. Hay and Morris (64) attribute the acidity of the ammonium groups in α,ω-diaminocarboxylic acids to the combined inductive (-I) effects of the nearby $-NH_3^+$ or $-NH_2$ and $-CO_2^-$ groups. As the ω-NH_3^+ is moved further away from the α-NH_3^+ group, the strong -I effect of a nearby $-NH_3^+$ group is reduced for both ammonium groups and the observed acidity of the molecules decreases.

The difference between pK_2 and pK_3 reflects the change in the acidity of the amino groups upon deprotonation of the other group. As can be seen from the results

TABLE 14

Macroscopic and Microscopic Acid Dissociation Constants[a] of α-Glycyllysine·HCl and Lysylglycine·HCl

	Glycyllysine[b]	Lysylglycine[c]
pK_2	8.13[d]	7.76
pK_3	10.58	10.73
pk_{12}[e]	8.14[f]	7.78[f]
pk_{13}	g	g
pk_{123}	10.57	10.71
pk_{132}	g	g

a) Mixed activity-concentration constants. To convert to approximate concentration constants, subtract 0.09.

b) .099 M glycyllysine·HCl; $\mu = 0.297 - 0.396$ M.

c) .105 M lysylglycine·HCl; $\mu = 0.105 - 0.210$ M.

d) The linear estimate of the standard deviation was < 0.02 for all pK and pk values listed.

e) For glycyllysine, subscript 1 denotes the carboxylic acid group, 2 the glycyl ammonium group and 3 the lysyl ammonium group. For lysylglycine, subscript 1 denotes the carboxylic acid group, 2 the lysyl α-ammonium group and 3 the lysyl ω-ammonium group.

f) Calculated by nonlinear curvefitting of $f_{2,d}$ data to Equation 74. $\Delta_{2,3} = 0.00$.

g) Values obtained were not reliable. See text for details.

in Tables 12 and 13, a decrease in the ratio K_2/K_3 reflects a decrease in the ratio k_{12}/k_{123} but does not indicate a decrease in the ratio k_{12}/k_{13}. Since the deprotonated amino group has only a moderate -I effect relative to the stronger $-NH_3^+$ group, deprotonation of the $\alpha-NH_3^+$ would be expected to reduce the acidity of the $\omega-NH_3^+$ and vice versa. This reduction would be more pronounced when the two amino groups are in close proximity. Consequently, the difference between the acidities of the $\alpha-NH_3^+$ in Forms I and III and between the acidities of the $\omega-NH_3^+$ in Forms I and II should be greater when the two ammonium groups are in close proximity. The effects of the number of intervening bonds between the alpha and omega ammonium groups upon the relative acidities of the two ammonium groups in 2,3-DAP, ornithine and lysine are presented in Table 15. The attenuation of the -I effect of the $-CO_2^-$, with distance, on the $\omega-NH_3^+$ is indicated by the increasing value for $pk_{13}-pk_{12}$ from 2,3-DAP to lysine.

In view of the previous discussion and the results presented in Table 15, a general consideration should be discussed at this time. Several authors have incorrectly assigned pK_2 to the α-ammonium group and pK_3 to the ω-ammonium group in the α,ω-diaminocarboxylic acids (54, 64, 65). As the macroscopic constants of simultaneously deprotonating functional groups are composites determined by the acidity of both deprotonating groups, discussion

TABLE 15

Effects of the Separation of the Alpha and Omega Ammonium Groups on their Acidities in α,ω-Diaminocarboxylic Acids

Acid	Bond Separation	pK_2-pK_3	$pk_{123}-pk_{12}$	$pk_{13}-pk_{12}$
2,3-DAP[a]	3	2.75	2.19	.04
ORN[b]	5	1.76	1.59	.70
Lys[b]	6	1.55	1.47	1.02

a) Calculated from constants in Tables 12 and 13.
b) Calculated from constants in Table 11.

of the relative acidities of the two groups, based on the macroscopic constants, are not well founded. From Equations 37 and 38, it can be seen that the smaller pK_a describes the loss of a proton when both acidic groups are protonated and the larger pK_a reflects the deprotonation of both groups after the titration of the competing functional group. Consequently, the ratio K_i/K_{i+1} reflects the changes in the acidity of both groups upon deprotonation of the other acidic group and does not necessarily indicate a wide separation in the acidity of the two functional groups. This point is clearly illustrated by the constants presented for EDMA in Table 4. Although the K_2/K_3 ratio is greater than 1200, the acidity of the two ammonium groups is quite similar, as is indicated by the k_{12}/k_{13} ratio of 2.8. Similar results are illustrated in Table 15 and have been previously obtained for diamines (32).

Examination of the microscopic constants for ornithine and lysine presented in Tables 11 and 13 indicates good agreement for the respective pk_{12} and pk_{123} values but some discrepancy in the values determined for pk_{13} and pk_{132}. For lysine, the CMR chemical shifts of the model compounds, presented in Chapter VI, are somewhat anomolous and thus reduce the reliability of carbon-13 calculations for this compound. In addition, the determination of the microscopic acid dissociation constants which describe the minor pathway (k_{13} and k_{132} in Figure 13), is subject to a lack of sensitivity due to low tautomer concentration, as discussed in Chapter IV. As can be seen from the results in Table 13, the reproducibility of the values for k_{13} and k_{132} decreases as the separation between k_{12} and k_{13} increases. The relatively low concentration of Form III (Figure 17), for ornithine and lysine, increases the sensitivity of the calculations to the errors in the chemical shift estimates and is responsible at least in part, for the decreased reliability of the calculated values of pk_{13} and pk_{132} in Table 13.

Attempts have been made to predict the microscopic acid dissociation constants of diamines using model compounds (20,34). The effect of substituent groups such as $-NH_3^+$ and $-NH_2$ on the pK_a of an amino group are considered to be additive, thus allowing the acid dissociation constants for diamines to be predicted from those for monoamines and symmetric diamines. The microscopic constants of symmetric diamines can be calculated directly from the macroscopic constants. From the following scheme, we can see that $k_1 = k_2$ and $k_{12} = k_{21}$.

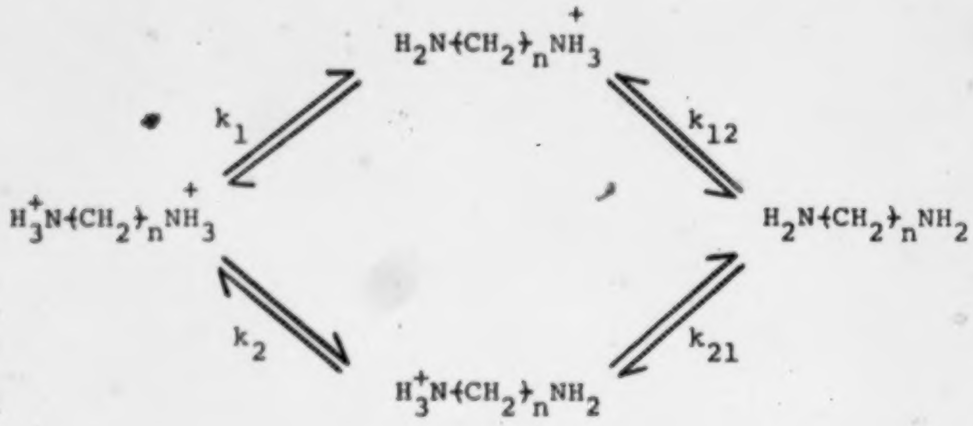

Scheme V

From Equations 37 and 38 we can write:

$$k_1 = K_1/2$$

$$k_{12} = 2K_2$$

The difference between pK_1 of ethylamine and pk_1 of ethylene diamine is assumed to be due to the effect of an $-NH_3^+$ group two bonds removed while the difference between pK_1 and pk_{12} is assumed to be due to the effect of an NH_2 group two bonds removed. By combining the pK_a values of the appropriate monoaminocarboxylic acids and the substituent effects for amino groups 'n' bonds removed, the microscopic acid dissociation constants of the four α,ω-diaminocarboxylic acids can be predicted. Table 16 contains literature values for the acid dissociation constants

TABLE 16

Acid Dissociation Constants for Symmetrical Diammines

	Ethylene Diamine	1,3-Diamino Propane	1,4-Diamino Butane	1,5-Diamino Pentane
pK_1[a]	7.22	8.88	9.61	10.02
pK_2	10.03	10.64	10.82	10.96
pk_1[b]	7.52	9.18	9.91	10.32
pk_{12}	9.73	10.34	10.52	10.66
NH_3^+ Substituent Effect[c]	-3.29	-1.74	-1.02	-0.61
NH_2 Substituent Effect[d]	-1.08	-0.58	-0.41	-0.27

a) All macroscopic constants from Reference 66.

b) Calculated from macroconstants. See text for details.

c) $pk_1 - pK_{NH_3^+(CH_2)_nCH_3}$, n varies from 1 to 4.

d) $pk_{12} - pK_{NH_3^+(CH_2)_nCH_3}$, n varies from 1 to 4.

of four symmetric diamines (66) along with the substituent parameters calculated from the appropriate alkyl amines. Table 17 contains similar data for the alpha and omega - monoaminocarboxylic acids. By assuming the substituent effects to be additive, the microscopic acid dissociation constants for the four α,ω-diaminocarboxylic acids under discussion were calculated. As an example, pk_{12} and pk_{123} of ornithine can be predicted from the pK_2 of 2-aminovaleric acid and the substituent effects in Table 16 for $-NH_3^+$ and $-NH_2$ groups four bonds removed. pk_{13} and pk_{123} can be predicted from the pK_2 of 5-aminovaleric acid in a similar manner. The microconstants estimated in this way for 2,3-DAP, 2,4-DAB, ornithine and lysine are given in Table 18.

Comparison of the microscopic acid dissociation constants presented in Table 18 with the constants in Tables 11 and 13 shows that the predicted functional group acidities are slightly greater than the observed acidities. Although the differences may arise due to ionic strength differences among the data sets used, a lack of additivity in substituent effects is probably the primary reason for the poor agreement. The lack of additivity may be due to the disubstitution at the alpha carbon; in Chapter VI it is noted that the alpha carbons of alpha amino acids exhibit anomolous chemical shift behavior with respect to the additivity of chemical shift parameters

TABLE 17

Acid Dissociation Constants[a] for Monoaminocarboxylic Acids

Monoaminocarboxylic Acid	pk_2
3-aminopropanoic acid	10.25
4-aminobutanoic acid	10.48
5-aminovaleric acid	10.81
6-aminocaproic acid	10.84
2-aminopropanoic acid	9.78
2-aminobutanoic acid	9.66
2-aminovaleric acid	9.70
2-aminocaproic acid	9.76

a) Data taken from Reference 3.

TABLE 18

Predicted Macroscopic and Microscopic Acid Dissociation Constants for α,ω-Diaminocarboxylic Acids

	2,3-DAP	2,4-DAB	ORNITHINE	LYSINE
pk_{12}	6.49	7.92	8.68	9.15
pk_{13}	6.96	8.74	9.79	10.23
pk_{123}	9.17	9.90	10.30	10.57
pk_{132}	8.70	9.08	9.29	9.49
pK_2	6.36	7.86	8.65	9.12
pK_3	9.30	9.96	10.34	10.61

derived from amine and carboxylic acid data. Similar effects have also been noted by other authors (77,78). The hypothesis by Hine and Li (34) that the difference between the substituent parameter predicted K_3 and the K_3 obtained by potentiometry represents the k_a of a hydrogen bonded, monoprotic tautomer requires further substantiation.

ii) Lysine Dipeptides

α-glysyllysine and lysylglycine were chosen as models for the acid-base chemistry of the ε-amino group of lysine in peptides and proteins. The macroscopic and microscopic acid dissociation constants calculated from chemical shift titration curves are presented in Table 14.

Comparison of the pk_{12} values for lysine (Table 11) and lysylglycine indicates an increase in the acidity of the $\alpha\text{-}NH_3^+$ of 1.55 pK units upon substitution of the carboxyl group by a peptide linkage. The greater acidity of the α-ammonium group of lysine as compared to monoalkylamines is due partly to the inductive effect of the CO_2^- group (64,67). When the CO_2^- is converted to a peptide linkage, its acid strengthening effect is even greater because of the increased inductive effect of the peptide bond and a decreased electrostatic attraction due to the increased separation of the alpha NH_3^+ and the CO_2^-. A virtually identical increase in acidity is observed when the k_{12} of glycyllysine is compared to the pK_2 of glycine (9.69 from reference 67). The pk_{123} of lysylglycine shows little change from the equivalent value in lysine and the pk_{123} of α-glycyllysine shows only a slight increase in acidity. These results indicate that the ε-NH_3^+ of lysine is not significantly increased by the incorporation of the α-amino and carboxylic acid groups into peptide bonds.

Examination of the chemical shift titration data in Figures 19 and 20 shows that the first deprotonation is essentially complete prior to the onset of the second deprotonation. It can be seen from the values presented in Table 14 that $pk_{12} \approx pK_2$ and $pk_{123} \approx pK_3$ for the two peptides. These observations lead to the conclusion that only a very small fraction of the molecules in solution dissociate via the pathway I → III → IV (see Figure 13). As a result, the analysis of the $f_{3,d}$ - pH data of both peptides, using Equation 90, is extremely sensitive to the common resonance effects discussed in Chapter IV. Consequently, the reliability of the estimates obtained for k_{13} and k_{132} from the chemical shift data of glycyllysine and lysylglycine is too low to warrant either the presentation of the values obtained for these constants or their utilization in further calculations. The only values of k_{12} and k_{123} reported are those obtained from the analysis of the $f_{2,d}$ - pH data.

CHAPTER VI

CARBON-13 CHEMICAL SHIFT PARAMETERS FOR AMINES, CARBOXYLIC ACIDS AND AMINO ACIDS

A. Introduction

During the course of the PMR work, the instrumentation required to perform Fourier transform carbon-13 magnetic resonance became available. Proton decoupled carbon-13 nmr spectra have several advantages relative to pmr spectra, including singlet resonance patterns for each magnetically non-equivalent carbon and a wider chemical shift range. However, the chemical shift effects, upon deprotonation are not as rapidly attenuated in CMR as they are in PMR and, for the compounds studied, all the observed carbons give rise to common resonances.

It has been shown in previous chapters that accurate estimates of the macroscopic constants of simultaneously deprotonating functional groups can be determined directly from common resonance chemical shift data. The determination of microscopic acid dissociation constants requires accurate estimates of either intermediate chemical shift values or of the net effect of the total deprotonation of each functional group on the observed chemical shift of a specific resonance.

Fairhurst (45) used carbon-13 chemical shift-pH data to study the acid-base chemistry of cysteine and

and several related compounds. Although she was able to determine the macroconstants, the model compound approach failed to provide unambiguous estimates for the microscopic constants. The shortcomings of the model compound approach were assumed to be due to the sensitivity of the ^{13}C chemical shifts to conformational changes brought about by deprotonation.

Due to the failure of the model compound approach to provide accurate estimates of intermediate chemical shift values, it was decided to determine if a linear parameterization scheme could be developed with which the intermediate chemical shifts could be predicted with sufficient accuracy to calculate microscopic acid dissociation constants from carbon-13 chemical shift data.

Linear parameterization schemes have been developed to predict the cmr chemical shifts of a variety of systems, including alkanes (68,69), aliphatic alcohols (70), amines (71,72), carboxylic acids (41), and amino acids (43,56). The first carbon-13 parameterization scheme was developed for alkanes by Grant and Paul (68), and was suggested by the systematic changes observed in the chemical shifts of a series of homologous alkanes. Their data indicated that the chemical shift of a given carbon could be predicted by an equation of the form

$$\delta_c^i = B + \sum_j A_j n_{ij} \qquad (98)$$

where δ_c^i is the chemical shift of carbon i, A_j is an additive parameter, n_{ij} is the number of atoms in the jth position relative to carbon i and B is a constant whose value is quite close to the chemical shift of the methane carbon.

Lindeman and Adams (69) modified the parameter scheme of Grant and Paul to yield improved predictions for branched alkanes. Their best parameter set was based on the equation

$$\delta_c(k) = B_S + \sum_{M=2} D_M A_{SM} + \gamma_S N_{k_3} + \Delta_S N_{k_4} \qquad (99)$$

where B_S, A_{SM}, γ_S, and Δ_S are constants, D_M is the number of carbon atoms which have M attached carbons and are bonded to the kth carbon and N_{k_3} and N_{k_4} are the number of carbon atoms three and four bonds removed. S represents the number of carbon atoms bonded to the kth carbon and A_{SM} is used to describe the steric configuration of adjacent carbon atoms. Consequently, Lindeman and Adams reported four different parameter sets; the parameter set used in the prediction of a given chemical shift depending upon whether the kth carbon is a primary, secondary, tertiary or quaternary carbon. For substituted alkanes, parameterization schemes have been developed in which the carbon-13 chemical shift is predicted by replacing the substituent with CH_3, CH_2, or CH and then employing the appropriate empirical parameters to account for the effect of the substituent. The validity of this approach for aqueous solutions has been questioned because of the different environments in which the alkane shifts were measured (56).

The linear parameterization scheme required for the prediction of the intermediate chemical shifts of polyfunctional molecules must accurately predict the chemical shifts of the carbons of interest in an aqueous environment and at a given degree of protonation. To develop a parameterization scheme for amino acids, the carbon-13 nmr spectra of a total of forty-five amines, amino acids, and carboxylic acids were obtained. Several approaches to the development of the parameterization scheme have been investigated, including individual sets of parameters for primary, secondary and tertiary carbons, parameters derived strictly from amino acid data, and a parameter set which includes carbons from all compounds examined, regardless of the degree of substitution.

As was noted in Chapter V, intermediate chemical shift values predicted by the linear parameterization schemes which are derived in this chapter are not of sufficient accuracy to be used in the calculation of microscopic acid dissociation constants from carbon-13 chemical shift data. However, the results presented in this chapter indicate that the estimates of chemical shifts obtained from these parameterization schemes are more than adequate to aid in the assignment of carbon-13 resonances.

B. Results and Discussion

i) Chemical Shift Data

The carbon-13 chemical shifts from which the parameter sets are derived are presented in Tables 19-25. The CMR spectra of the amines and carboxylic acids were obtained at pH values corresponding to the fully protonated and deprotonated states. The amino acid spectra were measured at pH values corresponding to the protonated, zwitterionic, and deprotonated forms. Alkyl carbon resonance assignments were made using the effects of substituents on the chemical shifts of directly-bonded carbon atoms, the dependence of the change in chemical shift accompanying the titration of ammonium and carboxylic acid groups on distance from the titrated group (43,56), relative intensities in molecules having two carbon atoms equivalent by symmetry and, where necessary, single frequency off-resonance decoupling.

Carbon-13 chemical shifts have been reported previously for aqueous or D_2O solutions of a number of the amines (72), carboxylic acids (41) and amino acids (40,42, 43,73,74) listed in Tables 19-25. A review has also appeared which discusses carbon-13 studies of a wide range of compounds (76). Variations in experimental conditions

TABLE 19

^{13}C Chemical Shifts of Selected Monoamines in Aqueous Solution[a,b]

Amine	pH	C_1	C_2	C_3	C_4	C_5
Methylamine	3.60	26.08				
	12.94	27.97				
Ethylamine	3.58	36.42	13.18			
	13.17	37.02	18.57			
n-Propylamine	4.40	42.59	21.55	11.30		
	13.17	43.94	26.30	11.84		
n-Butylamine	4.25	40.70	30.02	20.09	13.94	
	13.53	41.67	35.31	20.58	14.43	
n-Pentylamine	2.62	41.03	27.65	28.89	22.63	14.32
	13.55	41.94	32.72	29.54	23.01	14.54
Isopropylamine	3.23	45.45	21.14			
	13.19	43.07	25.50			
sec-Butylamine	2.79	50.64	18.56 (CH_3) 28.46 (CH_2)	10.31		
	13.20	48.70	22.88 (CH_3) 32.56 (CH_2)	11.04		
iso-Butylamine	2.95	47.78	27.49	20.07		
	13.29	49.92	31.18	20.55		
iso-Amylamine	3.52	39.48	36.76	26.09	22.64	
	13.14	40.06	42.30	26.14	23.13	
2-Methylbutylamine	3.08	46.23	33.71	17.06 (CH_3) 27.15 (CH_2)	11.38	
	13.24	47.73	37.64	17.54 (CH_3) 27.45 (CH_2)	11.82	

(a) In ppm vs external TMS. Positive shifts indicate deshielding relative to TMS.

(b) 0.3 M amine in H_2O; 25°C.

TABLE 20

^{13}C Chemical Shifts of Selected Diamines in Aqueous Solution[a,b,c]

Amine	pH	C_1	C_2	C_3
Ethylenediamine	2.66	38.07		
	12.21	44.29		
1,3-Diaminopropane	4.88	38.11	26.24	
	13.61	39.57	36.01	
1,4-Diaminobutane	5.25	40.27	25.11	
	13.56	41.76	30.40	
1,5-Diaminopentane	4.35	40.70	27.54	23.82
	13.58	41.84	32.83	24.57
1,2-Diaminopropane		46.69 (CH)	17.02 (CH_3) 43.40 (CH_2)	
		49.23 (CH)	20.74 (CH_3) 49.87 (CH_2)	

(a) In ppm vs external TMS. Positive shifts indicate deshielding relative to TMS.

(b) 0.3 M diamine in H_2O; 25°C.

(c) Carbon atoms numbered from a nitrogen.

TABLE 21

^{13}C Chemical Shifts of Selected Monocarboxylic Acids[a,b,c] in Aqueous Solution

Carboxylic Acid	pH	CO_2	C_1	C_2	C_3	C_4	C_5
Acetic Acid	1.49	177.95	21.72				
	8.03	182.61	24.48				
Propionic Acid	1.68	181.16	28.46	9.63			
	10.64	186.11	31.86	11.38			
Butyric Acid	1.61	180.43	37.01	19.15	13.95		
	10.42	185.23	40.79	20.50	14.44		
Valeric Acid	1.52	180.62	34.82	27.69	22.74	14.15	
	11.11	185.48	38.61	29.34	23.22	14.39	
Hexanoic Acid	d						
	10.33	185.48	38.80	26.77	32.20	22.98	14.54

(a) In ppm vs external TMS. Positive shifts indicate deshielding relative to TMS.

(b) 0.3 M carboxylic acid in H_2O; 25°C.

(c) Carbon atoms are numbered from the carboxylic acid group.

(d) Not sufficiently soluble at low pH.

TABLE 22

^{13}C Chemical Shifts of Selected Dicarboxylic Acids[a,b,c] in Aqueous Solution

Dicarboxylic Acid	pH	CO_2	C_1	C_2	C_3
Malonic Acid	0.10	172.13	42.35		
	12.80	178.49	49.04		
Succinic Acid	0.36	178.15	30.07		
	11.75	183.54	35.26		
Glutaric Acid	0.55	179.12	34.05	20.80	
	9.55	184.31	38.51	24.14	
Adipic Acid	d				
	10.45	184.85	38.56	26.96	
Pimelic Acid	d				
	12.28	185.24	38.75	26.91	29.92

(a) In ppm vs external TMS. Positive shifts indicate deshielding relative to TMS.

(b) 0.3 M dicarboxylic acid in H_2O; 25°C.

(c) Alkyl carbons numbered from a carboxylic acid group.

(d) Fully protonated form not sufficiently soluble.

TABLE 23

^{13}C Chemical Shifts of Selected Aminocarboxylic Acids[a,b,c] in Aqueous Solution

Aminocarboxylic Acid	pH	CO_2	C_α	C_β	C_γ	C_δ	C_ϵ
Glycine	0.45	171.21	41.46				
	4.53	173.58	42.81				
	12.01	182.66	45.99				
α-alanine	0.43	173.97	50.09	16.53			
	4.96	176.98	51.87	17.45			
	12.52	185.67	52.73	21.66			
2-Aminobutyric Acid	0.40	173.39	55.32	24.46	9.63		
	5.11	176.06	57.21	25.00	9.74		
	12.81	184.75	58.67	28.89	10.44		
2-Aminovaleric Acid	0.51	173.63	54.06	33.04	18.91	14.05	
	4.97	176.32	56.02	33.80	18.96	14.11	
	12.97	185.06	57.10	38.17	19.56	14.54	
2-Aminocaproic Acid	0.55	173.63	54.30	30.67	27.38	22.17	14.58
	d						
	13.34	185.01	57.32	35.50	28.40	23.69	15.48
β-alanine	0.49	175.72	36.55	32.23			
	5.03	179.36	37.95	34.82			
	12.56	182.66	39.25	41.57			
4-Aminobutyric Acid	0.45	178.15	40.22	23.33	31.80		
	5.12	182.22	40.70	24.79	35.20		
	12.75	184.46	41.89	30.18	36.28		
5-Aminovaleric Acid	0.37	179.26	40.65	27.43	22.25	34.28	
	5.04	183.49	40.59	27.70	23.44	37.25	
	13.04	184.84	41.67	32.88	24.36	38.49	
6-Aminocaproic Acid	0.27	179.90	40.86	27.70	26.24	24.90	34.77
	5.13	183.82	40.81	27.76	26.51	26.08	37.68
	12.93	185.12	41.78	32.72	27.16	26.84	38.71
Valine	0.30	172.86	59.77	30.31	17.98,18.47[e]		
	5.64	175.43	61.76	30.31	17.84,19.15		
	12.60	184.07	63.17	32.93	17.88,20.26		
Leucine	0.37	173.97	52.79	40.11	25.12	22.06,22.74[e]	
	d						
	13.00	185.43	55.89	45.50	25.55	22.54,23.66	
Isoleucine	0.28	172.81	58.70	37.06	25.94(CH_2),15.26(CH_3)	12.06	
	6.04	175.33	60.89	37.10	25.60(CH_2),15.85(CH_3)	12.30	
	12.84	184.12	62.34	39.82	25.21(CH_2),16.72(CH_3)	12.25	

(a) In ppm vs external TMS. Positive shifts indicate deshielding relative to TMS.
(b) 0.3 M aminocarboxylic acid in H_2O; 25°C.
(c) Carbon atoms are numbered from the nitrogen.
(d) Zwitterion form of 2-aminocaproic acid and leucine not sufficiently soluble.
(e) Nonequivalent geminal methyl groups.

TABLE 24

^{13}C Chemical Shifts of Aminodicarboxylic Acids[a,b,c] in Aqueous Solution

Aminodicarboxylic Acid	pH	$CO_{2(alpha)}$	CO_2	C_α	C_β	C_γ	C_δ	C_ϵ
Aspartic Acid	0.41	172.03	174.36	50.60	34.96			
	6.73	175.48	178.73	53.46	37.78			
	12.73	183.39	181.26	55.26	44.48			
Glutamic Acid	0.32	172.62	177.42	53.41	26.13	30.70		
	6.95	175.77	182.42	55.98	28.22	34.68		
	12.51	183.88	184.02	57.20	33.03	35.31		
α-Aminoadipic Acid	0.46	173.05	178.83	53.99	30.26	20.94	34.09	
	7.04	176.01	183.73	55.89	31.47	22.64	38.02	
	12.55	184.60	184.60	57.20	35.93	23.46	38.66	
α-Aminopimelic Acid	0.40	173.39	179.80	54.09	30.65	24.78	24.78	34.48
	6.96	176.21	184.60	56.03	31.47	25.41	26.57	38.27
	12.92	185.04	185.04	57.20	35.84	26.18	27.06	38.66

(a) In ppm vs external TMS. Positive shifts indicate deshielding relative to TMS.

(b) 0.3 M aminodicarboxylic acid in H_2O; 25°C.

(c) Carbon atoms numbered from the nitrogen atom.

TABLE 25

^{13}C Chemical Shifts of α,ω-Diaminocarboxylic Acids[a,b,c] in Aqueous Solution

α,ω-diaminocarboxylic acid	pH	CO_2	C_α	C_β	C_γ	C_δ	C_ϵ
2,3-diaminopropionic acid	0.03	170.01	51.01	39.68			
	3.06	172.27	51.71	40.27			
	13.42	182.56	59.37	46.80			
2,4-diaminobutyric acid	0.31	171.93	51.76	28.89	37.47		
	4.47	174.85	53.87	29.48	37.95		
	13.51	184.43	55.43	38.98	38.98		
Ornithine	0.46	172.76	53.65	28.08	23.98	40.22	
	5.02	175.28	55.48	28.67	24.03	40.32	
	13.53	184.60	57.16	33.31	29.43	41.94	
Lysine	0.50	173.20	53.97	30.51	22.58	27.59	40.54
	6.03	175.78	55.86	31.15	22.58	27.65	40.54
	13.85	184.79	57.26	35.74	23.55	32.99	41.78

(a) In ppm vs external TMS. Positive shifts indicate deshielding relative to TMS.

(b) 0.2-0.3 M diaminocarboxylic acid in H_2O; 25°C.

(c) Carbon atoms numbered from the alpha-amino group.

such as different temperatures, reference compounds (both internal and external) and concentrations make comparison of chemical shift data difficult. However, with few exceptions (73), the agreement with literature values obtained under conditions similar to those used in this thesis is within 0.5 ppm. The protonation shifts calculated from the data in Tables 19-25 also are in agreement with those reported for a variety of amines (72,75), carboxylic acids (75), and amino acids (56,75).

ii) Alkyl Carbon Chemical Shift Parameters

The carbon-13 chemical shift parameters for alkyl carbons were derived from the alkyl carbon chemical shift data in Tables 19-25 by the stepwise, multiple regression analysis of Equation 100.

$$\delta_k = \delta_{S°} + \sum_{i=1}^{23} N_i\delta_i + \delta_{ac} \qquad (100)$$

δ_k is the chemical shift of the kth carbon; $\delta_{S°}$ a constant which accounts for the degree of substitution, S°, of the kth carbon; δ_i is an additive parameter for substituent i; and N_i the number of i substituents. δ_{ac} is a pair interaction term to account for the combined effects of both an amino and a carboxyl group bonded to the kth carbon; subscript a refers to the protonation state of the amino group (+ and 0 indicating protonated and deprotonated respectively) and subscript c represents that of the carboxyl group (0 and -). The substituent effect to which a parameter refers and the values derived for the parameters are presented in Table 26. The parameters were derived from 353 observational equations, with a multiple correlation coefficient of 0.998. The alkyl carbon of malonic acid was not used in the final derivation of the parameters because the quality of the fit for its methylene carbon indicated the need for a pair-interaction parameter for carbons having two directly bonded carboxylic acid substituents. Insufficient data was available to derive such a parameter.

The carbon-13 chemical shifts predicted by the parameters in Table 26 for the alkyl carbons of the molecules listed in Tables 19-25 have a standard error of the estimate of 0.88 ppm. Eighty-three percent of the predicted chemical shifts are within 1.0 ppm of the observed shift and the mean of the absolute value of the residuals is 0.60 ppm. These results compare favourably with the recent work of Sarneski et al (72). These authors determined the carbon-13 protonation shifts of aqueous amines and developed a parameter set based on the alkane parameter set of Lindeman and Adams (69) plus five additional parameters. With their parameter set, Sarneski et al predicted the carbon-13 chemical shifts of 48 aliphatic amines, with 69% of the predicted shifts falling within 1 ppm of the observed shifts.

TABLE 26

Chemical Shift Parameters for Alkyl Carbons of Amines, Carboxylic Acids and Amino Acids

			Value (ppm)	Standard Error (ppm)
δ_{1°	Primary carbon		20.07	
δ_{2°	Secondary carbon		39.75	0.26
δ_{3°	Tertiary carbon		56.56	0.55
δ_1	CH_3	1[a]	-11.21	0.27
δ_2	CH_3	2[a]	1.53	0.17
δ_3	CH_3	3	- 0.34	0.18
δ_4	CH_2	1	- 5.20	0.28
δ_5	CH_2	2	0.00	
δ_6	CH	1	0.47	0.39
δ_7	CH	2	- 1.52	0.21
δ_8	NH_2	1	7.14	0.28
δ_9	NH_2	2	3.00	0.19
δ_{10}	NH_2	3	- 2.21	0.20
δ_{11}	NH_2	4	0.22	0.22
δ_{12}	NH_2	5	0.20	0.34
δ_{13}	NH_3^+	1	6.22	0.27
δ_{14}	NH_3^+	2	- 1.53	0.18
δ_{15}	NH_3^+	3	- 2.70	0.20
δ_{16}	NH_3^+	4	- 0.40	0.19
δ_{17}	NH_3^+	5	0.00	
δ_{18}	CO_2^-	1	3.72	0.28
δ_{19}	CO_2^-	2	- 2.61	0.18
δ_{20}	CO_2^-	3	0.24	0.18
δ_{21}	CO_2H	1	0.00	
δ_{22}	CO_2H	2	- 3.65	0.21
δ_{23}	CO_2H	3	0.00	
δ_{+0}	NH_3^+-CO_2H Interaction[b]		- 3.82	0.42
δ_{+-}	NH_3^+-CO_2^- Interaction		- 5.82	0.40
δ_{o-}	NH_2-CO_2^- Interaction		- 5.13	0.40

a) CH_3 1 bond removed from the kth carbon, CH_3 2 bonds removed from the kth carbon, etc.

b) between amino and carboxyl substituents bonded to the kth carbon.

The protonation shifts given by Batchelor, Feeney and Roberts (75, Table II) suggest that the prediction of chemical shifts for amines, carboxylic acids and amino acids might be improved by having a separate parameter set for each type of carbon (1°, 2°, and 3°) in each type of molecule. Parameter sets have been calculated for primary, secondary and tertiary carbons from the data in Tables 19-25 for all three types of compounds and also from the amino acid data only. The four parameter sets are given in Tables 27 and 28. Although the standard error of the estimate was reduced somewhat over that obtained with the parameters in Table 26, the improvement is small considering the many more parameters required to fit the data.

As a consequence of the above results, the parameters given by Batchelor _et al_ (75) were re-examined and were found to be based on the observed shifts of single compounds. However, several of the compounds chosen give rise to anomalous shifts. For example, the amino protonation shifts of the CH_2 (3.28 ppm) and the CH (0.88 ppm) carbons of glycine and α-alamine, respectively are listed for the protonation shifts of CH_2 and CH carbons alpha to the amino group of amino acids. The values calculated from the appropriate model compound data given in this chapter are 1.54 ppm for the alpha CH_2 and 1.27 ppm for the alpha methine.

The model represented by Equation 100 considers the deshielding of the kth alkyl carbon, due to substitution

TABLE 27

Chemical Shift Parameters[a] for Primary, Secondary, and Tertiary Carbons of Amines, Carboxylic Acids, and Amino Acids.

Parameter			-CH-	$-CH_2-$	$-CH_3$
B_S			39.69	34.52	26.08
δ_1	CH_3	1[b]	-4.17	-8.98	0.00
δ_2	CH_3	2[b]	2.18	3.31	4.37
δ_3	CH_3	3	-0.10	-0.36	-0.93
δ_4	CH_2	1	-0.94	-4.01	-14.21
δ_5	CH_2	2	1.06	1.80	1.51
δ_6	CH	1	2.17	0.00	-10.14
δ_7	CH	2	-0.29	0.92	2.56
δ_8	NH_2	1	12.77	9.49	1.89
δ_9	NH_2	2	2.13	4.68	5.45
δ_{10}	NH_2	3	-3.21	-2.63	-2.39
δ_{11}	NH_2	4	-0.27	0.00	0.00
δ_{12}	NH_2	5	-0.17	0.00	0.57
δ_{13}	NH_3^+	1	13.57	8.48	0.00
δ_{14}	NH_3^+	2	-1.76	0.00	1.27
δ_{15}	NH_3^+	3	-2.91	-3.09	2.91
δ_{16}	NH_3^+	4	-0.37	-0.66	0.43
δ_{17}	NH_3^+	5	-0.02	-0.24	0.00
δ_{18}	CO_2^-	1	1.06	6.18	-1.60
δ_{19}	CO_2^-	2	-0.64	-1.14	0.00
δ_{20}	CO_2^-	3	-0.13	-0.15	-0.35
δ_{21}	CO_2H	1	0.62	2.48	-4.36
δ_{22}	CO_2H	2	0.76	-2.20	-1.47
δ_{23}	CO_2H	3	-0.80	-0.50	-0.73
δ_{+0}	$NH_3^+-CO_2H$[c]		0.00	-4.02	-
δ_{+-}	$NH_3-CO_2^-$		1.41	-6.36	-
δ	$NH_2-CO_2^-$		3.78	-4.19	-

a) In ppm vs external TMS.
b) CH_3 group 1 bond removed from kth carbon, CH_3 group 2 bonds removed from kth carbon etc.
c) Parameters for the interaction between amino and carboxyl substituents bonded to same carbon.

TABLE 28

Chemical Shift Parameters[a] for Primary, Secondary and Tertiary Alkyl Carbons of Amino Acids

Parameter			-CH-	-CH$_2$-	-CH$_3$
B_S			62.67	51.49	19.98
δ_1	CH_3	1[b]	-11.85	-17.89	0.00
δ_2	CH_3	2[b]	3.60	-0.63	0.00
δ_3	CH_3	3	0.49	0.00	2.58
δ_4	CH_2	1	-9.22	-8.48	-5.97
δ_5	CH_2	2	2.20	-2.43	-1.99
δ_6	CH	1	-8.25	0.00	0.00
δ_7	CH_2	2	-0.71	-3.37	0.00
δ_8	NH_2	1	0.00	1.10	0.00
δ_9	NH_2	2	3.06	0.66	0.00
δ_{10}	NH_2	3	-2.60	-2.44	-1.96
δ_{11}	NH_2	4	-0.30	0.37	0.00
δ_{12}	NH_2	5	-0.20	0.47	0.97
δ_{13}	NH_3^+	1	-1.64	0.00	0.00
δ_{14}	NH_3^+	2	-0.30	-4.09	-4.04
δ_{15}	NH_3^+	3	-2.34	-2.92	-2.64
δ_{16}	NH_3^+	4	-0.35	-0.39	-0.48
δ_{17}	CO_2^-	1	1.81	-2.55	0.00
δ_{18}	CO_2^-	2	0.00	-5.40	1.09
δ_{19}	CO_2^-	3	-0.33	-0.32	0.00
δ_{20}	CO_2H	1	0.00	-6.04	0.00
δ_{21}	CO_2H	2	-0.31	-6.28	0.00
δ_{22}	CO_2H	3	-1.09	0.00	-0.31
δ_{+-}	$NH_3^+CO_2H$[c]		0.00	-3.99	0.00
δ_{+-}	$NH_3^+CO_2^-$[c]		0.00	-6.13	0.00
δ_{0-}	$NH_2CO_2^-$[c]		0.00	-4.05	0.00

a) In ppm vs external TMS.

b) CH_3 group 1 bond removed from kth carbon, CH_3 group 2 bonds removed from kth carbon, etc.

c) Parameters for the interaction between amino and carboxyl substituents bonded to the same carbon.

at the various carbon atoms in the molecule, to be the sum of substituent independent and dependent parameters. The well known β effect (77), deshielding due to substitution at carbon atoms one bond removed (C_k-CH_3 → C_k-CH_2X, where X can be CH_3, CH_2, CH, NH_3^+, NH_2, CO_2H or CO_2^-) is represented by δ_1 and δ_4 as a substituent independent deshielding of 6.01 ppm upon substitution of one β hydrogen and by δ_4 and δ_6 as an additional deshielding of 5.67 ppm upon further substitution (to C_k-CHXY). The appropriate substituent parameters, for example δ_9 when X or Y is NH_2, account for the dependence of the total deshielding upon the nature of the substituting group. The shielding of the kth carbon at carbon atoms two bonds removed from the kth carbon, the γ effect, (C_k-C-CH_3 → C_k-C-CH_2X) has been factored into similar components. Parameters δ_2 and δ_5 indicate an increase in shielding of 1.53 ppm upon the initial substitution and δ_5 and δ_7 suggest further substitution (to C_k-C-CHXY) causes an additional substituent-independent shielding of 1.52 ppm.

In addition to the substitution at remote carbons, the model represented by Equation 100 also correlates the chemical shift of the kth carbon to its degree of substitution and to the nature of the directly bonded substituents. The degree to which the effect of these molecular features is additive is indicated by the agreement between calculated and observed shifts. The success of this model is comparable to that achieved by Lindeman and Adams for branched alkanes (69).

The alpha carbons of alpha amino acids exhibit anomolous chemical shift behavior with respect to the additivity of parameters derived from amine and carboxylic acid data for directly-bonded amine and carboxyl substituents. This anomolous behavior was observed previously for the zwitterionic form of alpha amino acids (40,42) and the calculated alpha carbon chemical shifts, as predicted by a model based on the alkane parameter set of Grant and Paul (68), were corrected by the addition of a 6.0 ppm upfield shift. The interaction parameters of Table 26 were derived to account for the unusual chemical shift behavior of carbons bearing both an amino and a carboxyl group. The value of -5.82 ppm for δ_{+-} is in excellent agreement with the value of 6.0 ppm used by Sternlicht and co-workers (40,42) for the zwitterionic form of amino acids. Examination of the other interaction parameters in Table 26 indicates that the magnitude of these parameters is dependent upon the protonation state of the directly bonded amino and carboxyl substituents. Litchman and Grant (78) also found that similar interaction parameters were necessary to correlate the cmr shifts of polyhalomethanes.

Further examination of the results reported in this chapter and in previous publications (68,69,72,79) allows several conclusions to be drawn regarding the use of linear parameterization schemes for the prediction of carbon-13 chemical shifts. It appears that mutual interaction between the functional groups in polyfunctional molecules produces small chemical shift effects which cannot be predicted from model compound data, for functional groups which undergo simultaneous deprotonation. For example, the C_2 carbon resonance of n-propyl amine and the C_β resonance of 2-aminobutyric acid and 4-aminobutyric acid shift by 4.75, 3.89 and 5.39 ppm, respectively, upon deprotonation of their amino groups. The presence of the carboxylate group obviously alters the chemical shift effect of an amino group two bonds removed. For simultaneously deprotonating groups, the effect of the second group cannot be observed since the influence of the two groups cannot be isolated in any pH range. These effects are particularly evident for carbons bonded to more than one functional group and for the zwitterionic form of amino acids (40,42,79). As a consequence, parameterization schemes which provide excellent results when used to predict the chemical shifts of the model compounds from which the parameters were derived, may yield only rough estimates for the intermediate shifts of polyfunctional molecules.

iii) Carboxyl Carbon Chemical Shift Parameters

Parameters for the prediction of the carbon-13 chemical shifts of the carboxyl carbons of the molecules in Tables 21-25 were derived from the stepwise, multiple regression analysis of Equation 101:

$$\delta_{CO_2} = \delta_p + \sum_{i=1}^{22} N_i \delta_i \qquad (101)$$

δ_p is a constant, with the subscript p indicating the protonation state of the carboxylic acid group (- if deprotonated and 0 if protonated); δ_i is an additive parameter for substituent i and N_i is the number of such substituents. The interaction parameter (δ_{ac}) used in Equation 100 is unnecessary as the parameters for the amino group will implicitly account for any interaction effects. The values listed in Table 29 for the parameters were derived from ninety-four observational equations with a multiple correlation coefficient of 0.995.

Using the parameters in Table 29 to predict chemical shifts for the carboxylic acid carbons of the molecules in Tables 21-25, the standard error of the estimate is 0.56 ppm and the mean of the absolute value of the residuals is 0.40 ppm. Ninety-eight percent of the calculated shifts are within 1.0 ppm of the observed shift.

The β effect for carboxyl carbons can be determined from δ_1 and δ_5 to be a 2.56 ppm downfield shift. Further

TABLE 29

Chemical Shift Parameters for Carboxyl Carbons of Carboxylic Acids and Amino Acids

			Value (ppm)	Standard Error (ppm)
δ_-	Deprotonated CO_2		182.09	
δ_0	Protonated CO_2		178.47	0.16
δ_1	CH_3	1^a	0.00	
δ_2	CH_3	2^a	0.64	0.29
δ_3	CH_3	3	- 0.27	0.23
δ_4	CH_3	4	0.15	0.18
δ_5	CH_2	1	2.56	0.43
δ_6	CH_2	2	0.00	
δ_7	CH	1	5.08	0.58
δ_8	CH	2	- 0.43	0.33
δ_9	NH_2	2	- 2.35	0.38
δ_{10}	NH_2	3	- 2.01	0.37
δ_{11}	NH_2	4	- 0.21	0.35
δ_{12}	NH_2	5	0.00	
δ_{13}	NH_2	6	0.28	0.35
δ_{14}	NH_3^+	2	-10.26	0.36
δ_{15}	NH_3^+	3	- 4.48	0.28
δ_{16}	NH_3^+	4	- 2.09	0.28
δ_{17}	NH_3^+	5	- 1.36	0.27
δ_{18}	NH_3^+	6	- 0.74	0.27
δ_{19}	CO_2^-	2	- 6.15	0.43
δ_{20}	CO_2^-	3	- 1.17	0.28
δ_{21}	CO_2^-	4	- 0.55	0.26
δ_{22}	CO_2H	2	- 8.90	0.44
δ_{23}	CO_2H	3	- 2.19	0.34
δ_{24}	CO_2H	4	- 1.50	0.33

a) CH_3 1 bond removed from the carboxyl carbon, CH_3 2 bonds removed from the carboxyl carbon, etc.

substitution (to C_k-CHXY) leads to an additional deshielding of 2.52 ppm. As was previously noted for alkyl carbons, the γ effect is marked by an increase in shielding. δ_2 and δ_5 indicate an initial shift of -1.52 ppm and further substitution at the gamma position results in an additional 1.52 ppm upfield shift. These values represent the substituent-independent portion of the observed shift, with additional parameters being used to predict the effects of the various substituents.

Comparison of the substituent independent fractions of the β and γ effects, as predicted by the parameters in Table 26 for alkyl carbons and in Table 29 for carboxyl carbons, indicates that the direction of the observed shift is the same for both types of carbon atoms. However, the β effect is approximately two times as great for alkyl carbons as for carboxyl carbons. The magnitude of the substituent independent fraction of the γ effect is approximately the same in both cases.

Parameters δ_- and δ_0 from Table 29 indicate that deprotonation of the carboxylic acid group results in a deshielding of the carboxyl carbon of 3.62 ppm. From Table 26, parameters δ_{21} and δ_{18} indicate a deshielding of 3.72 ppm for an alkyl carbon one bond removed and, from δ_{22} and δ_{19}, a deshielding of 1.04 ppm for an alkyl carbon two bonds removed upon deprotonation of a carboxylic acid group in carboxylic acids or amino acids.

The results presented in this chapter indicate that linear parameterization schemes can be developed to predict the carbon-13 chemical shifts of alkyl and carboxyl carbons of amines, carboxylic acids and amino acids in aqueous solution. The mutual interaction effects of simultaneously deprotonation functional groups cannot be predicted with sufficient accuracy for use in the calculation of microscopic acid dissociation constants from common resonance chemical shift data. The chemical shift parameters should, however, be of value in the assignment of observed chemical shifts to the carbons of peptides and proteins as well as amines, carboxylic acids and amino acids.

BIBLIOGRAPHY

1. A.L. Lehninger, "Biochemistry", Worth Publishers Inc., New York, N.Y., 1970. p. 74.
2. A.I. Vogel, "Quantitative Inorganic Analysis", 3rd ed., John Wiley and Sons Inc., New York, N.Y., 1961. Appendix 17, pp. 1167-1168.
3. J. Clark and D.D. Perrin, Quart. Rev., 18, 295 (1964).
4. H. Borsook, E.L. Ellis, and H.M. Huffman, J. Biol. Chem., 117, 281 (1937).
5. E.J. Cohn and J.T. Edsall, "Proteins, Amino Acids and Peptides", Reinhold Publ. Corp., New York, N.Y., 1943. p. 84.
6. M. Calvin, "Glutathione", Academic Press Inc., New York, N.Y., 1954. p. 9.
7. L.R. Ryklan and C.L.A. Schmidt, Arch. Biochem., 5, 89 (1944).
8. S.J. Rogers, J. Chem. Ed., 46, 239 (1969).
9. J.T. Edsall and M.H. Blanchard, J. Amer. Chem. Soc., 55, 2337 (1933), and references therein.
10. A. Bryson, N.R. Davies, and E.P. Serjeant, J. Amer. Chem. Soc., 85, 1933 (1963).
11. J.T. Edsall, R.B. Martin, and B.R. Hollingworth, Proc. Nat'l. Acad. Sci., (U.S.A.) 44, 505 (1958).
12. R.B. Martin, J. Phys. Chem., 75, 2657 (1971).
13. M.A. Grafius and J.B. Neilands, J. Amer. Chem. Soc., 77, 3389 (1955).

14. P.J. Niebergall, R.L. Schnaare, and E.T. Sugita, J. Pharm. Sci., 61, 232 (1971).

15. R.B. Martin and J.T. Edsall, Bull. Soc. Chim. Biol., 40, 1763 (1958).

16. R.B. Martin, J. Phys. Chem., 65, 2053 (1961).

17. K.N. Pearce and L.K. Creamer, Aust. J. Chem., 28, 2409 (1975).

18. D.P. Wrathall, R.M. Izatt, and J.J. Christensen, J. Amer. Chem. Soc., 86, 4779 (1964).

19. E.W. Wilson and R.B. Martin, Arch. Biochem. Biophys., 142, 445 (1971).

20. E. Coates, C.C. Marsden, and B. Riggs, Trans. Faraday Soc., 65, 3032 (1969).

21. P. Paoletti, R. Barbucci, A. Vacca, and A. Dai, J. Chem. Soc.(A), 310 (1971).

22. R.E. Benesch and R. Benesch, J. Amer. Chem. Soc., 77, 5877 (1955).

23. G.E. Clement and T.P. Hartz, J. Chem. Ed., 48, 395 (1971).

24. G. Schill and K. Gustavii, Acta. Pharm. Suecica, 1, 24 (1964).

25. S. Riegleman, L.A. Strait, and E.Z. Fisher, J. Pharm. Sci., 51, 129 (1962).

26. E.L. Elson and J.T. Edsall, Biochemistry, 1, 1 (1962).

27. E. Grunwald, A. Lowenstein, and S. Meiboome, J. Chem. Phys., 27, 641 (1957).

28. A. Lowenstein and J.D. Roberts, J. Amer. Chem. Soc., 82, 2705 (1960).

29. N.E. Rigler, S.P. Bag, D.E. Leyden, J.L. Sudmeir, and C.N. Riley, Anal. Chem., 37, 892 (1965).

30. U.W. Kesselring and L.Z. Benet, Anal. Chem., 41, 1535 (1969).

31. D.B. Walters and D.E. Leyden, Anal. Chim. Acta., 72, 275 (1974).

32. H.S. Creyf, L.C. van Poucke, and Z. Eeckaut, Talanta, 20, 973 (1973).

33. J. Hine, F.A. Via, and J.H. Jensen, J. Org. Chem., 36, 2926 (1971).

34. J. Hine and W-S. Li, J. Org. Chem., 40, 1795 (1975).

35. D.L. Rabenstein, J. Amer. Chem. Soc., 95, 2797 (1973).

36. J.S. Cohen, R.I. Shrager, M. McNeel, and A.N. Schechter, Nature, 228, 642 (1970).

37. D.H. Sachs, A.N. Schechter, and J.S. Cohen, J. Biol. Chem., 246, 6576 (1971).

38. J.S. Cohen, C.T. Yim, M. Kandel, A.G. Gornall, S.I. Kandel, and M.H. Freedman, Biochem., 11, 327 (1972).

39. A.R. Quirt, J.R. Lyerla, Jr., I.R. Peat, J.S. Cohen, W.F. Reynolds and M. Freedman, J. Amer. Chem. Soc., 95, 570 (1974).

40. W.J. Horsley and H. Sternlicht, J. Amer. Chem. Soc., 90, 3738 (1968).

41. R. Hagen and J.D. Roberts, J. Amer. Chem. Soc., 91, 4504 (1969).

42. W.J. Horsley, H. Sternlicht, and J.S. Cohen, Biochem. Biophys. Res. Comm., 37, 47 (1969); W.J. Horsley, H. Sternlicht and J.S. Cohen, J. Amer. Chem. Soc., 92, 680 (1970).

43. M. Christl and J.D. Roberts, J. Amer. Chem. Soc., 94, 4565 (1972).

44. M.H. Freedman, J.R. Lyerla, I.M. Chaiken, and J.S. Cohen, Eur. J. Biochem., 32, 215 (1973).

45. M.T. Fairhurst, Ph.D. Thesis, University of Alberta, 1975.

46. Y. Fujii, E. Kyuno, and R. Tsuchiya, Bull. Chem. Soc. Japan, 43, 786 (1970).

47. A. Albert and E.P. Serjeant, "The Determination of Ionization Constants", 2nd ed., Chapman and Hall, London, 1971. p. 13.

48. Reference 2, p. 242.

49. C.W. Davies, "Ion Association", Butterworths, Washington, D.C., 1962. p. 39.

50. L. Meites, "Handbook of Analytical Chemistry", McGraw Hill, New York, N.Y., 1963. pp. 1-8.

51. H. Irving and H.S. Rossotti, J. Chem. Soc., 3397 (1953).

52. J.L. Dye and V.A. Nicely, J. Chem. Ed., 48, 443 (1971).

53. W.E. Wentworth, J. Chem. Ed., 42, 162 (1965).

54. J.H. Bradbury and L.R. Brown, Eur. J. Biochem., 40, 565 (1973).

55. P.J. Niebergall, R.L. Schnaare, and E.T. Sugita, J. Pharm. Sci., 62, 656 (1973).

56. R.I. Shrager, J.S. Cohen, S.R. Heller, D.H. Sachs and A.N. Schechter, Biochem., 11, 541 (1972).

57. H-L. Fung and L. Chen, J. Chem. Ed., 51, 107 (1974).

58. F.J.C. Rossotti, H.S. Rossotti, and R.J. Whewell, J. Inorg. Nucl. Chem., 33, 2051 (1971).

59. H.S. Rossotti, Talanta, 21, 809 (1974).

60. S.D. Christian, E.H. Lane, and F. Garland, I. J. Chem. Ed., 51, 475 (1974); II. J. Phys. Chem., 78, 557 (1974).

61. D.E. Sands, J. Chem. Ed., 51, 473 (1974).

62. W.E. Deming, "Statistical Adjustment of Data", Dover, New York, N.Y., 1964.

63. H.L. Youmans, "Statistics for Chemistry", C.E. Merrill, Columbus, Ohio, 1973.

64. R.W. Hay and P.J. Morris, J. Chem. Soc., Perkin II, 1021 (1972).

65. M.H.T. Nyberg and M. Cefola, Arch. Biochem. Biophys., 111, 327 (1965).

66. G. Schwarzenbach, B. Massen, and H. Ackerman, Helv. Chim. Acta., 35, 2333 (1952).

67. D.L. Rabenstein, R. Ozubko, S. Libich, C.A. Evans, M.T. Fairhurst and C. Suvanprakorn, J. Coord. Chem., 3, 263 (1974).

68. D.M. Grant and E.G. Paul, J. Amer. Chem. Soc., 86, 2984 (1964).

69. L.P. Lindeman and J.Q. Adams, Anal. Chem., 43, 1245 (1971).

70. J.D. Roberts, F.J. Weigert, J.I. Kroschurtz, and H.J. Reich, J. Amer. Chem. Soc., 92, 1338 (1970).

71. H. Eggert and C. Djerassi, J. Amer. Chem. Soc., 95, 3710 (1973).

72. J.E. Sarneski, H.L. Suprenant, F.K. Molen, and C.N. Reilly, Anal. Chem., 47, 2116 (1975).

73. S. Tran-Dinh, S. Fermandjian, E. Sala, R. Mermet-Bouvier, M. Cohen, and P. Fromageot, J. Amer. Chem. Soc., 96, 1484 (1974).

74. W. Voelter, G. Jung, E. Brietman and E. Bayer, Z. Naturforsch, 26, 213 (1971).

75. J.G. Batchelor, J. Feeney, and G.C.K. Roberts, J. Mag. Res., 20, 19 (1975).

76. M.B. Hayes, J.S. Cohen, and M.L. McNeel, Mag. Res. Rev., 3, 1 (1974).

77. J.B. Stothers, "Carbon-13 Nuclear Magnetic Resonance Spectroscopy", Academic Press, New York, N.Y., 1972. p. 56.

78. W.M. Litchman and D.M. Grant, J. Amer. Chem. Soc., 90, 1400 (1968).

79. J.L. Sudmier and C.N. Reilley, Anal. Chem., 36, 1698 (1964).

Part II

THE AQUEOUS SOLUTION CHEMISTRY OF TRIMETHYLLEAD AND TRIMETHYLLEAD CARBOXYLIC ACID COMPLEXES

CHAPTER VII

INTRODUCTION

The importance of heavy metals in environmental pollution is well established (1). Of the heavy metals commonly found in the environment, lead is of great concern because of its high toxicity and its widespread occurence, both in nature (2) and in use by man (3). Due to their use as antiknock agents in fuel for internal combustion engines (3), organic compounds of lead are especially widespread throughout the environment. Although much of the lead dispersed by man is eventually washed into natural waters (4), very little is known about the aqueous solution chemistry of organolead compounds. In their monograph on the organic compounds of lead, Shapiro and Frey (5) note that although the first coordination compound of organolead was reported in 1887, very little subsequent work has appeared in the literature. Studies in aqueous solution are particularly sparse, most reviews concentrating on reactions in non-aqueous solvents (6,7) or on related systems such as organomercury and -tin (8).

Recently, Wong, Chau, and Luxon (9) have reported the methylation of certain organic and inorganic lead compounds by microorganisms in lake sediments. Although not all of the sediment samples examined produced tetramethyllead ($(CH_3)_4Pb$) from inorganic lead, in all cases the transformation of trimethyllead ($(CH_3)_3Pb^+$) acetate to $(CH_3)_4Pb$ was observed. Although the organometallic chemistry of trimethyllead has been the subject of much study (3,5,7,8), its aqueous solution chemistry and coordination chemistry have not been characterized (8). Such fundamental information is essential for developing treatments for organolead poisoning. Inhalation or absorption of tetraalkyl lead compounds results in the presence of lead in the fluids and tissues of the body, primarily as dissolved trialkyl lead salts (10). Chelation therapy, a common form of treatment for inorganic lead poisoning (11), has thus far proven to be ineffective in the treatment of organic lead poisoning due to the lack of an effective chelating agent for organic lead salts (10).

In response to the need for information on the fundamental solution chemistry and coordination chemistry of alkyl lead salts in an aqueous environment, a programme directed towards characterizing the aqueous solution chemistry of trimethyllead and its complexes has been initiated at the University of Alberta. In Part II of this thesis, the results of a study of trimethyllead and of trimethyllead complexes of selected carboxylic acids, in an aqueous environment, is reported. The acid-base chemistry of $(CH_3)_3Pb^+$ has been studied at various concentration levels by both potentiometry and proton magnetic resonance spectroscopy. The formation constants of the trimethyllead complexes of five carboxylic acids with pK_A values ranging from 3.40 to 4.65 have been determined from pmr chemical shift data. The relationship between the magnitudes of the $(CH_3)_3Pb^+$ formation constant and the ligand pK_A is discussed.

A. The Study of the Solution Chemistry of Metal Complexes by Nuclear Magnetic Resonance Spectroscopy

The use of nuclear magnetic resonance (nmr) spectroscopy to study the solution chemistry of ions and complexes is well established (12) and the technique has been applied to a variety of systems (13). The wide range of application of the nmr technique is due to the variety of ligands which contain nmr active nuclei whose chemical shifts are sensitive to complexation reactions. In addition, for organometallic ions, the chemical shift and, if the metal has an isotope of $I = \frac{1}{2}$, the metal-proton coupling constant also provide information about the complexation reactions at the molecular level. (Naturally-occurring lead contains 22.6% lead-207, whose $I = \frac{1}{2}$). In view of the detailed information which has been obtained from pmr studies of the coordination chemistry of methylmercury (14), proton magnetic resonance is the principal technique being used in this study of trimethyllead chemistry.

CHAPTER VIII

EXPERIMENTAL

A. Chemicals

The carboxylic acids were of the highest grade commercially available and were used without further purification. Sodium formate was used as the source of formate ligand. The trimethyllead-acetic acid studies were carried out using trimethyllead acetate (Alfa Inorganics) as the source of both $(CH_3)_3Pb^+$ and acetate.

Trimethyllead acetate was the only water soluble form of trimethyllead commercially available and was converted to a stock solution of trimethyllead perchlorate prior to use in the acid-base and complexation studies. An initial attempt to extract $(CH_3)_3PbOH$ from benzene, using a method developed for triethyllead chloride (15), yielded only an insoluble, gelatinous mass of unknown composition. Ion exchange has been used to remove acetate from methylmercuric hydroxide solutions (16), and the following method was developed for the conversion of $(CH_3)_3PbO_2CCH_3$ to trimethyllead perchlorate.

An approximately 0.25 M solution of trimethyllead acetate is passed through an anion exchange column (Dowex 2 x 8) in the hydroxide form. The eluate is then checked for acetate by examining the pmr spectrum, at high signal amplitude, for the acetate resonance. (In basic solution, the resonance due to the protons of the acetate methyl group is located approximately 0.67 ppm downfield from the tert-butyl resonance of tertiary butanol and is detectable at concentration levels $\geq$ 0.001 M). If a detectable concentration of acetate is present, the solution is passed through the column a second time. The ion exchange resin was regenerated with 100 ml of 1 M NaOH prior to each passage of trimethyllead through the column. Due to residual impurities on the column, the resin was changed after every 500 ml of trimethyllead solution. The ion exchanged $(CH_3)_3PbOH$ solution was neutralized with concentrated perchloric acid and was stored, tightly sealed, in the dark (15). Before use, the stock solution of $(CH_3)_3PbClO_4$ was standardized with NaOH as described below.

The sodium hydroxide solutions used in all phases of this work were prepared from a saturated solution of carbonate-free NaOH and doubly distilled water. Standardization of NaOH was carried out using potassium hydrogen phthalate as described by Vogel (17).

B. pH Measurements

All pH measurements were made at 25 ± 1°C using an Orion Model 701 digital pH meter equipped with a standard glass electrode-porous ceramic junction, saturated calomel electrode pair. For solutions containing perchlorate ion, electrical contact between the solution and the calomel electrode was made via a salt bridge containing 4.0 M NaCl solution to avoid precipitation of $KClO_4$ in the liquid junction. The pH meter was calibrated using Fisher certified standard solutions of pH 4.00, 7.00 and 10.00.

C. NMR Measurements

The proton magnetic resonance measurements were obtained on a Varian A-60-D high resolution spectrometer at a probe temperature of 25 ± 1°C (see Chapter III, Part C).

Chemical shifts were measured relative to the central resonance of the tetramethylammonium (TMA) ion or the tert-butyl resonance of t-butanol, the choice of standard depending upon which allowed use of the narrower sweep width. The chemical shifts are reported vs DSS, as described in Chapter II, and are the average of at least two scans.

D. Solution Preparation

i) PMR Studies

Solutions for the pmr studies were prepared from an aliquot of stock $(CH_3)_3PbClO_4$ solution and the appropriate amount of sodium perchlorate and/or carboxylic acid. All solutions were prepared using doubly distilled water.

For the acid-base studies, the initial sample was taken at a pH no higher than 5. Samples were taken approximately every 0.3 pH unit to a maximum pH between 11 and 12.

The initial pH of the $(CH_3)_3Pb^+$-carboxylic acid solutions was reduced to a value about 3.0 pH units below the pK_a of the acid in order to obtain the chemical shift of the fully protonated acid and of the free $(CH_3)_3Pb^+$ ion. For acids with a pK_a below 3.75, a minimum pH of 0.75 was used. Samples were taken every 0.3 of a pH unit to a pH value 3.0 pH units above the pK_a of the acid and then every pH unit to a maximum pH of 11.00.

All pH adjustments were made with concentrated $HClO_4$ or carbonate-free NaOH solution. The temperature was maintained at 25 ± 1°C using a water bath.

ii) Potentiometric Studies

The solutions used in the potentiometric studies were prepared from an aliquot of the stock trimethyllead perchlorate. Crystalline $NaClO_4$ was added to give a total ionic strength of about 0.3 M. If necessary, the initial pH was adjusted to a value below pH 3.0 with $HClO_4$ prior to the beginning of the titration. A stream of nitrogen was passed over the solution to reduce exposure of the solutions to atmospheric carbon dioxide. All titrations were carried out using carbonate-free NaOH and all solutions were maintained at 25 ± 1° C using a water bath.

E. Calculations

The calculations were performed using a Hewlett-Packard Model HP-65 programmable electronic calculator.

F. Standardization of Trimethyllead Stock Solutions

The ion exchanged $(CH_3)_3Pb^+$ stock solutions were standardized by potentiometric titration using a glass electrode. The titrations were carried out using carbonate-free NaOH and the ionic strength was controlled using $NaClO_4$.

To insure complete neutralization of all the $(CH_3)_3PbOH$ present in solution, the initial pH was reduced to a value between 2 and 3 using concentrated $HClO_4$. The solution is thus a mixture of a strong acid ($HClO_4$) and a weak acid ($(CH_3)_3Pb^+$) and the titration yields two inflection points. Titration of the added perchloric acid yields a sharp inflection point at pH 6.0 and the $(CH_3)_3Pb^+$ a rather poorly defined inflection point between pH 10 and 11. The exact position of the $(CH_3)_3Pb^+$ endpoint was determined using a second derivative plot of the titration curve (18). The titration with base converts the trimethyllead from $(CH_3)_3Pb^+$ to $(CH_3)_3PbOH$. Consequently, the amount of NaOH added between the first and second endpoints provides the concentration of trimethyllead in the stock solution.

Since the possibility of dimer formation exists in basic solution, (see Chapter IX), the potentiometric method was verified by determining the trimethyllead concentration of several stock solutions using atomic absorption spectroscopy.

The atomic absorption measurements were made at the 283.3 nm line using a Perkin-Elmer 290-B atomic absorption spectrophotometer. A working curve was prepared using $Pb(NO_3)_2$ and a 0.1 M solution of the disodium salt of ethylenediaminetetraacetic acid was used as a common matrix. Standard solutions were prepared containing 10 to 40 μg per ml of lead and an aliquot of the trimethyllead stock solution was diluted to yield a solution of approximately 20-30 μg/ml of lead. Although the atomic absorption results tended to be slightly higher than the trimethyllead concentrations obtained by potentiometry, the agreement is sufficient to support the potentiometric standardization.

In addition, a method based upon the oxidation of trimethyllead to Pb^{2+} followed by an EDTA titration (19), has yielded results in excellent agreement with those obtained by pH titration. Consequently, we may safely assume that only $(CH_3)_3PbOH$ is present at the endpoint of the potentiometric titration.

CHAPTER IX

NUCLEAR MAGNETIC RESONANCE STUDIES OF THE AQUEOUS SOLUTION CHEMISTRY OF TRIMETHYLLEAD

A. The Acid-Base Chemistry of Trimethyllead

The proton magnetic resonance spectrum of trimethyllead is shown in Figure 21. The spectrum consists of a singlet flanked by two less intense satellite lines. The central resonance is assigned to the protons of methyl groups bonded to isotopes of lead having a nuclear spin of zero while the satellites are due to methyl groups bonded to lead-207 ($I = \frac{1}{2}$, 22.6% natural abundance). The chemical shift is given by the position of the central resonance; the lead-proton coupling constant by the separation of the satellite lines. The chemical shift of the methyl resonance and the lead-proton spin-spin coupling constant for a trimethyllead solution containing no coordinating ligand other than hydroxide ion are pH dependent. The chemical shift of the central resonance is shown as a function of pH in Figure 22 for a 0.140 M solution of trimethyllead perchlorate (bottom curve). The coupling constant is shown as a function of pH in Figure 23. The pH dependence is due to the formation of trimethyllead hydroxide complex(es) as the pH is increased from acidic to basic.

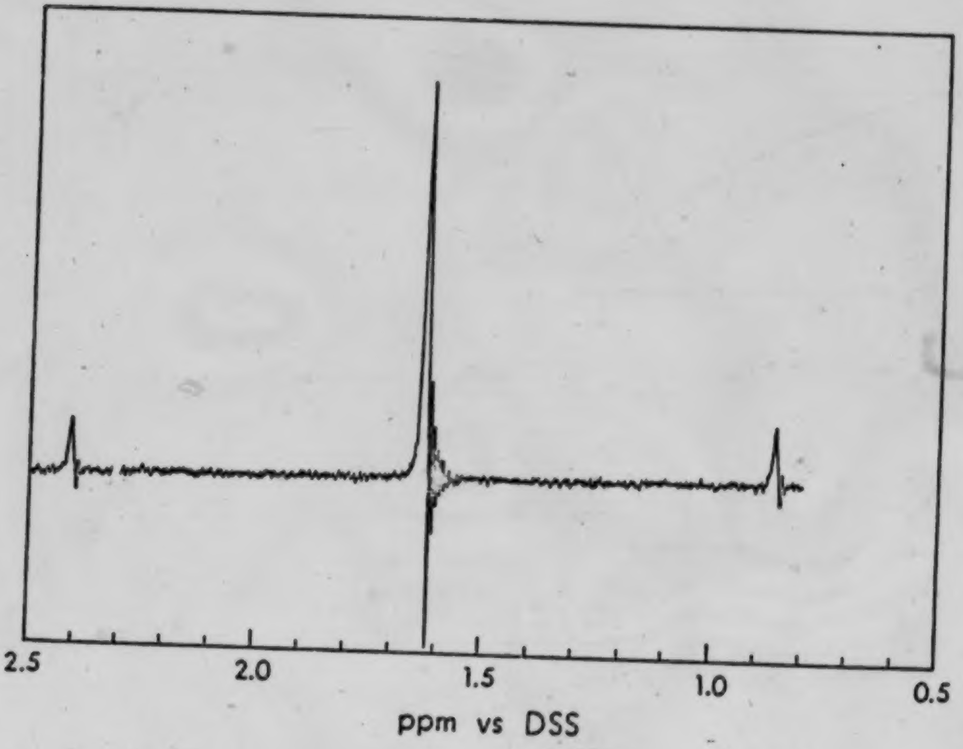

Figure 21. PMR spectrum of the methyl groups of trimethyllead in a 0.140 M solution at approximately neutral pH.

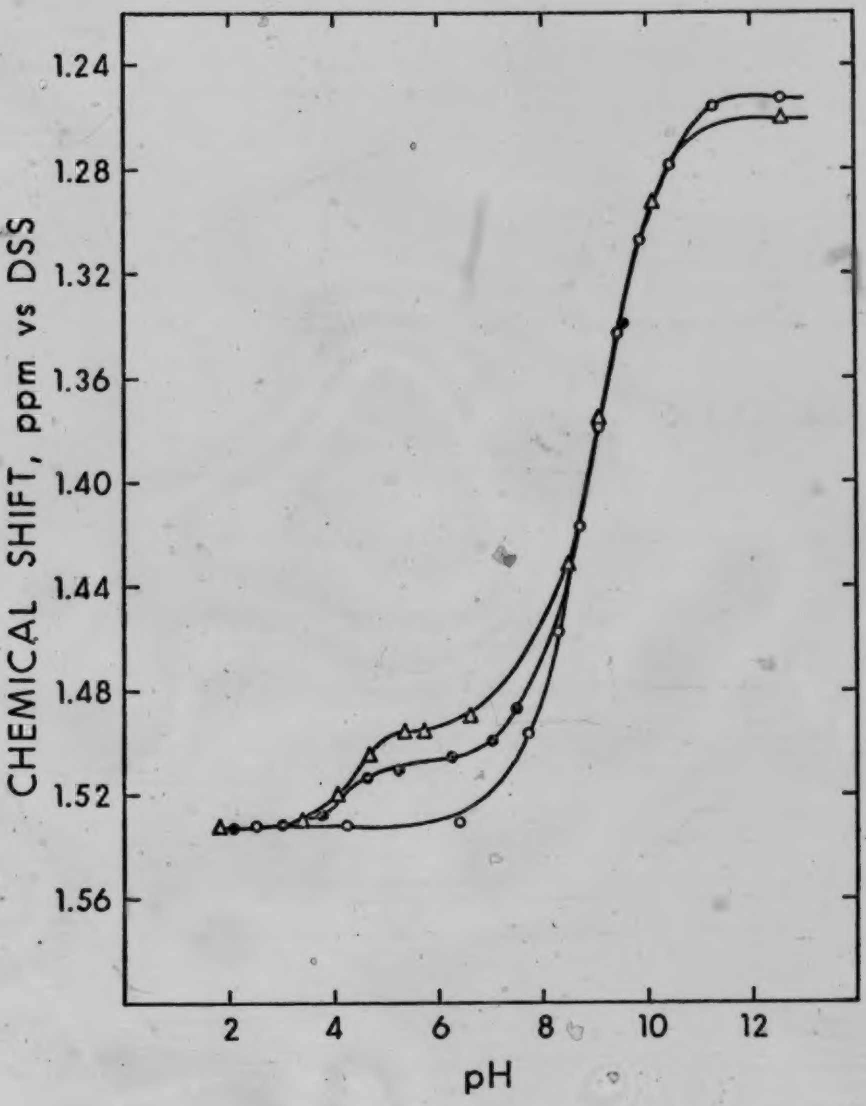

Figure 22. pH dependence of the methyl protons of trimethyllead in a 0.140 M aqueous solution, in an aqueous solution containing 0.153 M trimethyllead and 0.071 M pivalic acid and in an aqueous solution containing 0.102 M trimethyllead and 0.093 M pivalic acid.

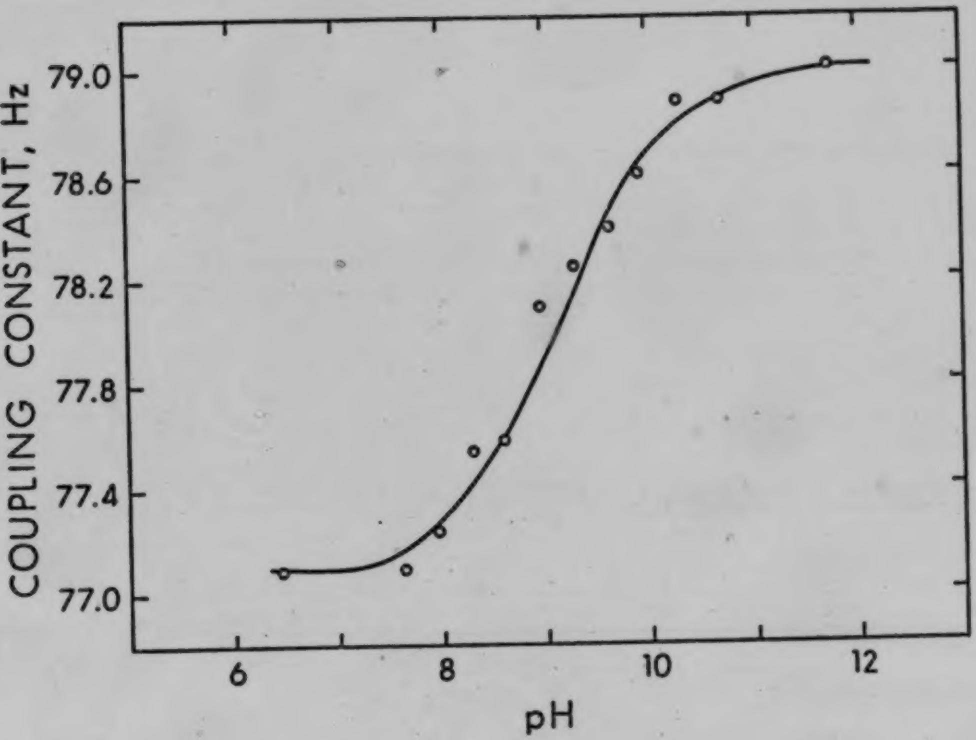

Figure 23. pH dependence of the lead 207-proton coupling constant in a 0.140 M aqueous solution.

$$(CH_3)_3Pb^+ + OH^- \rightleftarrows (CH_3)_3PbOH \qquad (1)$$

$$K_1 = \frac{[(CH_3)_3PbOH]}{[(CH_3)_3Pb^+]a_{OH^-}} \qquad (2)$$

K_1 is the formation constant for $(CH_3)_3PbOH$ and a_{OH^-} is the hydroxyl ion activity. Waters of solvation have been neglected for simplicity.

As was shown in Chapter III, if chemical exchange is rapid on the nmr time scale, the observed chemical shift will be a weighted average of the chemical shifts of the various molecular forms present in solution. For a system described by Equation 1 we may write:

$$\delta_{obs} = P_f\delta_f + P_c\delta_c \qquad (3)$$

where δ_{obs} is the observed chemical shift of the methyl resonance; P_f and P_c are the fractions of the total concentration of trimethyllead which are in the free ($(CH_3)_3Pb^+$) and complexed ($(CH_3)_3PbOH$) forms, respectively; δ_f and δ_c are the chemical shifts of the free and complexed forms. If the trimethyl lead is present only in the free and 1:1 complexed[1] forms, $P_f + P_c = 1$ and Equation 3 can be rewritten as:

---

[1] A 1:1 complex contains 1 molecule of trimethyllead and 1 ligand molecule.

$$\delta_{obs} = (1 - P_c)\delta_f + P_c\delta_c \tag{4}$$

which rearranges to

$$P_c = \frac{\delta_{obs} - \delta_f}{\delta_c - \delta_f} \tag{5}$$

To determine K_1 from the chemical shift titration data, Equation 2 is written in terms of P_c and a_{H^+}.

$$K_1 = \frac{P_c}{1-P_c} \cdot \frac{a_{H^+}}{K_w} \tag{6}$$

where a_{H^+} is the hydrogen ion activity and $K_w = 1.0 \times 10^{-14}$.

When the chemical shift titration data represented by the open points in Figure 22 was analysed using Equations 5 and 6, the log K_1 values obtained decreased continuously with decreasing pH. A systematic drift of this type indicates the presence of a second equilibrium (20).

By analogy to the solution equilibria for methylmercury (16,21,22) dimer formation is a possible second equilibrium.

$$(CH_3)_3PbOH + (CH_3)_3Pb^+ \rightleftarrows ((CH_3)_3Pb)_2\overset{+}{O}H \tag{7}$$

$$K_2 = \frac{[((CH_3)_3Pb)_2^+OH]}{[(CH_3)_3Pb^+][(CH_3)_3PbOH]} \qquad (8)$$

If a second equilibrium of the type described by Equation 7 is present, reducing the total concentration of trimethyl lead present in solution should reduce the concentration of dimer formed. Consequently, the values obtained for log K_1 from the chemical shift data should become pH independent at a sufficiently low concentration. As a result, pmr titrations were performed on solutions containing total trimethyllead concentrations of 0.069 M, 0.034 M, 0.014 M, and 0.004 M.

The ionic strength was maintained at about 0.3 M with sodium perchlorate. The chemical shift and coupling constant data and the log K_1 values calculated using the chemical shifts are presented in Tables 30-33 for the 0.07 M to 0.004 M solutions. Due to the small relative change observed in the coupling constant values (approximately 2 Hz out of a coupling constant of 78 Hz or ~2.5%), the coupling constant data was not used to characterize the acid-base equilibria.

Examination of the results in Tables 30-33 indicates that the drift with pH in the calculated log K_1 values is reduced with decreasing trimethyllead concentrations. The essentially constant value of 4.83 obtained with the

TABLE 30

Proton Magnetic Resonance Data and Log K_1 Values For 0.069 M Trimethyllead Perchlorate[a]

pH	Chemical Shift[b]	$J_{^{207}Pb-^{1}H}$[c] (Hz)	log K_1[d]
6.72	1.532	77.00	-
7.43	1.523	77.40	5.06
7.80	1.508	77.25	5.16
8.13	1.488	77.35	5.14
8.46	1.461	77.85	5.08
8.82	1.420	78.05	5.01
9.12	1.386	78.40	4.92
9.41	1.355	78.20	4.84
9.75	1.320	78.60	4.76
10.10	1.293	78.80	4.69
10.46	1.275	78.80	4.65
11.14	1.260	79.20	4.59
11.40	1.255	79.00	-

a) μ = ~.3 M.
b) ppm vs DSS.
c) Uncertainty is ~ ±.05 Hz.
d) Mixed activity-concentration constant, 25°C.

TABLE 31

Proton Magnetic Resonance Data and Log K_1 Values For 0.034 M Trimethyllead Perchlorate[a]

pH	Chemical Shift[b]	$J_{^{207}Pb-^{1}H}$[c]	log K_1[d]
2.96	1.535	77.10	-
7.00	1.530	77.50	-
7.27	1.524	77.50	-
7.91	1.511	77.30	5.00
8.23	1.491	77.30	5.01
8.53	1.464	77.80	4.98
8.85	1.425	78.50	4.94
9.29	1.369	78.30	4.86
9.54	1.337	78.30	4.83
9.93	1.301	79.20	4.75
10.25	1.279	78.75	4.72
10.71	1.263	78.80	4.72
11.06	1.258	79.20	4.68
11.54	1.255	79.00	-
12.47	1.253	79.00	-

a) μ = 0.3 M.
b) ppm vs DSS.
c) Uncertainty is ~ ±0.05 Hz.
d) Mixed activity-concentration constant, 25°C.

TABLE 32

Proton Magnetic Resonance Data and Log K_1 Values For 0.014 M Trimethyllead Perchlorate[a]

pH	Chemical Shift[b]	$J_{^{1}H-^{207}Pb}$[c]	log K_1[d]
2.90	1.535	77.35	-
4.20	1.535	-	-
6.44	1.534	77.10	-
7.12	1.532	77.15	-
7.60	1.516	77.25	-
8.29	1.494	77.55	4.94
8.63	1.461	77.60	4.92
8.95	1.417	78.10	4.90
9.30	1.366	78.25	4.87
9.60	1.324	78.40	4.87
9.92	1.297	78.75	4.83
10.33	1.272	79.00	4.83
10.69	1.261	78.80	4.82
11.02	1.256	78.90	4.90
11.38	1.255	78.90	-
11.74	1.255	79.05	-

a) $\mu \simeq 0.3$ M.
b) ppm vs DSS.
c) Uncertainty is ~ ±0.05 Hz.
d) Mixed activity-concentration constant, 25°C.

TABLE 33

Proton Magnetic Resonance Data and Log K_1 Values For 0.005 M Trimethyllead Perchlorate[a,b]

pH	Chemical Shift[c]	log K_1[d]
5.96	1.531	-
6.35	1.531	-
6.72	1.526	-
7.18	1.528	-
7.83	1.522	4.70
8.13	1.513	4.70
8.39	1.492	4.83
8.69	1.462	4.83
8.92	1.431	4.83
9.18	1.390	4.83
9.34	1.367	4.82
9.59	1.335	4.79
9.81	1.306	4.82
10.09	1.286	4.78
10.37	1.272	4.78
10.67	1.261	4.84
11.16	1.255	-
11.59	1.253	-
11.99	1.253	-

a) μ ~0.3 M.
b) Coupling constant not measurable due to low concentration.
c) ppm vs DSS.
d) Mixed activity-concentration constant, 25°C.

0.004 M solution is considered to be a good estimate of log K_1 for the conditions used.

To verify the conclusions drawn from the nmr data, potentiometric titrations were carried out on solutions with trimethyllead concentrations of 0.07 M and 0.007 M and ionic strength approximately 0.3 M. By neglecting dimer formation (Equation 7), K_1 was calculated from potentiometric data using Equation 2 and the following procedure.

For the titration of a solution of $(CH_3)_3PbClO_4$ with NaOH, the charge balance equation is:

$$[(CH_3)_3Pb^+] + [H^+] + [Na^+] = [OH^-] + [ClO_4^-] \quad (9)$$

$[OH^-]$ can be obtained from the pH meter readings; $[H^+]$ may be neglected in the pH range of interest. $[Na^+]$ is obtained from the volume of titrant added and $[ClO_4^-]$ from the initial concentration of added trimethyllead salt. (Since $[Na^+] = [ClO_4^-]$ when added as $NaClO_4$, the contribution of the inert salt is neglected). The sodium and perchlorate ion concentrations are easily corrected for dilution since both the initial volume and the volume of titrant added are known quantities (20). $[(CH_3)_3Pb^+]$ can thus be written in terms of known quantities.

$$[(CH_3)_3Pb^+] = [OH^-] + [(CH_3)_3PbClO_4] - [Na^+] \quad (10)$$

where $[(CH_3)_3PbClO_4]$ is the total concentration of trimethyllead in solution. Since only two forms of trimethyllead are being considered, we can write:

$$[(CH_3)_3PbOH] = [(CH_3)_3PbClO_4] - [(CH_3)_3Pb^+] \quad (11)$$

Thus all three variables on the right hand side of Equation 2 can be obtained from the experimental data.

The log K_1 values obtained from the potentiometric data at the 0.07 M concentration level exhibited the same range of values and continuous drift with pH as was observed with the nmr data obtained at 0.069 M whereas the calculations using the data obtained at 0.007 M yielded an essentially constant log K_1 value of 4.96. The reason for the difference between the nmr and potentiometrically determined log K_1 values at low concentration is not immediately apparent but is probably due, in part, to the higher trimethyllead concentration used in the potentiometric experiment. Also, the pH titration is more susceptible to carbon dioxide interference and to errors in the determination of the trimethyllead concentration.

Assuming that Equations 1 and 7 represent the equilibria which exist between trimethyllead and hydroxide ion in basic solution, the equation for the observed chemical shift becomes:

$$\delta_{obs} = P_f\delta_f + P_c\delta_c + P_d\delta_d \qquad (12)$$

where the subscript d represents the dimeric form, $((CH_3)_3Pb)_2^+OH$. Examination of the trimethyllead chemical shift values at high pH and at various total concentrations of trimethyllead (see Tables 30-33) shows that the limiting chemical shift, at high pH, is independent of the concentration level of the trimethyllead. This indicates that either δ_c and δ_d are the same, which is very unlikely considering the results for CH_3Hg (16) or that only $(CH_3)_3PbOH$ is present at high pH, which is much more likely considering that only one equivalent of hydroxide is consumed in the standardization titrations (see Chapter VIII). As a result, δ_f and δ_c may be obtained directly from the chemical shift titration curves at pH's below 6.5 and above 11.0, respectively. However, there is no pH at which the dimeric species is the only form of trimethyllead present and, as a consequence, δ_d cannot be measured directly. K_2 and δ_d have been estimated to be 20.6 and 1.345 ppm, respectively, by nonlinear least squares analysis of chemical shift titration data (19).

B. The Determination of Formation Constants of Trimethyllead Complexes of Selected Carboxylic Acids

Tables 34 through 37 contain the chemical shift vs pH data for both the trimethyllead and ligand resonances

TABLE 34

Proton Magnetic Resonance Data For The Trimethyllead-Pivalic Acid System[a]

pH	Chemical Shift[b]		$J_{^1H-^{207}Pb}$ [c]
	Pivalic Acid	Trimethyllead	
1.62	1.193	1.533	77.2
2.05	1.193	1.533	77.1
2.52	1.193	1.533	77.1
3.01	1.191	1.531	77.0
3.43	1.185	1.530	77.2
3.79	1.175	1.528	77.2
4.21	1.158	1.521	77.1
4.59	1.138	1.514	77.4
4.92	1.123	1.511	77.3
5.30	1.111	1.510	77.3
5.74	1.103	1.506	77.5
6.29	1.100	1.505	77.4
7.00	1.100	1.500	77.2
7.51	1.100	1.486	77.5

a) 0.153 M $(CH_3)_3PbClO_4$, 0.071 M Pivalic Acid.
b) ppm vs DSS.
c) Hz.

TABLE 35

Proton Magnetic Resonance Data for the Trimethyllead-Pivalic Acid System[a]

pH	Chemical Shift[b]	
	Pivalic Acid	Trimethyllead
1.83	1.193	1.533
3.09	1.188	1.530
3.39	1.186	1.530
3.70	1.180	1.525
4.01	1.170	1.521
4.37	1.155	1.513
4.72	1.136	1.505
5.03	1.123	1.500
5.39	1.111	1.496
5.70	1.106	1.496
6.61	1.100	1.490
9.11	1.098	1.378

a) 0.102 M $(CH_3)_3PbClO_4$, 0.093 M Pivalic Acid
b) ppm vs DSS

TABLE 36

Proton Magnetic Resonance Data for the Trimethyllead-Propionic Acid System[a]

pH	Chemical Shift[b] Trimethyllead
1.10	1.535
3.04	1.532
3.41	1.532
3.74	1.528
4.14	1.523
4.40	1.518
4.83	1.512
5.12	1.508
5.54	1.506
6.01	1.503
7.23	1.496
7.95	1.476

a) .079 M $(CH_3)_3PbClO_4$, .079 M sodium propionate.
b) ppm vs DSS.

TABLE 37

Proton Magnetic Resonance Data for the Trimethyllead-Acetic Acid System[a]

pH	Chemical Shift[b]	
	Acetic Acid	Trimethyllead
1.97	2.085	1.533
2.52	2.085	1.533
2.87	2.083	1.531
3.15	2.074	1.531
3.46	2.061	1.526
3.78	2.045	1.533
4.14	2.013	1.516
4.76	1.961	1.506
5.01	1.943	1.503
5.37	1.931	1.501
5.68	1.922	1.500
6.01	1.919	1.500
6.76	1.913	1.495
7.25	1.915	1.495

a) 1.402 M $(CH_3)_3PbO_2CCH_3$
b) ppm vs DSS

for 1:1 and 2:1(1) solutions of trimethyllead and pivalic acid and 1:1 solutions of trimethyllead and acetic acid and acetyl glycine. The chemical shift vs pH data for the trimethyllead resonance alone for 1:1 solutions of trimethyllead and propionic acid and formic acid is presented in Tables 38 and 39.

Figure 22 presents the chemical shift of the trimethyllead resonance as a function of pH for trimethyllead perchlorate and 1:1 and 2:1 solutions of trimethyllead and pivalic acid. Qualitatively, the effect of complexation can be observed as the upfield displacement of the trimethyllead resonance in the pH region below pH 7 in the solutions containing the carboxylic acid. Above pH 7, the hydroxyl ion competes with the carboxylate ligand for the trimethyllead and by a pH of 10 essentially all of the trimethyllead is present as a hydroxyl complex. The small plateau in the 1:1 plot at approximately pH 6.0 indicates that complexation by the pivalic acid is essentially complete at this pH. This is not an unexpected result since the acid is almost completely deprotonated by this pH. The plot for trimethyllead perchlorate shows that hydroxyl complexation does not occur to any significant degree below pH 6.5. As a consequence, it is apparent that neglecting the trimethyllead-hydroxide equilibria will have

---

(1) 1:1 solutions contain approximately 1 mole of trimethyllead per mole of ligand. 2:1 solutions contain 2 moles of trimethyllead per mole of ligand.

TABLE 38

Proton Magnetic Resonance Data for the Trimethyllead-Formic Acid System[a]

pH	Chemical Shift[b] Trimethyllead
1.94	1.533
2.64	1.533
3.00	1.530
3.30	1.526
3.60	1.526
3.91	1.525
4.31	1.523
5.24	1.523
7.34	1.511

a) .0785 M $(CH_3)_3PbClO_4$, .0786 M sodium formate.
b) ppm vs DSS.

TABLE 39

Proton Magnetic Resonance Data for the Trimethyllead-Acetylglycine System[a]

pH	Chemical Shift[b]		
	Acetyl Methyl	Glycine Methylene	Trimethyllead
0.85	2.056	3.988	1.535
1.41	2.054	3.980	1.535
1.70	2.054	3.977	1.535
2.01	2.055	3.969	1.534
2.32	2.054	3.955	1.532
2.64	2.051	3.929	1.530
3.00	2.048	3.893	1.527
3.32	2.041	3.848	1.523
3.60	2.039	3.814	1.521
3.94	2.036	3.783	1.518
4.47	2.031	3.753	1.515
5.47	2.033	3.740	1.514
6.60	2.031	3.740	1.511
7.29	2.031	3.742	1.501

a) 0.153 M $(CH_3)_3PbClO_4$, 0.140 M acetylglycine.
b) ppm vs DSS.

no effect upon the determination of the trimethyllead-carboxylic acid formation constants.

The lead-207-methyl proton coupling constant ($J_{^{207}Pb-^{1}H}$) was measured for the mixtures in Tables 34-37 and was observed to be essentially constant at 77.0 ± 0.5 Hz over the pH range 1.0-7.0. It appears, therefore, that $J_{^{207}Pb-^{1}H}$ is not sufficiently sensitive to coordination by the carboxylate ligand to be of use in the determination of formation constants for trimethyllead-carboxylate complexes. The coupling constant values observed are quite similar to the value of 77.5 Hz observed for 30% $(CH_3)_3PbF_4$ in aqueous solution (23).

It has been previously illustrated (16), for methylmercury-carboxylic acid systems, that the chemical shift vs pH data for the carboxylic acid protons can be used to determine formation constants. In contrast to the trimethyllead resonances, below pH 7 the observed chemical shifts of the carboxylic acid resonances are affected by the protonation-deprotonation equilibrium as well as by complex formation. As a consequence, the observed chemical shift of the ligand resonance(s) is the weighted average of the protonated, deprotonated and complexed limiting shifts. Accounting for the additional equilibrium brings about a significant increase in the complexity of the calculations required to determine formation constants from the chemical shift titration data and, as a result, the formation constants for the trimethyllead-carboxylic acid complexes studied in this thesis were calculated only from the observed changes in the chemical shifts of the trimethyllead protons.

Although previous studies of the aqueous solution chemistry of the chloro-complexes of triethyllead (24,25) were inconclusive with regards to the preferred coordination state of triethyllead, a study of the trimethyllead-diphenylthiocarbazone system (26) indicated that a 1:1 complex was the dominant form in aqueous solution. Also, the tendency for $(CH_3)_3Pb^+$ to form 1:1 complexes has been documented for a variety of ligands in several nonaqueous solvents (23,27). Consequently, only 1:1 trimethyllead-carboxylic acid complexes were considered for the solution conditions used in this work.

The formation constant of the trimethyllead complex can be defined by Equations 13 and 14:

$$(CH_3)_3Pb^+ + RCO_2^- \rightleftarrows (CH_3)_3PbO_2CR \qquad (13)$$

$$K_f = \frac{[(CH_3)_3PbO_2CR]}{[(CH_3)_3Pb^+][RCO_2^-]} \qquad (14)$$

where $(CH_3)_3PbO_2CR$ represents the trimethyllead-carboxylic acid complex and RCO_2^- the deprotonated, uncomplexed, carboxylic acid.

K_f can be determined from nmr chemical shift data by recalling that, for a 1:1 complex, the observed chemical shift is defined by Equation 3, with δ_c referring to the limiting shift of $(CH_3)_3PbO_2CR$. The fraction of the trimethyllead in the complexed form is described by Equation 5 and the fraction in the free form by Equation 15.

$$P_f = (\delta_{obs} - \delta_c)/(\delta_f - \delta_c) \qquad (15)$$

The equation for K_f can be written in terms of P_f and P_c,

$$K_f = \frac{P_c}{P_f[RCO_2^-]} \qquad (16)$$

and $[RCO_2^-]$ can be determined from:

$$[RCO_2^-] = \alpha([RCO_2H]_t - P_c[CH_3)_3Pb^+]_t) \qquad (17)$$

where $[RCO_2H]_t$ and $[(CH_3)_3Pb^+]_t$ are the total concentrations of carboxylic acid and trimethyllead respectively. α is the fraction of uncomplexed, deprotonated carboxylic acid at a given pH.

$$\alpha = K_A/(K_A + a_{H^+}) \qquad (18)$$

Substitution of Equations 5, 15, and 17 into Equation 16 gives:

$$K_f = \left(\frac{\delta_{obs}-\delta_f}{\delta_c-\delta_{obs}}\right) \Bigg/ \left(\left\{[RCO_2H]_t - \frac{(\delta_{obs}-\delta_f)}{(\delta_c-\delta_f)}[(CH_3)_3Pb^+]_t\right\}\alpha\right) \qquad (19)$$

Equation 19 gives K_f in terms of the total concentration of ligand and trimethyllead, α, and the chemical shift data. K_f and δ_c are the only unknowns and can be calculated using Equation 19 by a series of successive approximations. From Figure 22, it can be seen that the pH range 5.5 to 6.0 is the range of maximum $(CH_3)_3PbO_2CR$ concentration. By assigning the experimentally observed value of δ_{obs} at pH 6.0 to δ_c, a value for K_f can be calculated from each chemical shift-pH data point in the region of the titration curve over which complexation occurs (as determined from chemical shift vs pH plots such as Figure 22). As it is unlikely that the trimethyllead is totally complexed under the solution conditions used, δ_c is most likely greater than δ_{obs} at pH 6.0 (recall Equation 3) and as a consequence, the assigned value of δ_c is increased by 0.0167 ppm and a new set of K_f values calculated. This cycle is repeated 4 or 5 times to obtain several sets of δ_f, δ_c and average K_f values. (δ_f is the same in all data sets and the K_f values are averaged for each δ_c). Each set of constants is then used to predict the chemical shift of the trimethyllead resonance at each pH value in the data set. The goodness of fit between the predicted, δ_{pred}, and observed chemical shifts is determined by calculating

$$R = \{\Sigma(\delta_{pred} - \delta_{obs})^2\}^{\frac{1}{2}}$$

the minimum value of R indicating the best fit. The two successive δ_c values between which R will be a minimum are thus determined and the entire calculation is repeated using smaller increments (.004 ppm) between successive estimates of δ_c for the range yielding a minimum for R. The δ_c and average K_f values which yield the minimum value of R are reported in Table 40 for the carboxylic acids in Tables 34-39. The uncertainties in the formation constants are the average absolute deviations from the reported value of K_f, for values calculated with the reported δ_c. The uncertainty in the δ_c values is ±0.004 ppm for all compounds.

There are no formation constants for trimethyllead complexes available for comparison with the results given in Table 40. A qualitative comparison can be made with the previously reported formation constants for the methylmercury complexes of the same carboxylic acids and, to facilitate comparison, the log K_f values of the appropriate methylmercury complexes reported in Reference 16 are given in Table 40. The values in Table 40 show that the log K_f of a given methylmercury complex is approximately 2.2

TABLE 40

Acid Ionization Constants and Formation Constants of the Trimethyllead and the Methylmercury Complexes of Selected Carboxylic Acids, and the Trimethyllead Chemical Shifts of Their Trimethyllead Complexes

Carboxylic Acid	pK_A[a]	$\delta_{Complex}$[c]	$\log K_f$[a,b] $(CH_3)_3Pb^+$	$\log K_f$[a,b,c] CH_3Hg^+
Pivalic	4.95	1.447	1.32±.02	3.53
Propionic	4.80	1.460	1.20±.01	3.37
Acetic	4.65	1.465	1.02±.02	3.16
Formic	3.55	1.460	0.37±.10	2.65
Acetylglycine	3.40	1.461	0.59±.02	2.61

a) 25°C
b) Mixed activity-concentration constant
c) Chemical shift of the methyl protons of trimethyllead, ppm vs DSS
d) From S. Libich and D.L. Rabenstein, Anal. Chem., 45, 118 (1973)

units greater than the log K_f of the equivalent trimethyllead complex. The greatest deviation occurs for formic acid which yields a difference of 2.3 units between the two log K_f values. This correlation lends some support to the previous use of the methylmercury-hydroxide equilibria as models for the trimethyllead-hydroxide system.

Of greater interest, however, is the correlation shown in Figure 24 between the formation constant of the complex and the acid dissociation constant of the ligand. From the plot in Figure 24 we obtain:

$$pK_A = 1.47 \log K_f + 3.0 \qquad (20)$$

Equation 20 predicts that for carboxylic acids with pK_A values less than 3.0, the log K_f for complexes with trimethyllead should be less than zero. In other words, no stable complexes would be expected. A nmr titration of a 1:1 solution of trimethyllead: monochloroacetic acid ($pK_A = 2.75$) was performed and the chemical shift data obtained indicates that no detectable complex is formed.

By analogy to the methylmercury work (16), it would be expected that the $^{207}Pb-^{1}H$ coupling constant would be sensitive to complex formation. However, the coupling-constant data presented in Tables 30-32 for hydroxyl complexes and the even smaller changes in $J_{^{207}Pb-^{1}H}$ observed

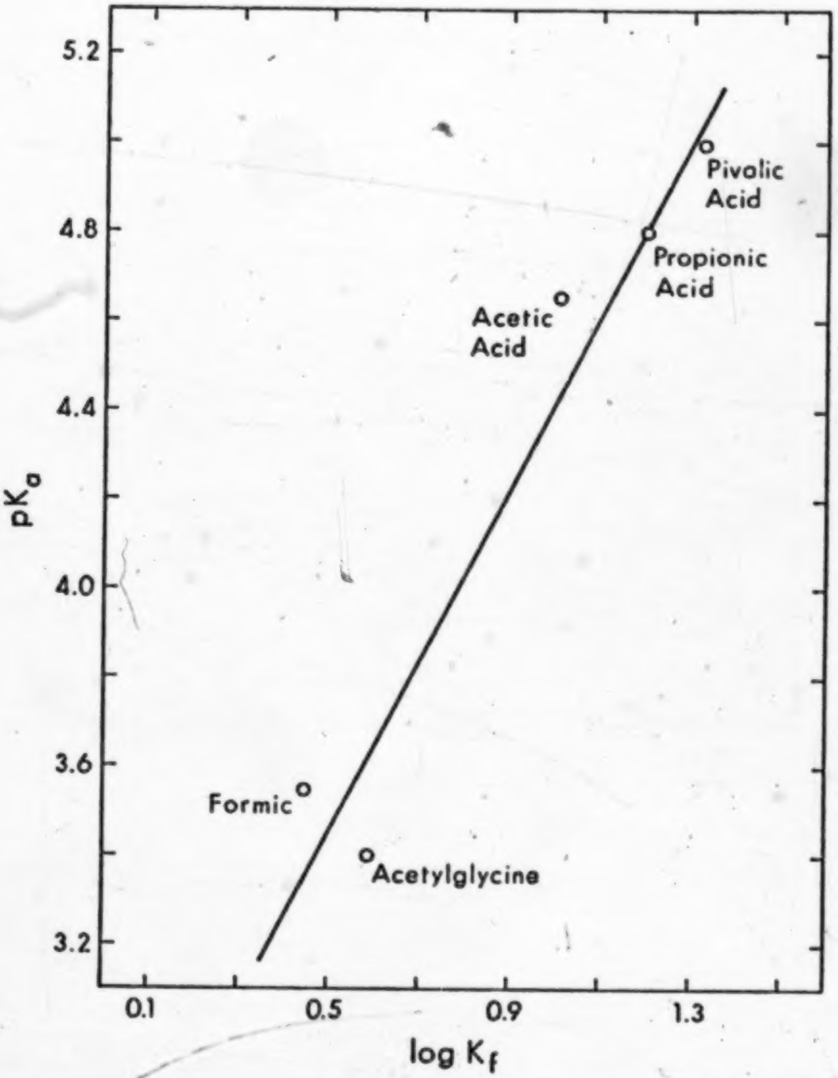

Figure 24. Plot of the pK_A's of selected carboxylic acids vs the formation constants of their trimethyllead complexes.

for the carboxylic acid complexes indicates that the lead-207 proton coupling constant is not sensitive to the complexation of trimethyllead by the ligands studied. Any changes in the hybridization of lead, due to complexation, which involve the bond angles at the lead atom should be reflected in changes in $J_{^{207}Pb-^{1}H}$ (23). Shier and Drago (23) have shown, however, that $J_{^{207}Pb-^{1}H}$ changes from 77.5 Hz for $(CH_3)_3PbBF_4$ in water to 85.0 Hz for $(CH_3)_3PbClO_4$ in hexamethylphosphoramide and that the change is not solely dependent upon any apparent geometrical change in the planar $(CH_3)_3Pb^+$ ion. Raman spectroscopy studies (28) have illustrated that $(CH_3)_3Pb^+$ is planar in aqueous solutions of perchlorate salt. It is possible, then, that complex formation with the carboxylic acids studied does not bring about any significant change in the geometrical configuration or in the hybridization of the lead ion in trimethyllead. As a result, a system of 1:1 trimethyllead-oxalic acid was studied to determine if the presence of two carboxyl groups on a single ligand molecule would bring about changes in the arrangement of methyl groups around the lead which in turn would be reflected in the lead-207 proton coupling constant. However, in dilute solution (.014 M $(CH_3)Pb^+$) no detectable binding occurred below pH 7.0 and in more concentrated solution (0.14 $(CH_3)_3Pb^+$), a highly insoluble precipitate formed above pH 2.4.

BIBLIOGRAPHY

1. J.M. Wood, in "Advances in Environmental Science and Technology", Vol. 2, J.N. Pitts, Jr., and R.L. Metcalf, Ed., Wiley-Interscience, New York, N.Y. 1971.
2. "Lead in the Canadian Environment", Publication No. BY 73-7 (ES), Ch. 2, National Research Council of Canada, 1973.
3. G.J.M. Van der Kerk, International Conference on Lead, 3, Permagon Press, London, 1969. p. 409.
4. N. Labarre, J.B. Milne, and B.G. Oliver, J. Water Res., 7, 1215 (1973).
5. H. Shapiro and F.W. Frey, "The Organic Compounds of Lead", Interscience Publishers, New York, N.Y., 1968, p. 298.
6. R.W. Leeper, L. Summers, and H. Gilman, Chem. Rev., 54, 101 (1954).
7. M. Gielern and M. Sprecher, Organometal. Chem. Rev., 1, 455 (1966).
8. I.P. Beletskaya, K. Butin, A.N. Ryabtsev, and O.H. Reutor, J. Organometallic Chem., 59, 1 (1973).
9. P.T.S. Wong, Y.K. Chau, and P.L. Luxon, Nature, 253, 263 (1975).
10. H. Shapiro and F.W. Frey, op. cit., pp. 17-21.

11. N.I. Sax, "Dangerous Properties of Industrial Materials", Reinhold Publishing Corporation, New York, N.Y., 1968. p. 886.

12. D.L. Rabenstein, Can. J. Chem., 50, 1036 (1972).

13. B.J. Fuhr, Ph.D. Thesis, University of Alberta, 1974.

14. M.T. Fairhurst, Ph.D. Thesis, University of Alberta, 1975, and references therein.

15. G. Calingaert, F.J. Dykstra, and H. Shapiro, J. Amer. Chem. Soc., 67, 190 (1945).

16. S. Libich and D.L. Rabenstein, Anal. Chem., 45, 118 (1973).

17. A.I. Vogel, "Quantitative Inorganic Analysis", 3rd ed., John Wiley and Sons Inc., New York, N.Y., 1961. Chap. [III, 6], p. 242.

18. A.I. Vogel, op. cit., Chapter [XVI, 3] p. 931.

19. S. Backs, E. Millar, C.A. Evans, and D.L. Rabenstein, unpublished results.

20. A. Albert and E.P. Serjeant, 'The Determination of Ionization Constants', Chapman and Hall, London, 1971. Chapter 2.

21. G. Schwarzenbach and M. Schellenberg, Helv. Chim. Acta., 48, 28 (1965).

22. D.L. Rabenstein, C.A. Evans, M.C. Tourangeau, and M.T. Fairhurst, Anal. Chem., 47, 338 (1975).

23. G.D. Shier and R.S. Drago, J. Organometal. Chem., 6, 359 (1966).

24. N. Bertazzi, G. Alonzo, and A. Silvestri, J. Inorg. Nucl. Chem., 34, 1943 (1972).

25. A.J. Barker and A.B. Clarke, J. Inorg. Nucl. Chem., 36, 921 (1974) and references therein.

26. H. Irving and J.J. Cox, J. Chem. Soc. (Lond.), 1421 (1961).

27. N.A. Matwiyoff and R.S. Drago, Inorg. Chem., 3, 337 (1964).

28. I.R. Beattie, Quart. Rev., 17, 382 (1963).